Effects of diode parasitics on the performance of lattice mixers

Gregory, J. F.

EFFECTS OF DIODE PARASITICS ON THE PERFORMANCE OF LATTICE MIXERS

BY

J. F. GREGORY B.Sc.(Dunelm)

(Van Mildert College)

A Thesis submitted to the Faculty of Science

in the University of Durham for the degree of

Doctor of Philosophy

Department of Applied Physics

and Electronics

April 1975

University of Durham

ABSTRACT

It has been known for a number of years that the noise figure of a simple receiving system is directly proportional to the conversion effeciency of the mixer. Any improvement in this will have great bearing on the performance of a communications system, offering the possibility of an increased range of reception.

The narrow-band open-circuit lattice mixer has been shown theoretically, under certain conditions, to produce a loss approaching zero. Exploratory low frequency circuits have given conversion power losses as low as 1 dB. The increasing use of communication systems at microwave frequencies brings with it the demand for low-loss mixers at these higher frequencies. As the frequency of operation increases, the parasitic diode reactances have a more pronounced effect on the mixer performance.

The original work presented here analyses the effect of the parasitic diode package capacitance on the performance of a narrow-band open-circuit lattice mixer. The main conclusion to be drawn from the analysis is that for practical diodes used with local oscillator powers normally encountered in microwave mixers, the conversion power-loss of the mixer will, generally, be less than 1.5 dB. Another important result from the analysis is that the optimum terminating resistances are considerably reduced when even small amounts of package capacitance (eg. 0.1 pF) are present. This may be considered as being an advantage when matching the lattice to a 50 Ω coaxial system.

An experimental mixer at L-band constructed by the author using lumped circuit components, gave a 2.8 dB conversion power loss at 20 mW of local oscillator drive. This was a considerable improvement on existing commercial models. Had it been a broad-band lattice mixer it would have given a 3.6 dB minimum conversion loss. On the other

hand a narrow-band mixer would have given 3.75 dB minimum.

The practical mixer circuit was a modification of the one first analysed in detail by Kulesza, in that the input transformer was resonated. This configuration solved the problem of feeding the local oscillator at the input of the lattice. The 25 MHz 3 dB band-width of the mixer would be considered sufficiently large enough for use in a communications network. Less power at the local oscillator frequency was required when comparing this mixer with some 2-diode mixers; in some cases producing a power saving of 50%.

Experimental verification of the analytical work on the effect of diode capacitance gave within 0.9 dB of the theoretical values for low values of capacitance and for local oscillator drive levels used in practice.

Finally, the 'K' mixer parameters for the case when diode package capacitance is present in a narrow-band open-circuit lattice mixer are solved. These will be of importance to any future analytical work on lattice mixers.

ACKNOWLEDGMENTS

I am deeply indebted to my supervisor, Dr. B.L.J. Kulesza, for his assistance, guidance and friendship during the research work and the production of the thesis. His method of apprach and his attention to detail when solving analytical or practical problems are qualities I will always try to emulate.

Thanks are extended to Prof. D.A. Wright, head of the Department of Applied Physics and Electronics, for allowing me to work in his department and for making the facilities available to me. Other members of the department deserve acknowledgment notably the members of the workshops, especially Mr. F. Spence and Mr. P. Friend.

I would also like to thank the Managing Director and Board of Directors of the English Electric Valve Co., for their sponsorship of my research work. Acknowledgments are also made to other members of E.E.V. namely Mr. M. Esterson, Mr. A.B. Cutting (now with E.M.I.-Varian) and especially Mr. G.O. Chalk, for their help, guidance and encouragement during my research period at Durham and later during the production of the thesis. My thanks are extended to Mr. P.M. Chalmers for the loan of the Hewlett-Packard calculator, which I hope did not have a detrimental effect on his children's homework.

Finally, I would like to thank my wife, Eva, who typed the manuscript and whose encouragement throughout the writing of the thesis has been beyond the call of matrimonial duty.

LIST OF CONTENTS

List of Principal Symbols

I_s	=	reverse saturation current
r_s	=	diode spreading resistance
r_b	=	diode incremental resistance at origin
q	=	electronic charge
k	=	Boltzmann's constant
T	=	temperature, K
$X(t)$	=	normalised local-oscillator drive
X	=	magnitude of normalised local-oscillator drive
$S(t)$	=	± 1 switching function
i_p	=	local-oscillator current amplitude through one diode
$r(t)$	=	time-varying resistance
$Z(t)$	=	time-varying impedance
ω_p	=	local-oscillator frequency
ω_q	=	signal frequency
$\omega_p - \omega_q$	=	intermediate frequency (also referred to as ω_{-1})
$2\omega_p - \omega_q$	=	image frequency (also referred to as ω_{-2})
A_n, A'_n, B_n, D_n, E_n, Q_n	=	Fourier coefficients
V_{-1}, V_q, V_{-2}, i_{-1}, i_q, i_{-2}	=	phasor voltages and currents at intermediate, signal and image frequencies, respectively
C_L	=	conversion-loss ratio
c.p.l.	=	conversion power loss
Z_i	=	input impedance at signal frequency

Z_0 = output impedance at intermediate frequency

Z_{-2} = image-frequency termination

Z_L = termination at intermediate frequency (load impedance)

r'_s = diode quality factor

x = normalised drive coefficient

P_0 = local-oscillator power

ln = natural logarithm

* denotes conjugate

CHAPTER 1

REVIEW OF MICROWAVE MIXERS

1.0 Introduction

Frequency changers, commonly called mixers, play an important part in communication systems. Their function is to convert the incoming modulated signal to a lower intermediate frequency which is then amplified and further processed in order to recover the original information.

In 1944, Friis[1] investigated radio receivers which basically consisted of a mixer followed by an i.f. amplifier. He concluded that the noise figure of such a system may be expressed by the following relation:

$$F_0 = (c.p.l.)\left\{t_n + F_{if} - 1\right\} \qquad \ldots 1$$

where

c.p.l. = conversion power loss ratio of the mixer

t_n = mixer noise temperature ratio

F_{if} = noise figure of the i.f. amplifier

Thus the noise figure of a receiver is directly proportional to the conversion power loss of the first mixer.

If a receiving system consists of an r.f. amplifier followed by a mixer and an i.f. amplifier, it may be shown that the noise figure for this arrangement is given by:

$$F_0 = F_1 + \frac{F_2 - 1}{G_1} + \frac{F_3 - 1}{G_1 G_2} \qquad \ldots 2$$

where

F_1, F_2, F_3 = noise figures of the first, second and third stages, respectively.

and

G_1, G_2 = available gains of the first and second stages, respectively.

Although in this case the noise figure of the r.f. amplifier is usually the dominant term, the noise figure of the mixer can still be significant.

With an increasing use of microwaves for communication links, there is a great demand for low noise receivers at these frequencies. Such a microwave link is normally required to transmit information, eg. telephone and/or television channels between two points by means of highly directional antennas. In terrestrial applications, the frequency bands most commonly used are situated in the lower microwave region (L, S and C) as coaxial and strip transmission line components are relatively easy to manufacture at these frequencies, also the absorption by water vapour in the atmosphere and the sky noise temperature at these frequencies are comparatively low[2]. A transmission of information can be effected in principle over any range using repeater stations, however, the cost of such systems can be prohibitive for long distances due to the number of repeaters required.

The artificial earth satellite offers a solution to the problem of intercontinental communication. Again the frequencies chosen are in the L, S and C bands for the reasons stated previously. For example, the 'sky-net' satellite system uses frequencies in the 1.5 GHz to 1.6 GHz range (L band) and the G.P.O. Goonhilly system receives signals in S band and transmits in C band. The noise produced in the constituent networks of a satellite system cannot be ignored because the signals are at low power levels.

In radio astronomy there is also a need for low noise reception. There are a number of frequencies radiated from parts of the Universe due to atoms and molecules. One such radiation is due to interstellar hydrogen at a frequency of 1.424 GHz. From observations at this frequency the structure and relative velocities of these hydrogen clouds

present in the galaxies can be determined. The power levels of the signals are so low that a sensitive low-noise receiver has to be used to detect them.

The information sent from planetary probes, even when correlation techniques are used, are approaching the limit of detectability due to noise. Any improvement in the noise figure of a receiving system in this case will increase its sensitivity and hence the range of such probes.

1.1 Early Research on Semiconductors and Semiconductor Diodes

The two fundamental properties of semiconductors, i.e. photoelectricity and negative temperature coefficient of resistance were observed in the 19th century. In 1833, Faraday[3] found that silver sulphide displayed a negative temperature coefficient of resistance. Six years later Becquerel[4] discovered the photovoltaic effect by shining light on the surface of one electrode immersed in an electrolyte.

Little further research into semiconductors was undertaken until 1874 when F. Braun[5] reported on the rectifying nature of the contacts produced between the metal points and lead sulphide crystal. In the same year Shuster[6] noticed a similar effect between contacts of clean copper and tarnished (oxidised) copper. It took over fifty years from this observation to the production of the copper-oxide rectifier by Grondahl and Geiger[7].

The importance of the discovery by Hall[8] in 1879, that current carriers in a metal may be deflected by a magnetic field applied perpendicularly to the motion of the current flow, was not significant as a measurement which can be used in the determination of the basic properties of the bulk semiconductors until the late 1930's.

The suitability and the importance of semiconductor rectifiers as detectors was not fully realised until sixteen years after the discovery

of radio waves in 1888 by Hertz. Patents for detectors of radio waves were taken out by Bose[9] (1904), Dunwoody[10] (1906) and Pickard[11] (1906), the latter used a whisker (point-contact) rectifier made with silicon. In 1907, Pierce[12] published a paper on the rectification characteristics of diodes made by sputtering metals on a variety of semiconductor materials.

The research and the development into thermionic valves at the turn of the century retarded the progress in the semiconductor field. The application of quantum mechanics to material sciences stimulated further study of the mechanisms of the various phenomena in semiconductors. Even in the late 1930's many thought that rectification was a bulk effect; Schottky and Deutschmann[13] introduced the idea of junctions by stating that the process of rectification occurred within a very narrow boundary layer of only 10^{-4} cm. to 10^{-5} cm. in thickness.

The development of radar in World War II brought the need for sensitive receivers at microwave frequencies. A comprehensive treatment of the research into semiconductors and point-contact diodes during this period was published by Torrey and Whitmer[14] in 1948. North[15] found that if he used a whisker containing a trace of antimony and welded the contact onto the germanium, a diode was formed which had a negative i.f. conductance and hence amplification under certain conditions. These parametric effects were due to the non-linear capacitance of a small hemispherical p-n junction.

During experimental work on the surface states of germanium, Bardeen and Brattain[16] in 1948 produced the transistor as a by-product. A year later Shockley[17] published a classic paper on the theory of p-n junction transistors which gave a clearer quantitative understanding of the semiconductor junction. From the research during these two years, grew the whole new technology associated with transistors. The metal-alloy diffusion techniques of fabricating p-n junctions were used

by Hall and Dunlap[18] in 1950. Another method, that of gaseous diffusion was patented by Scaff and Theurer[19] in 1951 and used in the production of devices three years later.

Chemically purer materials were required. The zone refining process developed by Pfann[20] in 1952 produced germanium and silicon crystals with the impurity content less than one part in 10^{10} by 1953.

The discovery that the layers of silicon oxide could be grown on the surface of pure silicon and act as masks during the diffusion of impurities into the semiconductor favoured silicon as a device material over germanium.

In 1950 Micheals and Meacham[21] reported the presence of charge storage effects in transistors and diodes they were investigating. Pell[22], three years later, was able to establish the minority carrier lifetime from the transient responses found by Micheals and Meacham. Because of these charge storage effects due to minority carriers in p-n junction diodes; devices which are based on majority carrier conduction are to be preferred in high frequency applications as a more efficient rectification is obtained.

In conclusion; the point-contact diode is one of the oldest semiconductor devices, types of which have been in existence for about a hundred years. The mechanisms involved in its operation are perhaps the least understood. Some diodes probably consisted essentially of a metal-semiconductor junction. Bonded (or formed) diodes have been analysed using the model of an abrupt hemispherical p-n junction produced by acceptor impurities, present in the whisker, diffusing into the semiconductor during the bonding process. Modern point contact diodes have been further developed using semiconductor technology and can operate upto millimetre wavelengths.

1.2 Modern Mixer Diodes

1.2.1 Introduction

In this section the construction and properties of point-contact, Schottky barrier, tunnel and backward diodes will be considered and their performances in some mixer applications assessed.

1.2.2 Point Contact Diodes

Modern point-contact diodes consist of a fine tungsten wire, electrolytically etched to produce the 'point' in contact with a silicon chip. This chip is manufactured with a lightly doped surface layer formed by a process called out-diffusion. During this process a coating of silicon-dioxide is grown onto the aluminium doped silicon. Some of the aluminium from the silicon diffuses into the silicon dioxide, leaving a lightly doped layer at the silicon surface. The oxide and the out-diffused dopant are then etched away. To obtain the required current-voltage characteristics the diodes are 'adjusted' by tapping the diode's case. The result of this is thought to produce crystalline imperfections which act as recombination centres and traps.

1.2.3 The Schottky-barrier Diode

The Schottky-barrier diode consists of a metal film evaporated onto a single-crystal semiconductor surface under the conditions of high cleanliness. A review of the physical processes which determine the height of the barrier and the current-voltage relationship in a metal-semiconductor Schottky barrier are given by Rhoderick[23]. These diodes can, under cetain conditions, show almost ideal rectification characteristics. The main feature of both, the point contact and Schottky barrier diode, is the very low parasitic capacitance produced by a small contact area. In

both diodes, when forward biased, current flows because of the injection of majority carriers from the semiconductor to the metal. Thus the minority carrier storage effects are eliminated.

The process for the manufacture of Schottky barrier diodes is developed from a planar technology. The semiconductor chip used is approximately 0.020" square in size and consists of a heavily-doped n^+ substrate on one surface of which an n-type epitaxial layer of a specific resistivity is grown. An ohmic contact is made to the other surface. In general, n-type silicon is preferred to p-type because a higher electron mobility results in an improved high frequency performance. On the epitaxial layer a further oxide layer is grown and by masking and etching techniques using photoresist a matrix of small holes is formed through the oxide. The evaporation of the metal then produces a metal-semiconductor junction. The diode characteristic will depend on the metal and the semiconductor used and the geometry of the junction. An ohmic contact is then made between the evaporated metal layer and the gold-plated metal whisker.

The main advantages of Schottky-barrier diodes; which have led to their superseding the point contact diode are:

(a) an increased resilience to mechanical vibrations

(b) they can withstand a higher incident energy without a permanent change in the characteristics (burn out)

(c) a lower $\frac{1}{f}$ noise

(d) they are mass produced, and are easily introduced into the integrated circuits

Silicon is the material most commonly used, but some diodes have been produced using gallium arsenide. The latter have a lower saturation current and a lower spreading resistance.

For use at high microwave frequencies the area of the metal-semiconductor junction has to be small ($<5\mu m$ in diameter) in order to minimise the junction capacitance. For use at frequencies above Q band would require an extremely fine control of the production techniques mentioned above. It is due to these fabrication difficulties and because of the planar geometry resulting in a relatively large capacitance, the receivers and the detectors at and above Q band still use point-contact diodes. Point-contact diodes have been produced which operate at frequencies up to 2,000 GHz.

1.2.4 The Tunnel Diode

Another device which offers possibilities for mixer applications is the tunnel diode. It was first reported by Esaki[24] (1957) and relies on the quantum-mechanical tunnelling in very narrow germanium p-n junctions. Mixer circuits using tunnel diodes have been investigated but it was found that to utilise the dynamic negative resistance region in the I/v characteristic, very careful biasing circuits had to be incorporated.

Hall[25] found that by frequent etching of the junction in a tunnel diode, a backward diode could be fabricated. A backward diode is a special form of tunnel diode in which the tunnelling process is restricted and the negative resistance region virtually disappears. These diodes have a great non-linearity of the volt-ampere characteristic at the origin and a lower $\frac{1}{f}$ noise than the silicon Schottky-barrier diode. This gives their main use as detector diodes and they are widely used in Doppler radar receivers. Because of the narrow functions involved (≈ 150 A^0) the depletion layer capacitance is large as compared to a Schottky-barrier diode.

1.2.5 Conclusion

The future research and development of mixer diodes will be towards the reduction of their noise figure, so that when used in conjunction with low loss mixer circuits it may be possible to develop a receiving system which does not require refrigeration to obtain an extremely low overall noise figure. Further reduction of the diode parasitics is an inevitable progression so that almost ideal devices will be obtained up to the frequencies in the higher microwave regions.

1.3 Practical Mixers

1.3.1 General Theory of Mixers

In theory, any non-linear element in which the local oscillator (angular frequency, ω_p) and the signal (angular frequency, ω_q) are combined will generate components which are the sum and difference products of the two frequencies and their harmonics. If the local oscillator (L.O.) level is much greater in magnitude than the signal, then in general there will be products produced of the form $n\omega_p \pm \omega_q$, $n\omega_p$ (where n = 1, 2, 3,... etc.) and ω_q only. In a receiver the frequency normally extracted is $\omega_p - \omega_q$ called the intermediate frequency (i.f.). The frequency $2\omega_p - \omega_q$ is called the image frequency, because of its position in the spectrum. As it is situated at twice the i.f. frequency away from the signal it may prove difficult to reject. There are two types of mixer operations normally considered. One, in which the signal termination is identical to the termination at the image frequency, called a broad-band circuit. The other, where the two terminations are not identical, is called a narrow-band circuit.

For a purely non-linear resistive mixer, with no external sources of power, there will always be a conversion loss from the signal to

the intermediate frequency. On the other hand, if the non-linear element is a pure reactance it is possible, under certain conditions, to obtain a conversion gain due to the energy storage from the pump.

Pre World War II superheterodyne receivers used vacuum tubes as the mixing element. With the requirements of radar, the vacuum tube was unsuitable for two main reasons:

(a) the transit time for the electrons from the cathode to the anode was approximately of the same order of magnitude as the period of the signal

(b) the interelectrode capacitances were high

This has led to the development of the point contact diodes for mixer applications.

At lower radio frequencies the bipolar transistor, and later the F.E.T. superseded the vacuum tube in most applications. At present, with transistors being produced at the lower microwave frequencies, there is a likelihood of transistor mixers being developed.

Microwave mixer circuits can be divided into 3 distinct types: the single diode mixer, the two diode balanced mixer and the lattice mixer.

1.3.2 The Single-diode Mixer

A detailed analysis of this type of circuit was carried out by Torrey and Whitmer[14]. The effects on the mixer performance of the image frequency termination, parasitic impedances and depletion layer capacitance were included.

In practice the diode was situated in a mount on a waveguide/coaxial transformer. The signal and the local oscillator were coupled into the waveguide section and the i.f. taken out via a

coaxial outlet. Conversion power losses of such mixers were approximately 8 dB to 12 dB.

The fact that the local oscillator and the signal use the same input terminals proves to be one of the main disadvantages of this circuit. Although the i.f. is at a much lower frequency, the rejection of the l.o. and the signal frequencies should be easy but there may not be complete rejection because of the level differences involved.

1.3.3 The Two-diode Balanced Mixer

A modulator circuit of this form has been in existence for a number of years. The circuit is balanced with respect to the L.O. frequency only, and consequently it is referred to as a single balanced mixer. It is not balanced with respect to the signal, so hence the signal is present at the i.f. terminals. The balance with respect to the local oscillator frequency has two main advantages, assuming that the two diodes are matched:

(a) the local oscillator noise contribution is minimised

(b) radiation of the local oscillator wave by the antenna is reduced

Van der Graaf[26] has analysed the single-balanced modulator under different terminating conditions. He showed that for the circuit shown in Fig. 1.2, with no frequency-selective terminations and using ideal diodes, the minimum c.p.l. is theoretically 9.9 dB.

The input transformer and l.o. feed, at the input, have an elegant microwave equivalent in the 'magic T'. Single-balanced microwave mixers based on the 'magic T' have been extensively used in receivers. Pound[27] states that an added advantage of this type over the single diode mixer is that a lower local oscillator power is required to obtain the same conversion loss.

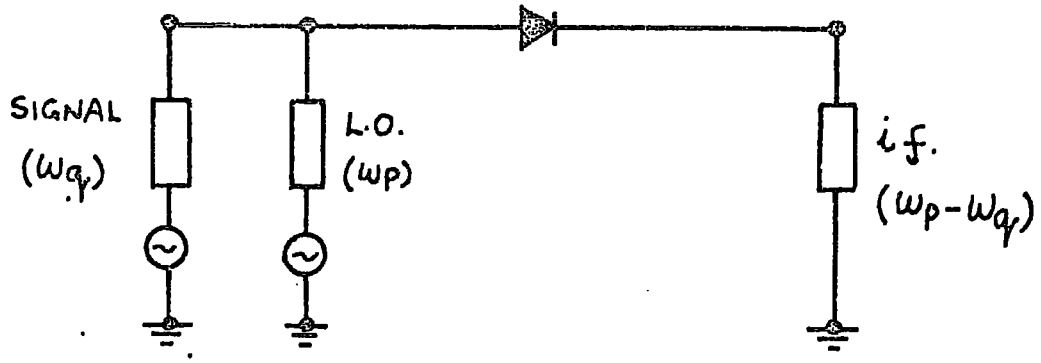

FIG. 1.1. THE SINGLE DIODE MIXER – AN EQUIVALENT CIRCUIT.

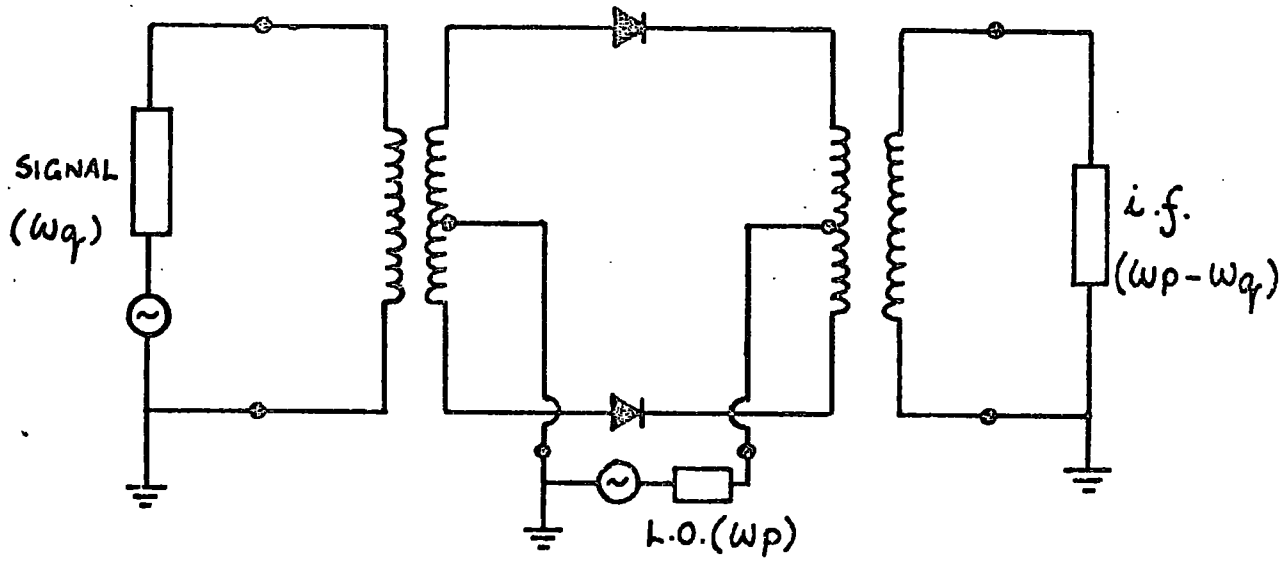

FIG. 1.2. THE SINGLE – BALANCED MIXER.

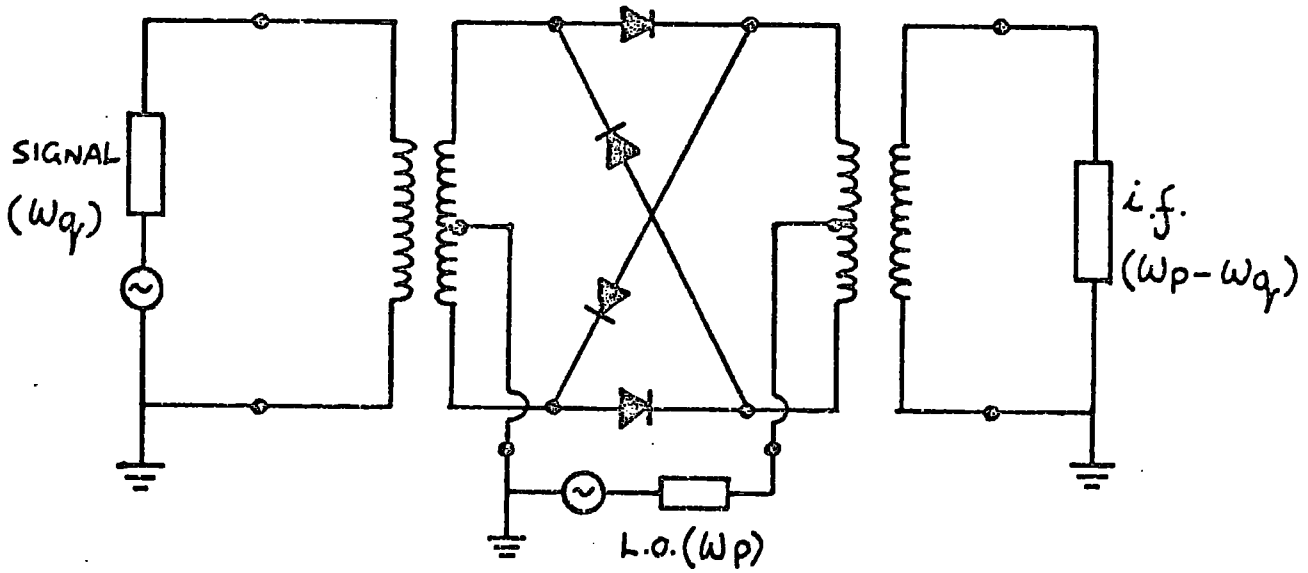

FIG. 1.3. THE LATTICE MIXER.

Using microstrip construction more compact and lighter versions of this mixer have been produced. The designs incorporated some form of image rejection. C.p.l.'s for commercially available mixers are in the range from 5.5 dB to 7.0 dB approximately.

1.3.4 The Lattice Mixer

Several workers[28,29] have shown that a low-loss frequency changer may be achieved by means of four externally-driven rectifiers connected in a ring (or lattice). The lattice mixer has been developed from this ring modulator. The circuit is balanced at both the signal and the local oscillator frequencies; this gives rise to the alternative name of a double-balanced mixer. Neither signal voltage nor local oscillator voltage appears, ideally, at the output terminals, and in practical circuits an adequate degree of suppression of these voltages can usually be obtained. A second major advantage of the lattice mixer is that due to its symmetry only even-order modulation products are present in its input i.e. currents or voltages at the frequencies of the form $(2n\omega_p \pm \omega_q)$. In the output the modulation products are, ideally, all odd-order i.e. have the form $(2n - 1)\omega_p \pm \omega_q$, where $n = 1, 2, 3 \ldots$. This segregation of the frequency components to either the input or the output of the lattice aids filtering.

1.4 Conclusion

It has been demonstrated that the performance of a low noise receiving system depends on a mixer with a low conversion power loss.

In the following chapters low loss lattice mixers will be considered and the effect of diode parasitics on their performance.

CHAPTER 2

GENERAL THEORY OF A LATTICE MIXER

2.0 Introduction

This chapter is based on the initial investigations into lattice mixer carried out by Kulesza[1,2].

Previous work[3,4,5,6] concerned with low-loss ring modulator (mixer) circuits, assumed that each diode was switched by the local-oscillator voltage between two resistance levels, low forward and high reverse. The incremental resistance as a function of time was approximated to a square wave. The equivalent networks of these modulators were then obtained as sinusoidally varying resistances (eg. $\sum r_m \cos m\omega_p t$) in which the mixing takes place and to which most of the small signal analysis laws apply.

Kulesza's approach to the analysis of the lattice mixer differs from these in two important respects, firstly, a sinusoidal local-oscillator current was assumed, and secondly, the practical diode law was used. In the analysis he also assumed a l.f. equivalent circuit for the diode (i.e. no parasitic reactances present). The effects of these parasitics on the performance of a lattice mixer will be discussed and analysed in Chapter 4.

The image frequency component $(2\omega_p - \omega_q)$, is of great importance in mixers because its proximity to the signal makes filtering high frequency, low i.f. circuits very difficult. The general theory of a lattice mixer assumes this image component to be terminated in an impedance, $Z_{-2} = R_{-2} + jX_{-2}$. There are four cases of a lattice mixer which may be distinguished, each one depending on the value of the termination at the image frequency. A broad-band mixer is defined as having the input terminating resistance, $\mathcal{R}e(Z_i)$, equal to $\mathcal{R}e(Z_{-2})$. It can be shown that[6], in general, for any broad-band resistive mixer a c.p.l. less than 3 dB cannot be obtained.

One of the two types of narrow-band mixers usually considered has an open-circuit in the input at the image frequency, i.e. $Z_{-2} = \infty$. The other has a short-circuit condition in the input, i.e. $Z_{-2} = 0$. These last two examples are impossible to achieve using practical circuits, therefore, the general solution must still initially be considered for the narrow-band cases. Another special case for the mixer is when the image is reactively terminated, i.e. $Z_{-2} = jX_{-2}$.

All these specific cases will also be reviewed later on in the chapter.

2.1 Practical Diode Laws

Investigations of point-contact diodes by Kulesza[7], based on the theory that the junction was abrupt and hemispherical under the whisker[8], led to the following expression for the forward characteristic of a practical diode:

$$V = Ir_s + \frac{kT}{q} \ln\left(1 + \frac{I}{I_s}\right) \qquad \ldots 1$$

Both point-contact and Schottky-barrier diodes, which are based on majority carrier conduction, have shown to satisfy the above V/I law experimentally within 3%. Thus the relationship given in eqn. 1 was the diode law assumed in the analysis.

2.2 The Incremental Resistance

The incremental or slope resistance of the diode is obtained by differentiating eqn. 1 with respect to I, where I is the current through one diode. If the assumption is now made that there is a frequency restriction imposed by the series resonant circuit at the l.o. frequency, then this current, to a good approximation, is sinusoidal during the forward conducting halfcycle and zero in the reverse direction. The substitution of this current into the expression for the incremental

resistance gives the time-varying resistance of the diode, i.e.,

$$r(t) = r_s + r_b \frac{1}{1 + X(t) + X(t)\ S(t)} \quad \ldots 2$$

where

$$X(t) = X \cos \omega_p t$$

$$S(t) = +1 \text{ between } -\frac{\pi}{2} \text{ and } +\frac{\pi}{2}$$

$$-1 \text{ between } +\frac{\pi}{2} \text{ and } +\frac{3\pi}{2}$$

$$X = \frac{i_p}{2I_s} \quad (i_p \text{ is the current amplitude through the diode})$$

and

$$r_b = \frac{kT}{qI_s} \quad (\text{the slope resistance at the origin})$$

2.3 The Lattice-Network Equations

The four diodes of the lattice are so connected that there is a 180° phase difference in the operations of the parallel and crossed diode pairs (Fig. 2.1). For the lattice mixer considered (Fig. 2.2) the expressions for the time varying resistances can therefore be written as:

$$r_+(t) = r_s + r_b \frac{1}{1 + X(t) + X(t)\ S(t)} \quad \ldots 3$$

$$r_-(t) = r_s + r_b \frac{1}{1 - X(t) + X(t)\ S(t)} \quad \ldots 4$$

Expressions can now be derived for the voltage across the input terminals (1,1') and the current through the output terminals (2,2'), both in terms of the input current and the output voltage (these are given in Appendix 7). These relations may be finally expressed in the following

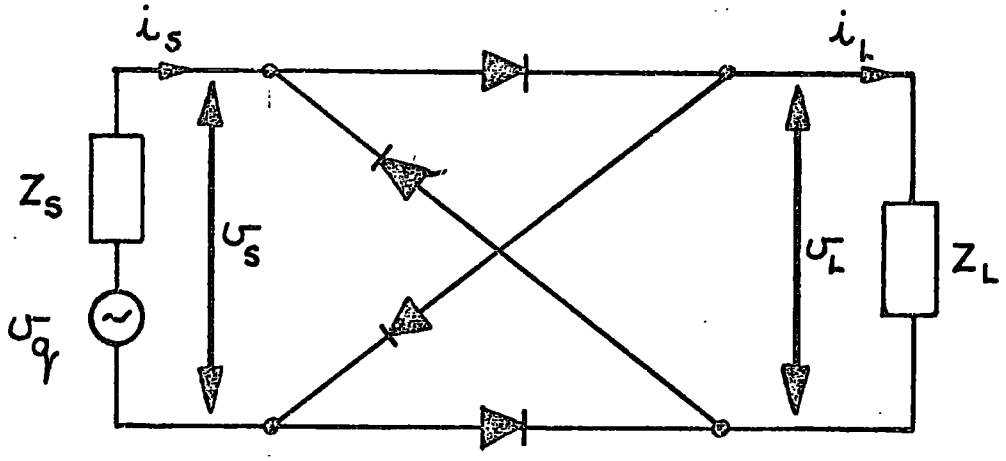

FIG. 2.1. BASIC MIXER CIRCUIT.

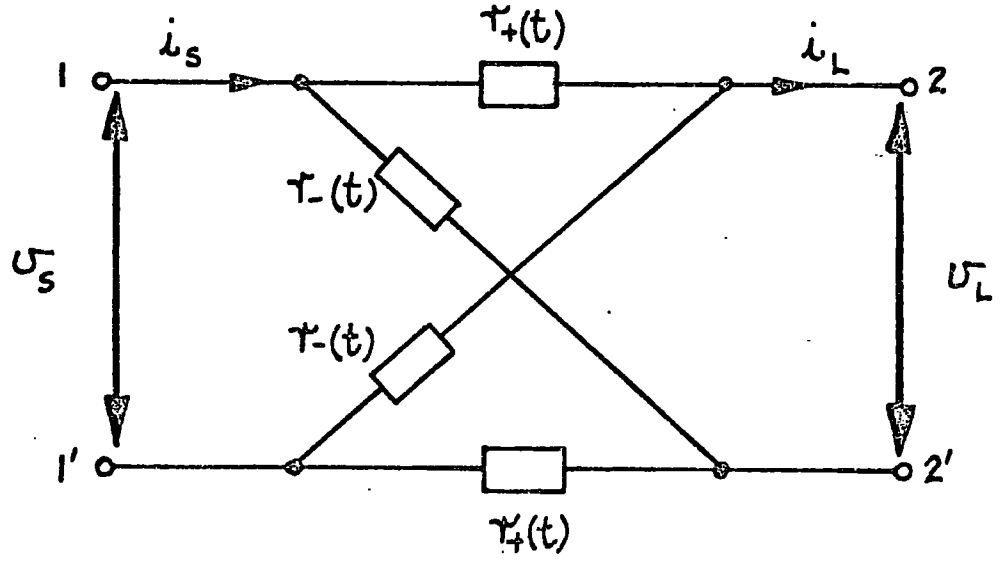

FIG. 2.2. MIXER CIRCUIT AS 4-TERMINAL NETWORK.

forms:

$$v_s = i_s r_b \sum_{n \text{ even}} A_n \cos n\omega_p t + v \sum_{n \text{ odd}} A_n \cos n\omega_p t \quad \ldots 5$$

and

$$i = i_s \sum_{n \text{ odd}} A_n \cos n\omega_p t - v \frac{1}{r_b} \sum_{n \text{ even}} A_n \cos n\omega_p t \quad \ldots 6$$

In a mixer there will be a restriction to select only the i.f. components, $(\omega_p - \omega_q)$, at the output, all other components of the load current will be ideally shorted out. It is assumed that the series resonant circuit in the input allows only two currents i_q at the signal frequency and i_{-2} at the image frequency to flow. Introduction of these constraints into eqns. 5 and 6 gives v_s as a summation of even-order products only and a component at ω_q and i_L as a summation of odd-order products. The mixer equations at ω_q, ω_{-2} and $\omega_p - \omega_q$ are then extracted and the image frequency voltage eliminated by the substitution, $v_{-2} = i_{-2} Z_{-2}$. Finally, the two equations containing only the voltages and currents at the signal and intermediate frequencies are obtained i.e.:

$$v_q = i_q r_b K_1 + v_{-1} (K_3)^{\frac{1}{2}} \quad \ldots 7$$

$$i_{-1} = i_q (K_3)^{\frac{1}{2}} - v_{-1} \frac{1}{r_b} K_2 \quad \ldots 8$$

The 'K' parameters for this general case are given in Appendix 7. They are generally complex and are functions of Z_{-2}, the local-oscillator drive (X), and the quality factor of the diode $r'_s = \frac{r_s}{r_b}$.

The solutions of the integrals for the required Fourier coefficients are given by Kulesza[1], and at drive levels greater than 10^4 may be approximated to:

$$A_0 = 2r_s' + \frac{2}{\pi X} \ln 2X$$

$$A_0' = 2$$

$$A_1 = \frac{4}{\pi}$$

$$A_2 = \frac{8}{\pi X} - \frac{4}{\pi X} \ln 2X$$

Using eqns. 7 and 8, the formula for the minimum conversion loss for this general case is given by:

$$c.p.l._{min} = \left\{ \frac{1 + 2|K|^{\frac{1}{2}} \cos\frac{\theta}{2} + |K|}{1 - 2|K|^{\frac{1}{2}} \cos\frac{\theta}{2} + |K|} \right\}^{\frac{1}{2}} \cdot \frac{\cos\theta_i}{\cos\theta_t} \qquad \ldots 9$$

where

$$K = \frac{K_1 K_2}{K_3 + K_1 K_2}$$

and

$$\exp(j2\phi) = \frac{K}{K^*}$$

An alternative method of expressing the trigonometrical functions in eqn. 9 is given in Appendix 7.

For the case when $|X_{-2}| \gg R_{-2}$ the image may be considered as being reactively terminated and X_{-2} may be substituted for Z_{-2} in the 'K' parameters.

2.4 Solutions of the Special Cases

2.4.1 Introduction

The three resistive cases of image frequency termination (i.e. narrow-band open-circuit, narrow-band short-circuit and broad-band) have been considered by Kulesza[2] and will be reviewed in this section.

For all three cases the mixer parameters are given by:

$$c.p.l._{min} = \frac{1 + K^{\frac{1}{2}}}{1 - K^{\frac{1}{2}}} \qquad \ldots 10$$

$$(R_i')_{opt} = \frac{K^{\frac{1}{2}}}{K_2} \quad \text{and} \quad (R_L')_{opt} = \frac{K_1}{K^{\frac{1}{2}}} \qquad \ldots 11, 12$$

The above are the general relationships which will be used in the following paragraphs.

2.4.2 Narrow-Band Open-Circuit Mixer

For an infinite image impedance and ideal diodes, the c.p.l. may theoretically approach 0 dB at high l.o. drives. An infinite impedance at the image frequency cannot be achieved in practice, even so very efficient frequency conversion may be obtained even at low image rejection ratios (defined as $\frac{Z_{-2}}{Z_i}$).

The 'K' parameters for the open-circuit case are:

$$K_1 = A_0$$
$$K_2 = A_0'$$
$$K_3 = \left(\frac{A_1}{2}\right)^2$$

For practical diodes at high drive levels an important relationship between the optimum terminating resistances is obtained i.e.

$$\frac{R'_{i(opt)}}{R'_{L(opt)}} = \frac{4}{\pi^2} \qquad \ldots 13$$

2.4.3 Narrow-Band Short-Circuit Mixer

Because of the short-circuit at the image frequency, losses will occur due to the dissipation of the image frequency component in the lattice itself. Thus the c.p.l. will always be greater than that for the open-circuit mixer.

The 'K' parameters for the short-circuit case are:

$$K_1 = A_0(1 - x^2)$$

$$K_2 = \left(\frac{A_1}{2}\right)^2 \frac{1}{A_0}$$

and

$$K_3 = \left(\frac{A_1}{2}\right)^2 (1 - x)^2$$

For an ideal diode, also in this case, the c.p.l. approaches 0 dB with an increasing l.o. drive. On the other hand, with practical diodes as the drive is increased the c.p.l., under matched conditions, gives in the limit a constant loss of 7.65 dB.

2.4.4 Broad-Band Mixer

For many practical mixers, especially those operating at microwave frequencies, the image frequency termination is very similar to the signal impedance. Kulesza[2] has also calculated the c.p.l. for this case and has found, similar to other authors, that it may never be below 3 dB, even when ideal diodes are used.

For practical devices, as the l.o. drive is increased the loss reads a limiting value of 4.77 dB.

2.5 Conclusions

It has been shown theoretically that a high conversion efficiency may be achieved with a narrow-band open-circuit lattice mixer. Using practical circuits the lowest c.p.l. may still be obtained with this configuration (eg. a loss below 1 dB for an image rejection ratio of 10:1 using good quality diodes).

Experimental results obtained from exploratory lattice mixers at 200 KHz (1 dB) and 900 MHz (1.85 dB) were sufficiently encouraging to investigate these circuits at microwave frequencies; where there is a demand for low-loss mixers in communication systems.

The diode parasitic reactances have an increased effect at these higher frequencies; there is thus a need for the mixer parameters, which take account of these parasitics, to be derived analytically. Because the narrow-band open-circuit mixer theoretically showed the lowest loss, it was chosen as the circuit on which to base this analysis. The discussion and analysis of the effects of diode parasitics is presented in Chapter 4.

CHAPTER 3

Practical Mixer Diodes

3.0 Introduction

The information supplied by most manufacturers of mixer diodes has been found to be inadequate for three main reasons. Firstly, there are certain diode parameters, required in the analysis of a lattice mixer, which are not easily obtained directly from the supplied data. Secondly, the conditions under which a diode parameter has been measured by the manufacturer are not always clearly defined; this measurement, in certain cases, may not be valid for the lattice mixer application. Thirdly, the lattice mixer requires a quad of diodes, whose certain parameters should be matched to within close tolerances. Most manufacturers supply quads of diodes which have not been matched to the required degree. The parameters used for the purpose of producing a matched quad are clearly defined in this chapter. The equivalent circuit of a mixer diode is considered and the measurement techniques are described by means of which the diode constants required for the analysis (r_s, r_b and C) are obtained. Although, in general, these techniques can be applied to a variety of microwave semiconductor devices only the measurements of Schottky-barrier diodes are considered, as these are predominantly used in high frequency mixer applications.

3.1 Equivalent Circuits and Diode Laws

The most comprehensive equivalent circuit generally accepted in the literature for the mixer diodes is shown in Fig. 3.1, where:

L_ℓ is the lead inductance

L_p is the inductance due to the whisker contact

R_s is the series resistance of the diode

C_p is the package capacitance

R_j is the voltage-dependent resistance of the metal-semiconductor junction

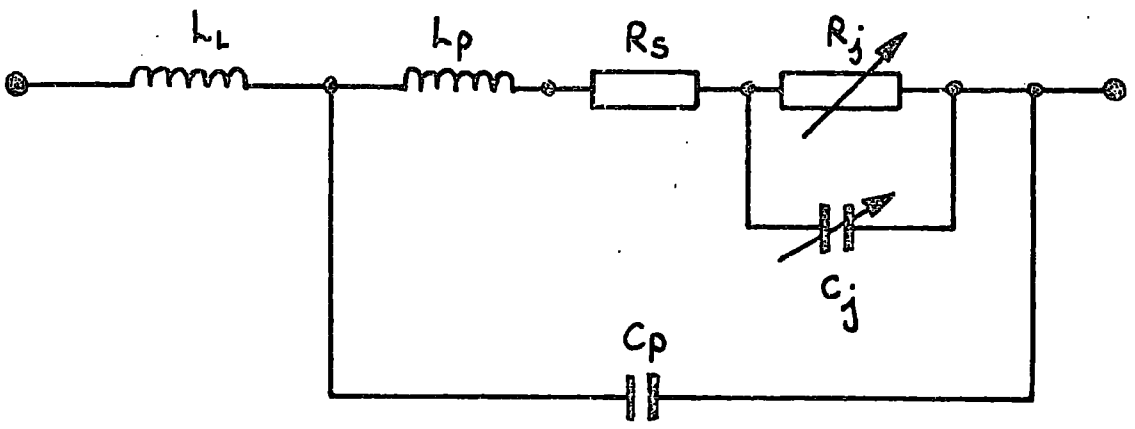

FIG. 3.1. THE EQUIVALENT CIRCUIT OF A MIXER DIODE.

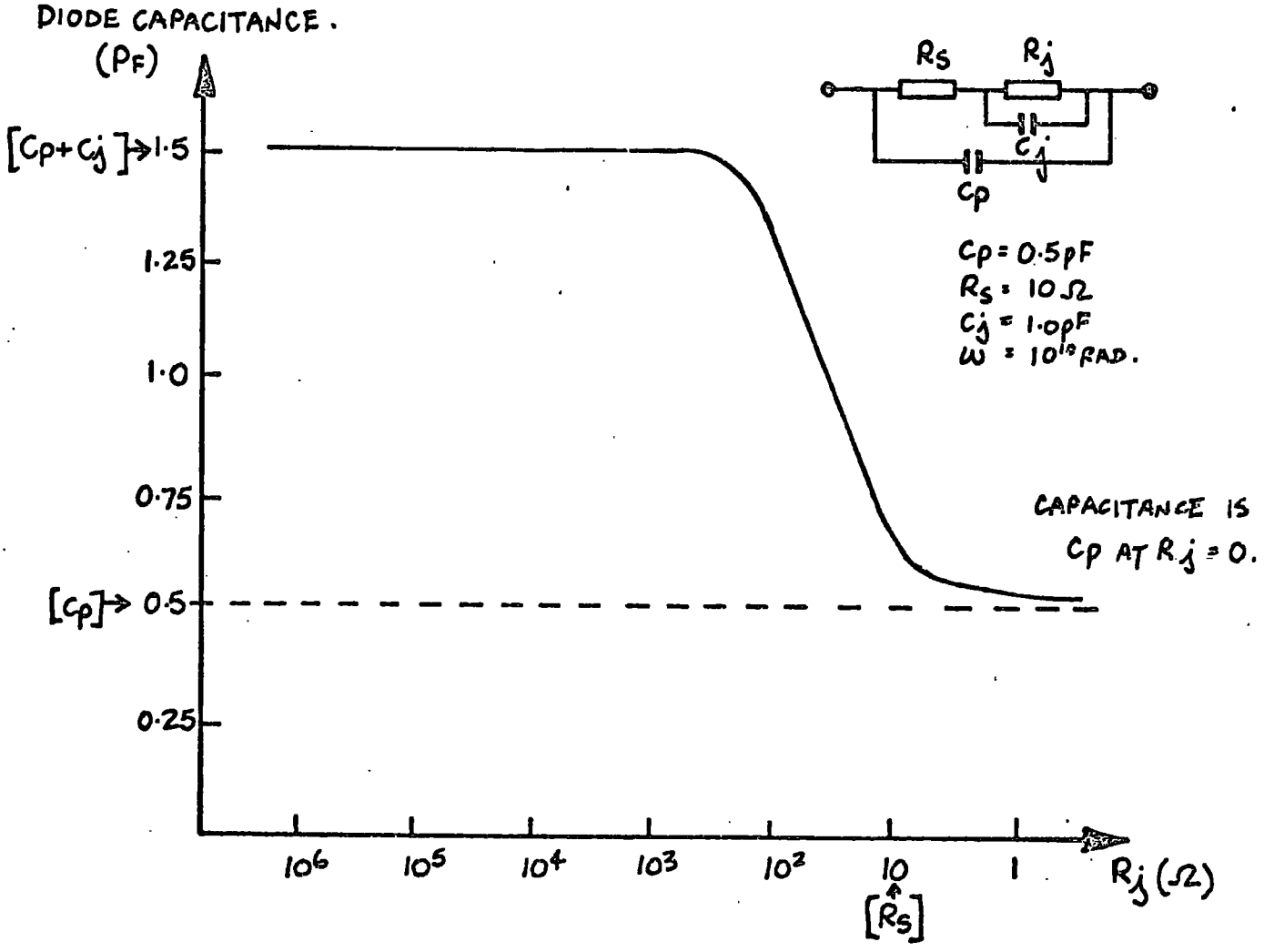

FIG. 3.2. GRAPH OF THE DIODE CAPACITANCE AS A FUNCTION OF R_j, FOR C_j A CONSTANT.

C_j is the voltage-dependent capacitance of the junction

The reactance of the parasitic inductances (L_ℓ and L_p) is in most cases much lower than the magnitude of the other components and these inductances are generally omitted in simplified equivalent circuits. Assuming this, the admittance of the diode at any point of the characteristic is given by:

$$Y_d = \frac{R_s + R_j + \omega^2 C_j^2 R_j^2 R_s + j\omega C_j R_j^2}{(R_s + R_j)^2 + \omega^2 C_j^2 R_j^2 R_s^2} + j\omega C_p \qquad \ldots 1$$

The above equation can be also expressed in a general form as:

$$Y_d = G_d + j\omega C_d \qquad \ldots 2$$

where, G_d is the diode conductance

and C_d is the diode capacitance

If typical values are now inserted for the constituent components of the diode and C_j is assumed to be voltage independent then the variation of the equivalent diode capacitance (C_d) can be found as a function of R_j; this is shown in Fig. 3.2. In the particular case chosen the diode capacitance approaches the value of the package capacitance for $R_j \gg R_s$. If $R_j \gg R_s$ (i.e. at low values of forward current) the diode conductance is given by:

$$G_d = \frac{\frac{1}{R_j} + \omega^2 C_j^2 R_s}{1 + \omega^2 C_j^2 R_s^2} \qquad \ldots 3$$

In most practical cases, neglecting $\omega^2 C_j^2 R_s^2$ with respect to unity, yields an error less than 5%. Also, for some mixer diodes (eg. GaAs and certain Si Schottky-barrier diodes), $\frac{1}{R_j} \ll \omega^2 C_j^2 R_s$. In such cases the equivalent diode slope resistance at the origin is given by $\frac{1}{\omega^2 C_j^2 R_s}$. It can be readily seen that if care is not taken in selecting a diode with low values of C_j and R_s for high frequency applications, its equivalent slope resistance at the origin will not be r_b but some greatly reduced value.

When considering Schottky-barrier diodes, used in most mixer circuits, the variation of depletion layer capacitance is small and to a first approximation may be neglected. For practical l.o. drive levels the diode capacitance may be considered, to a good approximation, as being the sum of the package and junction capacitances at zero bias voltage.

The theoretical semiconductor-diode equation has been shown not to accurately represent the forward current-voltage law of practical diodes, especially for relatively high levels of forward current. The departure from theory may be partially accounted for by the presence of a series resistance and to a lesser extent, in Schottky-barrier diodes, by the image force lowering of the barrier and an insulating interfacial layer. Instead of introducing this series resistance into the diode law, some workers[2,3] have chosen to introduce an empirically derived 'ideality factor' into the theoretical diode equation. These equations are generally accurate over only limited ranges of diode current.

Kulesza[1] has found from his work on point contact diodes that, for a low frequency equivalent circuit of the diode, the forward V/I characteristic is given by eqn. 1 (Chapter 2). Both point-contact and Schottky-barrier diodes have been shown to obey this V/I law to within 2 or 3 percent, and, therefore, this is the law which is assumed in the analysis.

3.2 Measurement Techniques

3.2.1 Introduction

In the following paragraphs a number of techniques are described for measuring the diode constants. The results of these measurements are given later on, in Chapter 5, when the practical mixer circuit is considered.

3.2.2 Diode d.c. Forward Characteristics

The object of these measurements was to find the constants r_s and I_s in the practical diode eqn. 1 (Chapter 2). The current through the diode was measured on an ammeter and the voltage across the diode was measured using a high-impedance voltmeter. Average values for r_s and I_s were obtained by taking several such pairs of readings. The slope resistance at the origin (r_b) is obtained when $I = 0$ in eqn. 1 (Chapter 2), i.e.:

$$r_b = \frac{kT}{qI_s} \qquad \ldots 4$$

3.2.3 Pulsed Measurements

The method outlined in the previous paragraph gave reproducibly accurate results for the diode parameters r_s and I_s at low values of current. At higher currents because of heating, the diode's V/I characteristics change and errors are introduced. The maximum value of current which gave consistent results coincided approximately with the one which produced the manufacturer's recommended maximum power dissipation for the diode.

If a pulsed method is employed, in which the duty cycle is chosen such that the power dissipated in the diode is much less than the maximum permitted power dissipation, the diode characteristics can be obtained for higher values of current and voltage.

The diode spreading resistance can be determined by introducing a known resistor of approximately the same value as r_s in series with the diode and measuring the pulse amplitude across the diode and the series combination of diode and resistor.

3.2.4 Low Amplitude a.c. Measurements

This method was devised to give a direct experimental determination of the diode slope resistance at the origin, r_b. Care was taken that no d.c. current could flow; thus removing any possibility of biasing the diode. The experimental circuit is shown in Fig. 3.3. A high value resistor of approximately 10MΩ was connected in series with the diode. The slope resistance at the origin is then given by the potentiometer ratio. A low frequency (approximately 100 Hz) was chosen for the a.c. signal so as to reduce the effect of parasitic capacitances.

3.2.5 The Measurement of the Diode Capacitance by a Bridge Method

The aim was to measure the diode capacitance at the origin i.e. I = 0. A universal bridge, Wayne Kerr type B221, was available, which unfortunately produced a voltage of approximately 5V peak-to-peak across the terminals. In order to reduce this voltage and to prevent any d.c. current flowing through the diode, a small capacitor of about 0.5 pF was placed in series with the diode. The bridge operated at an angular frequency of 10^4, and thus the reactance of this capacitance was in the order of 2×10^8 .

The equivalent circuit at the terminals of the bridge is shown in Fig. 3.4. For a bridge which measures the impedance as a series equivalent R and X :

$$r_b = \left\{ \frac{R^2 + X'^2}{R} \right\} \qquad \ldots 4a$$

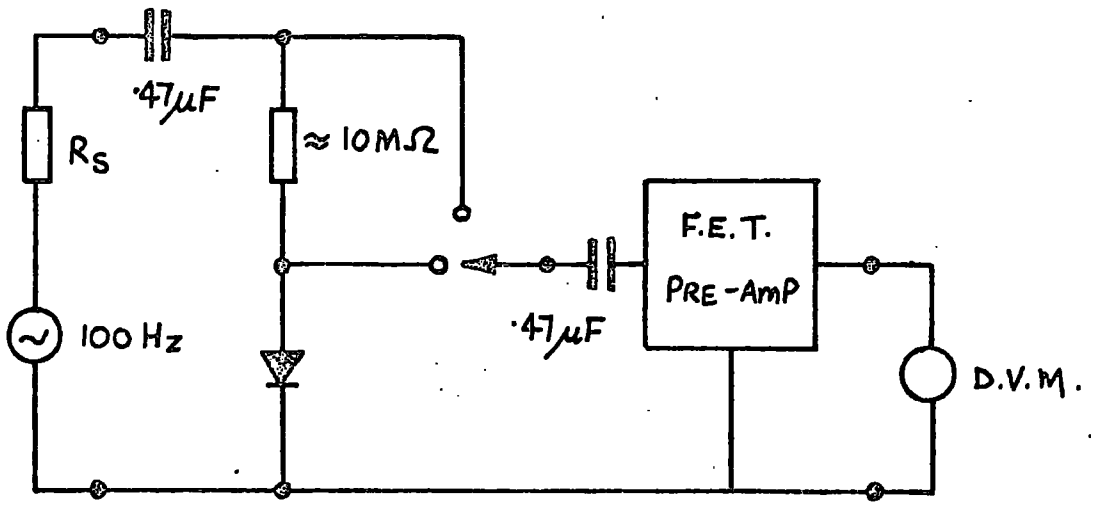

FIG. 3.3. APPARATUS FOR MEASUREMENT OF r_b.

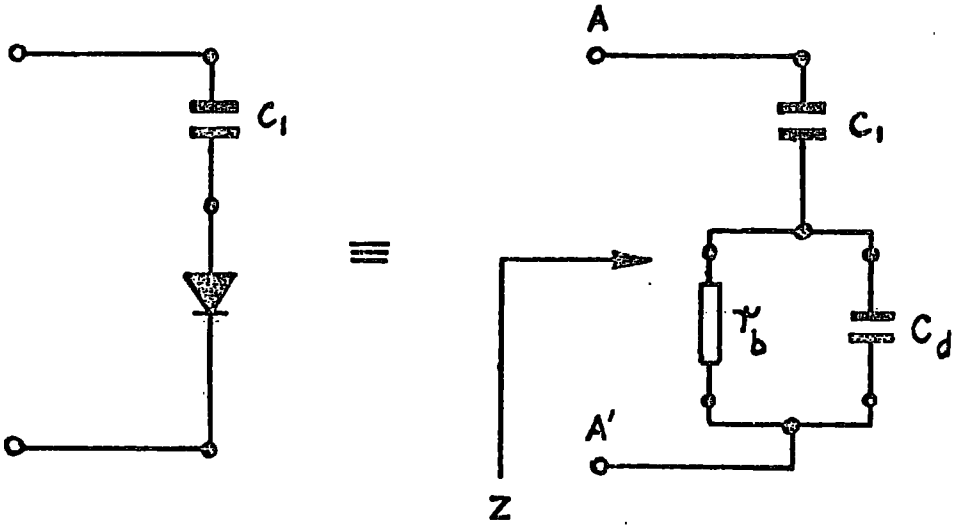

FIG. 3.4. EQUIVALENT CIRCUIT CONSIDERED IN SECTION 3.2.5.

$$C_d = \left\{ \frac{X'}{(R^2 + X'^2)} \right\} \quad \ldots 4b$$

where

C_d = diode capacitance

$$X' = X - \frac{1}{\omega C_1} = \frac{\omega C_d r_b^2}{1 + \omega^2 C_d^2 r_b^2}$$

C_1 = value of small capacitance placed in series with the diode

For a bridge which gives the impedance as a parallel combination of conductance (G) and capacitance (C), the following substitutions are made in eqns. 4a and 4b.

$$R = \left\{ \frac{G}{G^2 + \omega^2 C^2} \right\} \quad \ldots 5a$$

$$X' = \left\{ \frac{\omega C}{G^2 + \omega^2 C^2} - \frac{1}{\omega C_1} \right\} \quad \ldots 5b$$

This method gives a precise and reproducible measurement of the diode capacitance, as the accuracy is primarily determined by that of the bridge.

3.2.6 C/V Characteristics

Two different types of C/V plotters have been constructed in this department, and experiments were conducted using both to determine the characteristics of the Schottky-barrier mixer diodes. The capacitance-voltage law of such junction diodes is given by:

$$C_d = C_p + \frac{C_{jo}}{(1 - \frac{V}{\phi})^n} \quad \ldots 6$$

where

C_p and C_d have been described previously

C_{jo} is the junction capacitance at zero bias

ϕ is the contact potential of the metal and semiconductor

n is a constant

By plotting a graph of $\log_{10} \left(\frac{C_{jo}}{C_d - C_p} \right)$ against $\log_{10} (1 - \frac{V}{\phi})$; 'n' is obtained from the slope.

3.2.7 Microwave Measurements

The aim of this method was to obtain the parasitic diode inductance and capacitance (at zero bias voltage). Two published works[4,5] have been found to be of particular relevance to the measurements of mixer diodes at microwave frequencies.

A diagram of the apparatus is shown in Fig. 3.5. It was important that no d.c. current should flow through the diode and thus bias it. The fixed 12dB attenuator had no d.c. path to earth, as most thin film attenuators do, as it relied for its operation on the loss of a section of coaxial line.

At the start of the project a V.S.W.R. amplifier was not available and thus an alternative method of V.S.W.R. measurement was found. The diode impedance is high relative to the 50Ω line and thus the V.S.W.R. is also high. The pattern of detected output from the slotted line is shown in Fig. 3.6. Assuming that the detector is used in the "square law" region and $\left(\frac{V'}{V\,min}\right)^2 = 2$ then:

$$\text{V.S.W.R.} = \left\{ 1 + \frac{1}{\sin^2 \frac{\pi d}{\lambda_g}} \right\}^{\frac{1}{2}} \quad \ldots 7$$

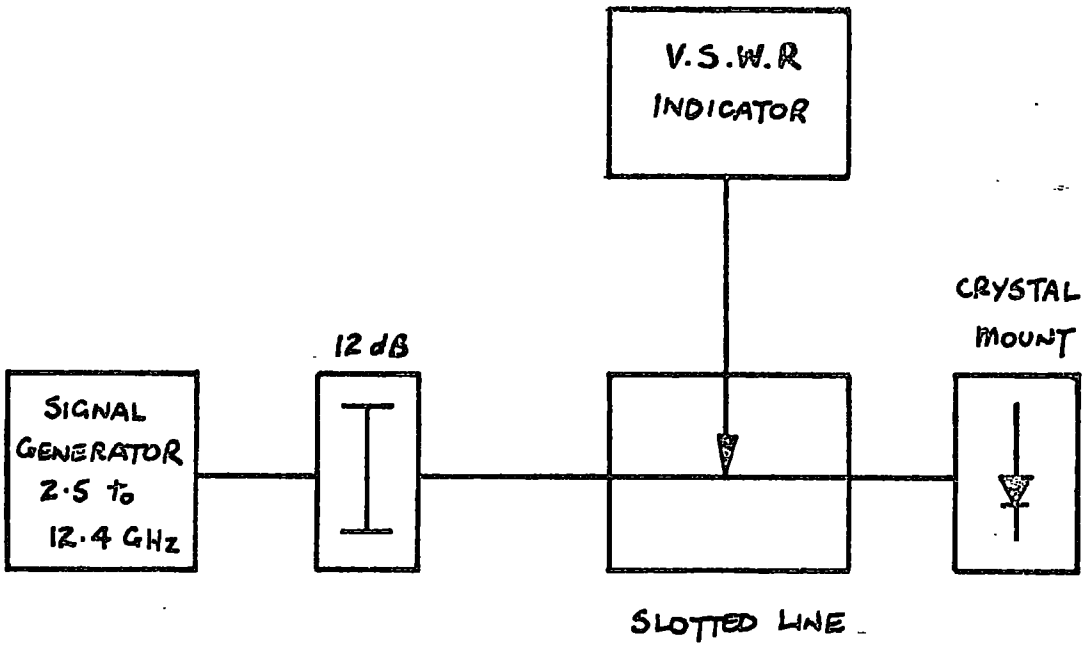

FIG. 3.5. MICROWAVE DIODE MEASUREMENT.

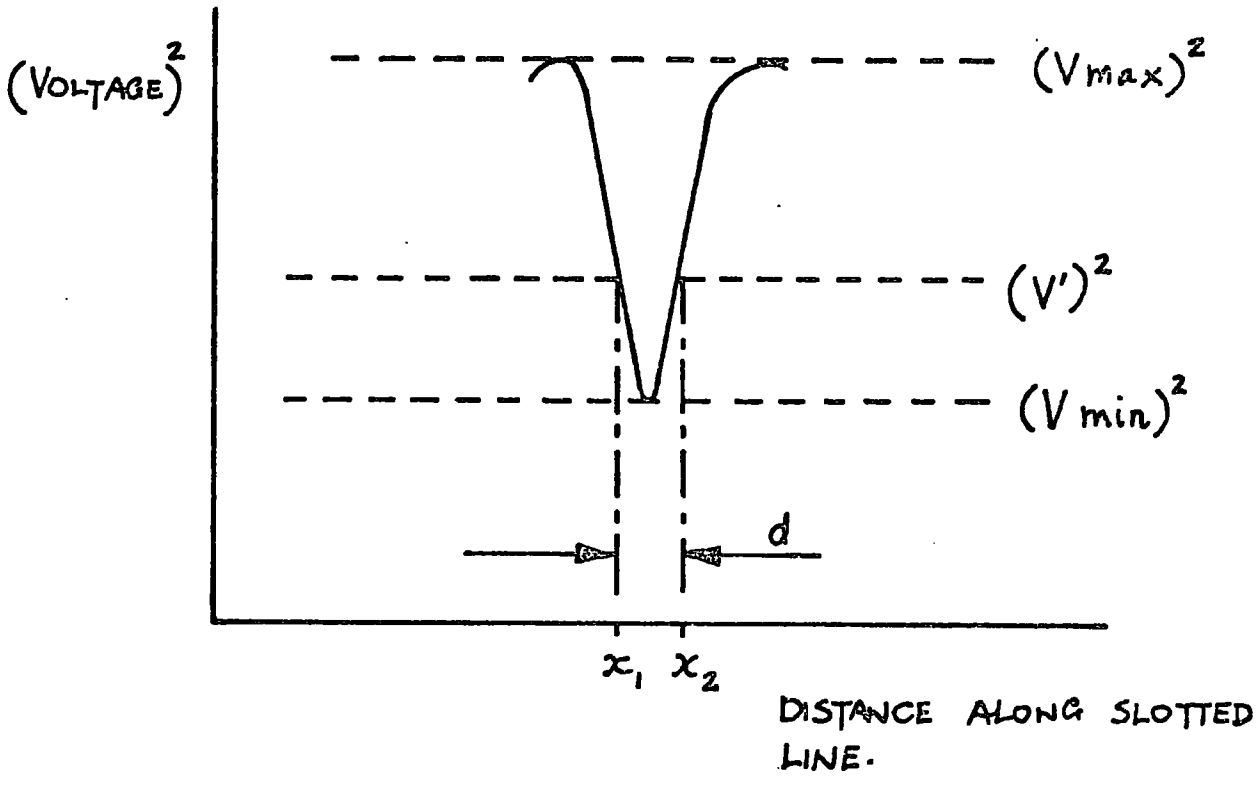

FIG. 3.6. MEASUREMENT OF HIGH V.S.W.R.

d is defined in Fig. 3.6

λ_g is the wavelength

This together with the phase information, obtained by shorting out the diode, is plotted on a Smith's chart.

3.3 Conclusion

The results of these measurement techniques will follow in Chapter 5, where specific diodes will be discussed together with the practical mixer circuit.

As a conclusion to this chapter the merits and limitations of each measurement now will be discussed.

The accuracy obtained for the values of r_b and r_s from the forward d.c. characteristics (see 3.2.2) can be better than 5% for calculations based on three points. The disadvantage of this method is that in order to obtain a high degree of accuracy a larger number of readings must be taken, which results in an equally large number of calculations. However, a computer can be used to process the data if these large number of points are required for high accuracy.

The experimental methods outlined in 3.2.3 and 3.2.4 were carried out to obtain results for r_s and r_b respectively, and to act as verification of the results given in the previous method. The pulsed method was found to produce localised heating effects which distorted the pulse shape and also resulted in non-repeatable results. In the low amplitude a.c. method stray capacitances are present at the input of the F.E.T. amplifier, across the 10 MΩ resistor and across the diode. These have an effect even when the frequency of measurement is low.

Thus it is considered that the forward d.c. measurements give the most accurate and reproducible method of obtaining r_b and r_s.

To obtain the diode capacitance at zero bias the measurement must be conducted at a low frequency in order that the parasitic diode inductances

can be considered negligable. The bridge method gave a reliable measurement of the diode capacitance. The accuracy is limited by that of the bridge.

The measurement of the diode capacitance with bias voltage was to give an indication of the variation of diode capacitance with voltage. The capacitance at zero bias could not be accurately determined from this method as:

(a) it was difficult to calibrate the instrument accurately

(b) the zero voltage point was not readily discernable

Two important results can be obtained from the microwave measurements. Firstly, the parasitic reactances present in the diode can be determined and the usefulness of the diode for mixer applications quickly assessed. Secondly, the slope resistance at the origin at microwave frequencies can be obtained from the Smith's Chart. As explained at the beginning of this chapter the value obtained at high frequencies may be different than that obtained at lower frequencies. The V.S.W.R. values enccuntered in these measurements are high due to the high impedance of the diode as compared to the 50 Ω of the coaxial measuring system. The diode impedance may be more accurately measured using a slotted line, if a $\frac{\lambda}{4}$ transformer is placed between the end of the line and the diode. A twin line of 100 Ω characteristic impedance was constructed and the V.S.W.R. measured at its input when terminated with a diode. The main disadvantage of this measurement is that only one frequency may be used, for which the length of the line is $\frac{\lambda}{4}$.

CHAPTER 4

THE ANALYSIS OF A LATTICE MIXER WITH DIODE CAPACITANCE PRESENT

4.0 Introduction

In this chapter a narrow-band open-circuit lattice mixer is analysed for the case when parasitic diode package capacitance is present.

Before the analytical work is presented, some methods of constructing equivalent circuits of lattice networks will be considered. These equivalent circuits are useful when carrying out analyses of lattice networks in general, and have a particular importance when used in the analysis of the lattice mixer when parasitic reactances are included.

Early published work on the effect of diode capacitance on the performance of low-loss frequency changers will be briefly examined.

4.1 The Construction of Equivalent Circuits of Lattice Networks

4.1.1 Linear Circuits

In the search for equivalent circuits of lattice networks, Bartlett's theorem, in its simplified form, has been found to be of considerable use.

Bartlett's theorem,[1] sometimes called the bisection theorem, was originally applied to an artificial line section (an iterative network) within which there is a pair of terminals such that the network may be equated to two equal asymmetric networks placed back to back (Fig. 4.1). If one half is removed, the impedance of the remaining network measured at the terminals T_1 T_2 is:

$Z_o \tanh \frac{\theta}{2}$ if T_1' T_2' is shorted $= Z_{sc}^{\frac{1}{2}}$

$Z_o \coth \frac{\theta}{2}$ if T_1' T_2' is open circuit $= Z_{oc}^{\frac{1}{2}}$

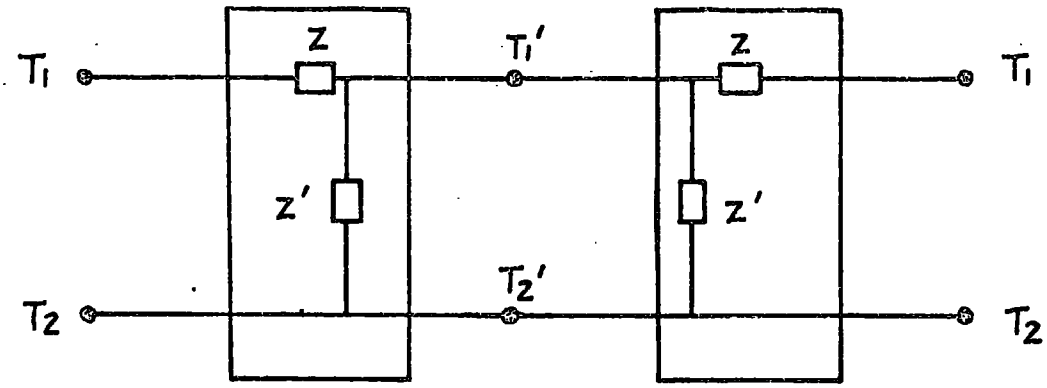

FIG. 4.1. BARTLETT'S ITERATIVE NETWORK.

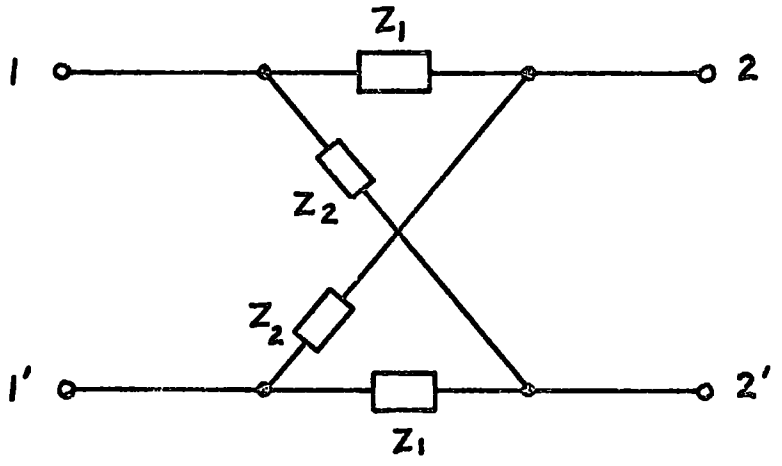

$Z_2 = Z_{oc}^{1/2}$

$Z_1 = Z_{sc}^{1/2}$

FIG. 4.2. MONTGOMERY'S SIMPLIFICATION.

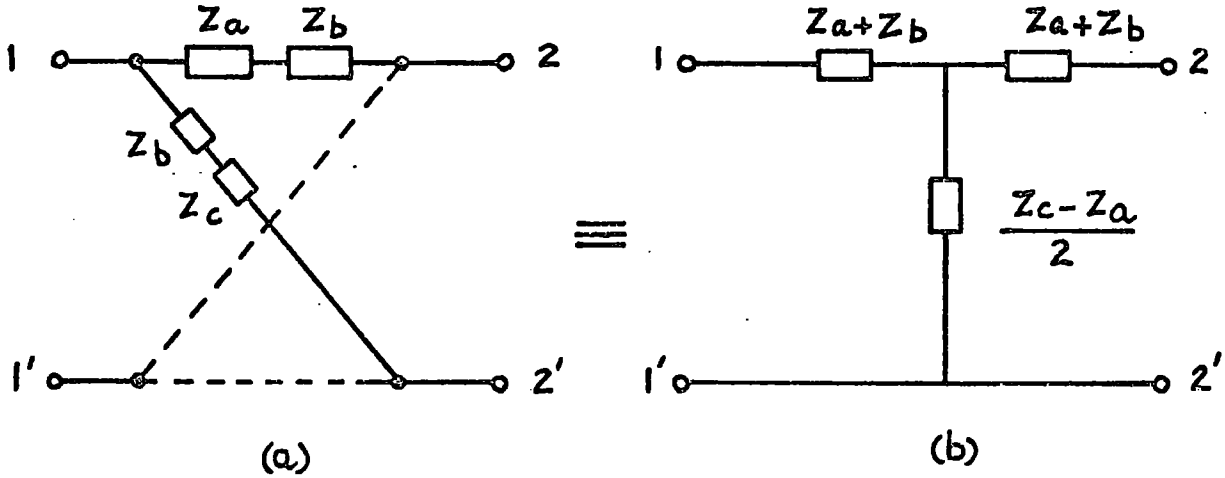

FIG. 4.3. 'T' EQUIVALENT OF THE LATTICE.

where Z_o and θ are the characteristic impedance and propagation constant of the artificial line section, respectively.

Montgomery[2] has applied Bartlett's theorem to a general symmetrical network and has derived the lattice equivalent in terms of $Z_{oc}^{\frac{1}{2}}$ and $Z_{sc}^{\frac{1}{2}}$. The result is shown in Fig 4.2. Using this transformation any symmetrical network may be replaced by an equivalent lattice network; each element will be physically realizable as $Z_{oc}^{\frac{1}{2}}$ and $Z_{sc}^{\frac{1}{2}}$ are obtained directly from the components of the symmetrical network.

Brune[3] has obtained the same result as above for the lattice equivalent of a symmetrical network. He has derived a number of other network equivalents of the general symmetrical network.

The inverse of this theorem, i.e. equating a lattice network to an equivalent T, also has applications. Fig. 4.3 shows this important transformation. A further application of the bisection theorem yields the networks shown in Fig. 4.4(a) and Fig. 4.4(b).

Thus a series element common to each arm of the lattice may be brought outside the lattice and placed in series with the input and in series with the output. By the same argument a shunt element common to each arm of the lattice may be brought out of the lattice and placed symmetrically at its input and output as shown in Fig. 4.5.

4.1.2 Non-Linear Switching Circuits

Tucker[4] has considered a lattice of switches in which each switch has a series loss resistance, r_s, as shown in Fig. 4.6(a). The polarity of the pairs of switches are reversed with a period of $\omega p/2\pi$. The components of the loss resistance may be taken outside the lattice and be placed at the input and output of the lattice as shown in Fig. 4.6(b).

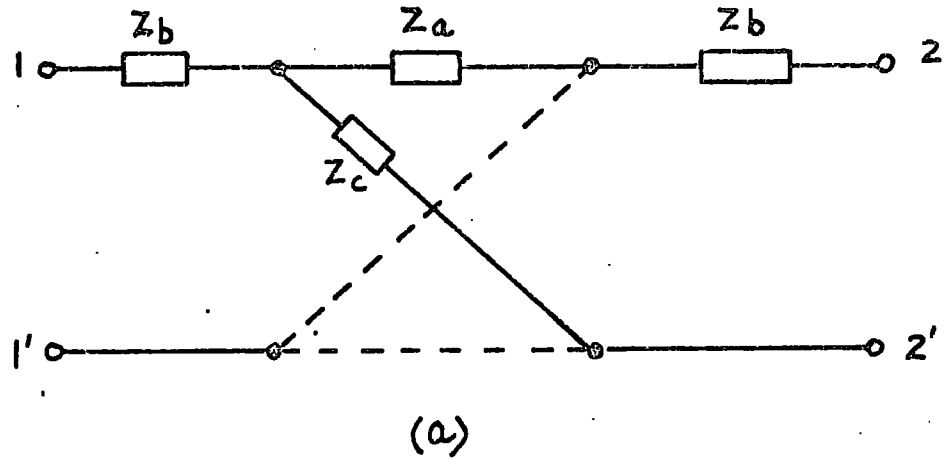

(a)

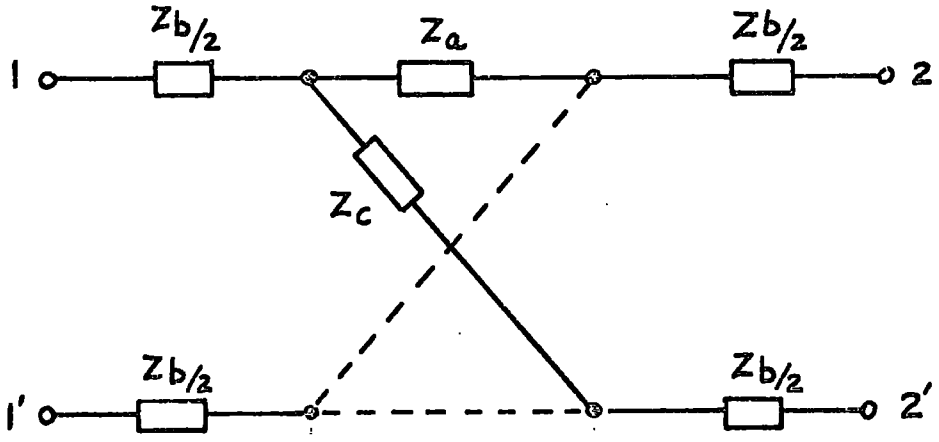

(b)

FIG. 4.4. FURTHER APPLICATION OF THE BISECTION THEOREM.

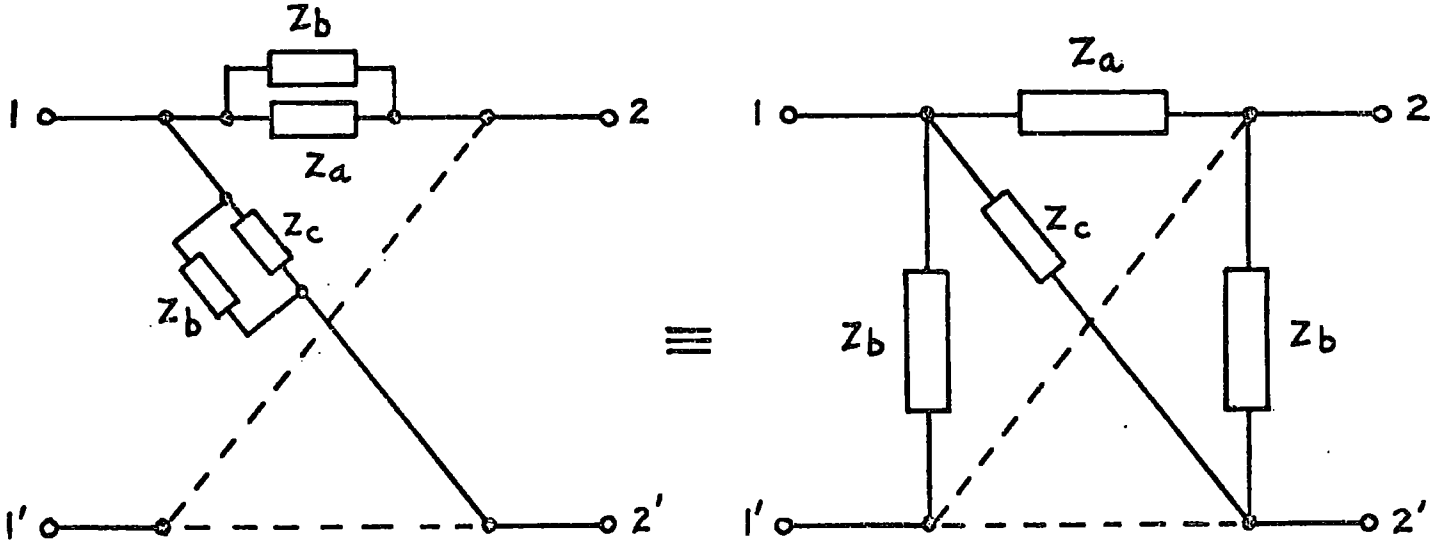

FIG. 4.5. THE BISECTION THEOREM FOR SHUNT CAPACITANCE.

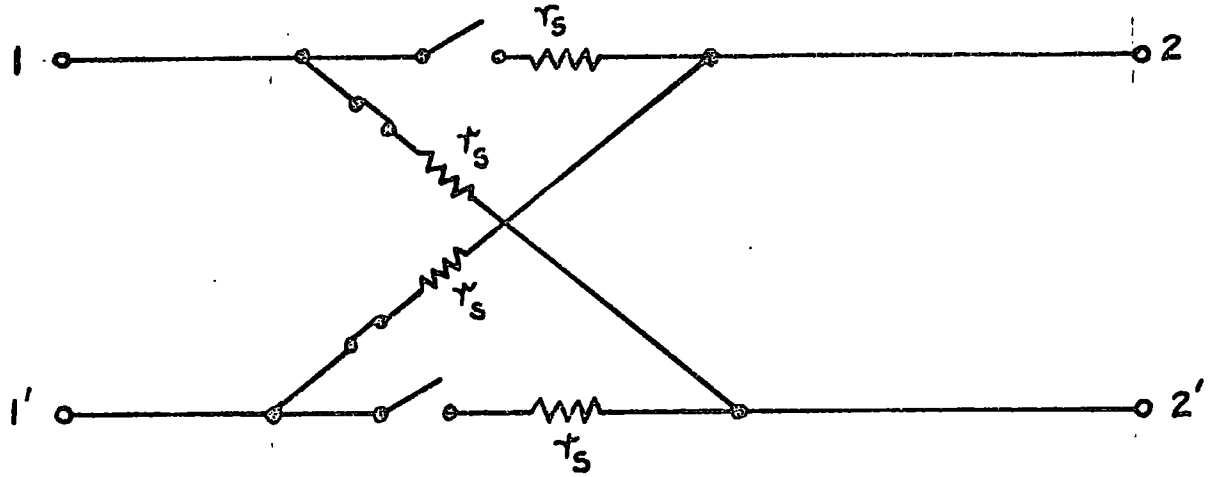

(a)

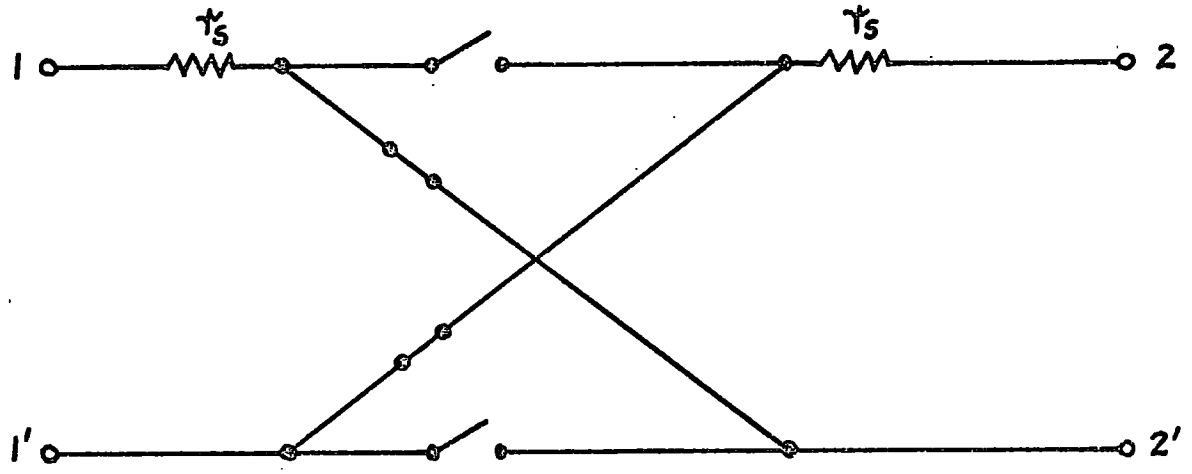

(b)

FIG. 4.6. THE BISECTION THEORM APPLIED TO A LATTICE OF SWITCHES.

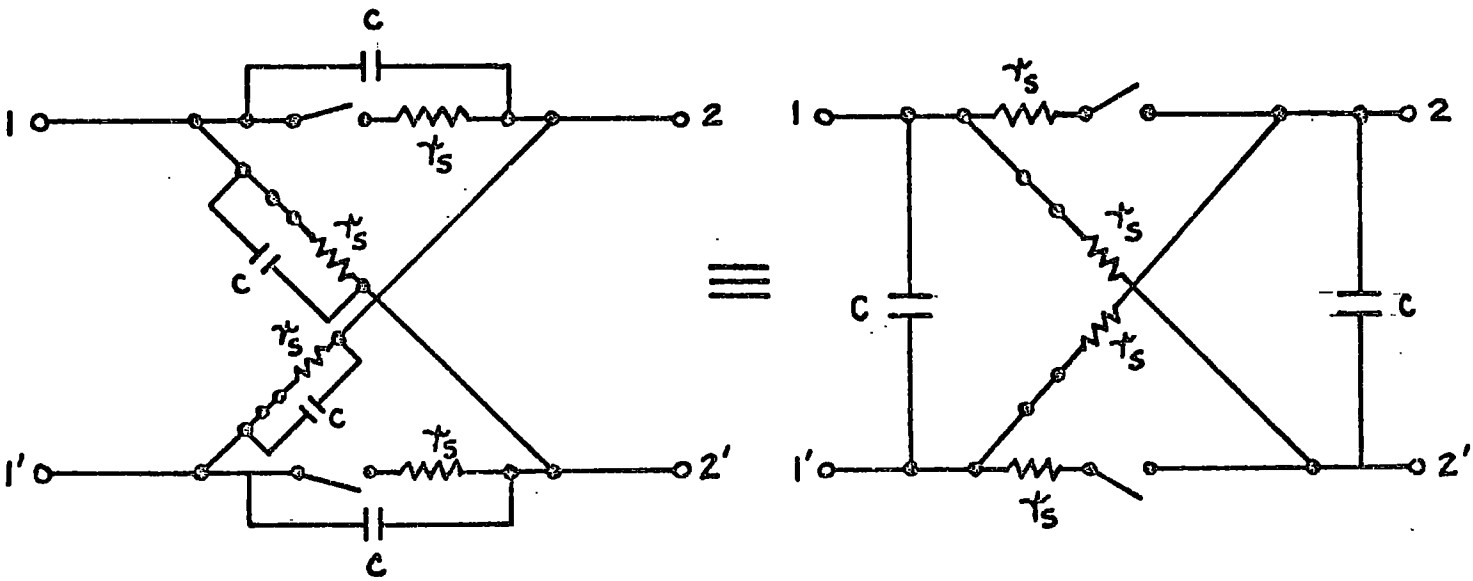

FIG. 4.7. THE BISECTION THEORM WHEN SHUNT CAPACITANCE IS PRESENT.

If there is a capacitor shunted across both the switch and the series resistance, this can be brought outside of the lattice and placed across both the input and output terminals as shown in Fig. 4.7.

This last equivalent circuit is not applicable when the capacitor is situated across the switch only, because during one half cycle the capacitor is shorted out. The resultant capacitance across the input and output terminals in this case will not be C, but rather some function of C and the switching frequency.

4.2 Early Work on the Effects of the Diode Capacitance

Previously published work of the effects of diode capacitance on low-loss frequency changes will be reviewed.

Kruse[5] and Belevitch[6] have analysed low-loss modulator circuits with parasitic diode capacitance present. In general, their analyses have taken the form of an additional corollary to their original work (assuming purely resistive diodes) and were based on the approximate equivalent circuits of the modulator. Although the details of their work will not be given here, it is thought of interest to discuss their methods of approach.

Kruse has considered a ring modulator with the diode package capacitances present. This is shown in Fig. 4.8(a), the equivalent circuit he considered is shown in Fig. 4.8 (b). He then considered the effect that these capacitors had on the magnitude of the voltages and currents at the input and output of the modulator.

Belevitch analysed a ring modulator in which he considered the diodes to be perfect switches, i.e. zero impedance in the forward direction and infinite impedance in the reverse direction, the lattice shunted on either side by a capacitance C. This he brought outside the lattice and placed symmetrically at the input and output of the lattice (Fig. 4.9). He calculated the change in c.p.l. due to the

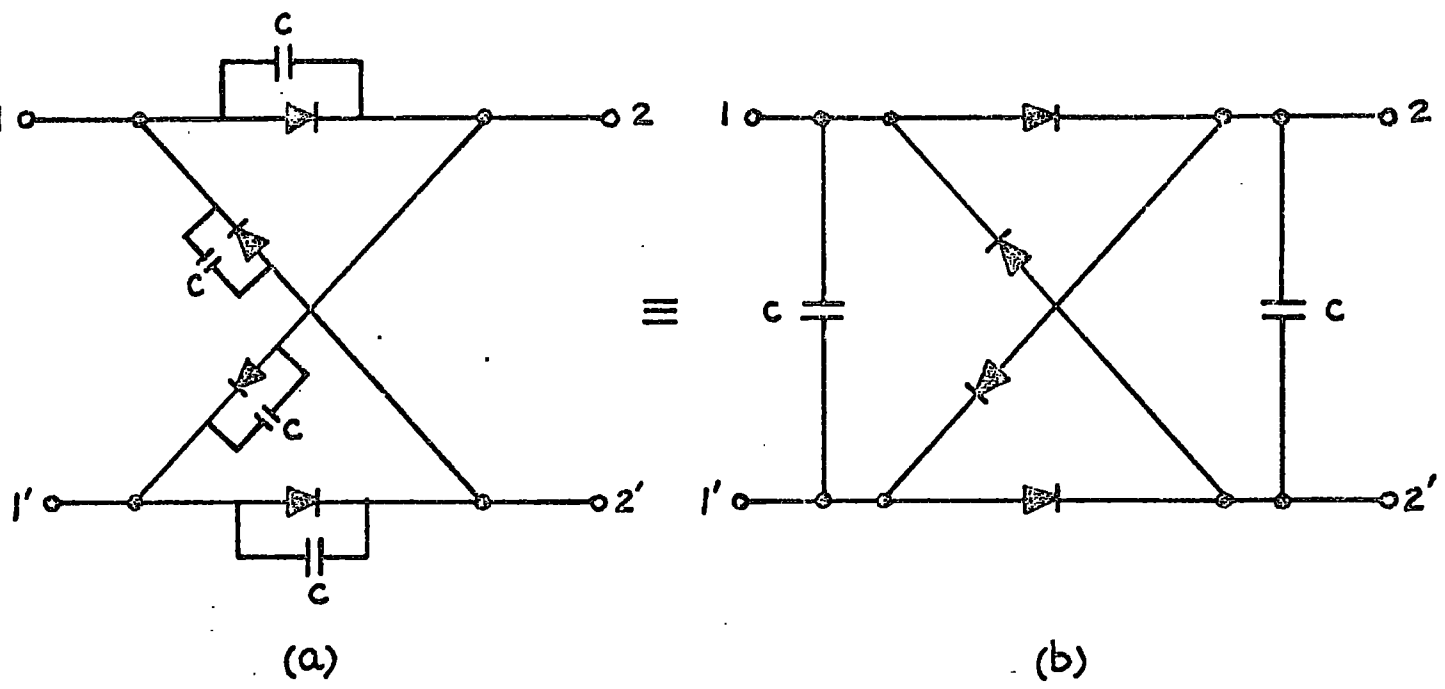

FIG. 4.8. THE EQUIVALENT CIRCUIT USED BY KRUSE.

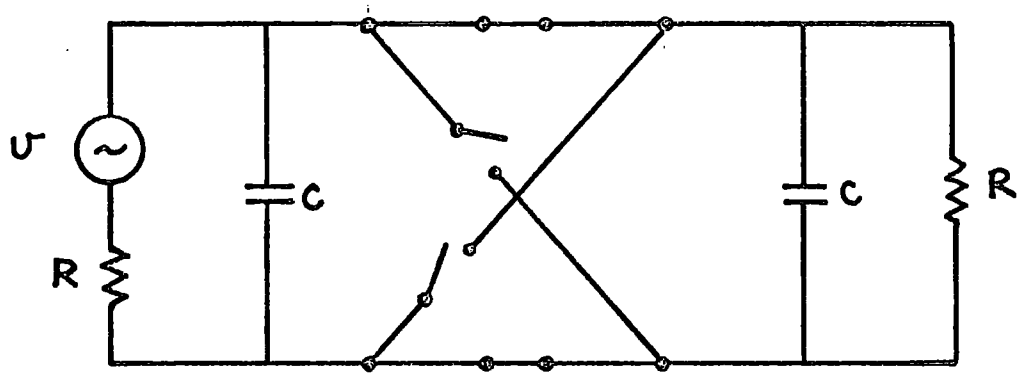

FIG. 4.9. THE EQUIVALENT CIRCUIT USED BY BELEVITCH.

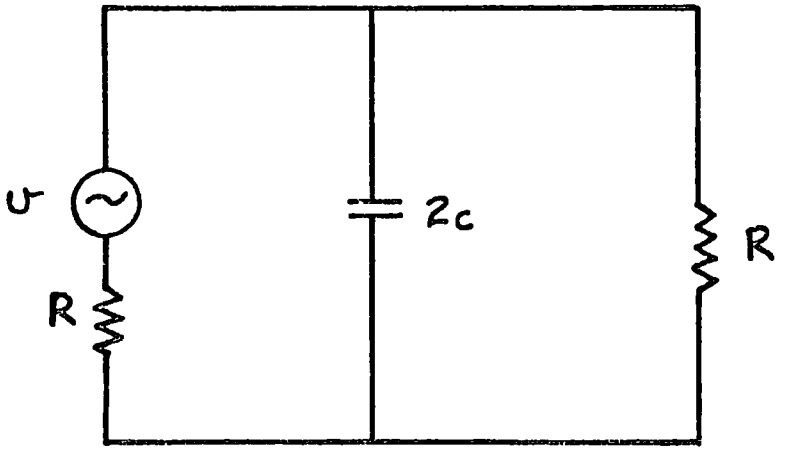

FIG. 4.10. THE EQUIVALENT OF Fig 4.9.

presence of this capacitor (2c) present at the input (Fig. 4.10). The major limitation to his analysis was that there was no way of introducing practical diode current-voltage laws into the expressions.

Belevitch[7] has also considered the effect of diode parasitic capacitance on the shunt bridge modulator. In this analysis he considered the capacitance due to each diode (C) to be equivalent to one capacitor (C) shunted across the output of the modulator at the useful sideband frequency (Fig. 4.11). The component values were so arranged that the whole circuit including the parasitic capacitance had a parallel resonance at ωp and a high impedance at $\omega p - \omega q$.

In conclusion, low-loss frequency changer circuits have been previously analysed when diode parasitics are present. The approach that is presented here differs from the above in that it employs the practical diode voltage-current laws and assumes a sinusoidal current drive at the local oscillator frequency.

4.3 The Diode Incremental Impedance

In Chapter 2 the general theory of a lattice mixer was presented, in which it was assumed that no diode parasitic reactances were present. This l.f. equivalent circuit of a diode may be successfully used in mixers up to frequencies in the lower radio frequencies using modern practical mixer diodes with the package capacitances $\leqslant$ 1pF and $r_s' \leqslant 10^{-5}$. At higher frequencies, in the U.H.F. and microwave bands, the parasitics cannot be ignored when selecting diodes for a mixer application.

The conversion power loss (c.p.l.), the optimum mixer input impedance at the signal frequency, $Z_i(opt)$, and the optimum mixer load impedance at the i.f. frequency, $Z_L(opt)$, all will be functions not only of the diode parameters, r_s and r_b, and the normalised current drive level X, but will also be functions of these reactive parasitics.

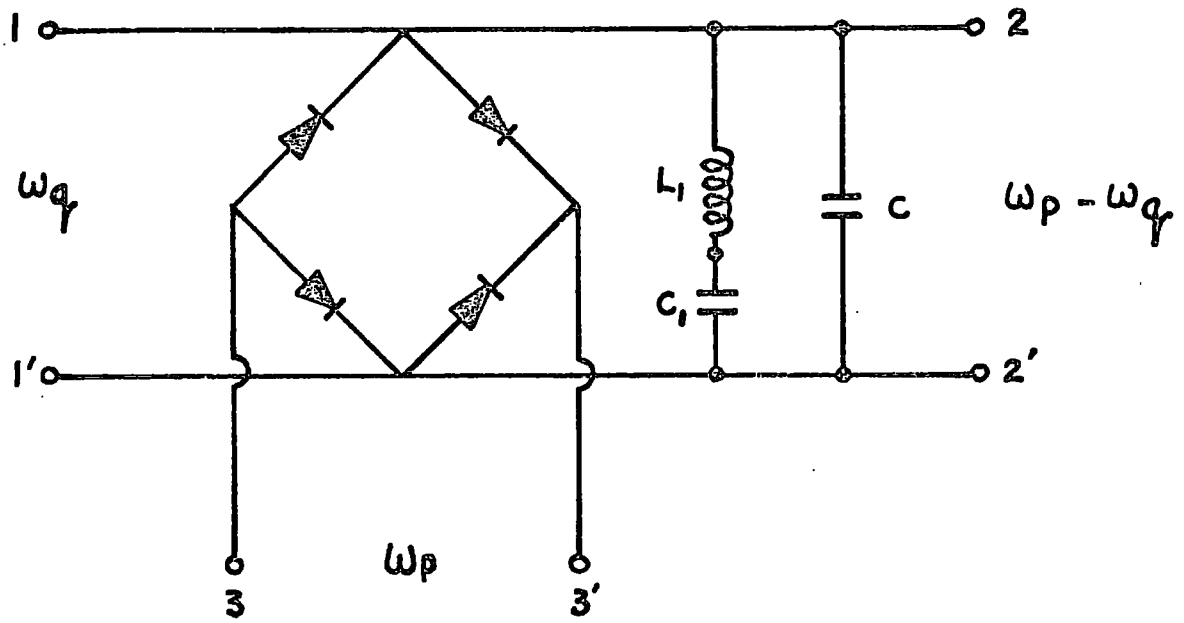

FIG. 4.11. THE SHUNT MODULATOR.

Thus to obtain a mixer with a low c.p.l. at high radio frequencies these optimum terminating impedances must be determined with reactive effects taken into account.

The diode high frequency equivalent circuit was discussed in the last chapter. For a modern Schottky-barrier diode the package capacitance falls in the range from 0.1pF to 1.5pF depending on the geometry of the package.

The zero bias junction capacitance is approximately 0.5pF to 1.0pF and is to a great extent a function of the metal-semiconductor junction. The package inductance depends on the diameter and length of the wire used to make the contact with this junction and has a value ranging from 2 nH to 5 nH for a typical diode. Added to this inductance there is an inductance due to the package (if cartridge or strip-line type) or to the diode leads (if appropriate).

When a non-linear element is used in a frequency converting application its incremental (or slope) impedance is perhaps the most important parameter in the analysis of the circuit.

It is assumed, in the following, that the longitudinal series resonance at the local oscillator frequency (ω_p) is still maintained. The current through each time-varying impedance will, therefore, approximate to being sinusoidal during the forward-conducting half cycle and zero in the reverse direction. It will be shown in section 4.8 that under these conditions, and when the package capacitance is considered, the local oscillator power, expressed as a function of X and r_s', is the same whether there is diode capacitance present or not, provided $(2\omega_p C_p r_s)^2 \ll 1$.

In the following three paragraphs various equivalent circuits are proposed and expressions derived from the time-varying incremental

impedance. Although the analysis presented here is primarily concerned with the effect of the diode package capacitance, the time-varying incremental impedances for the cases of the junction capacitance and the diode inductance are also examined.

(a) The Time-Varying Incremental Impedance When the Package Capacitance is Considered

The equivalent circuit is shown in Fig. 4.12(a). It is assumed that the package capacitance appears as a non-varying capacitance across the series combination of the diode spreading resistance and the time-varying incremental resistance of the junction. The resultant impedance is then given as:

$$Z(t) = \frac{r(t)}{1 + j\omega_f C_p r(t)}$$

where C_p is the package capacitance

$r(t)$ is the time-varying incremental resistance, which in the case of a lattice mixer is given by:

$$r(t) = r_s + \frac{r_b}{1 + X(t) + X(t)\, S(t)}$$

and ω_f is the angular frequency component which is specifically being considered (i.e. ω_q, ω_{-1} or ω_{-2}) when appropriate frequency constraints are introduced into the equations containing these time varying impedances.

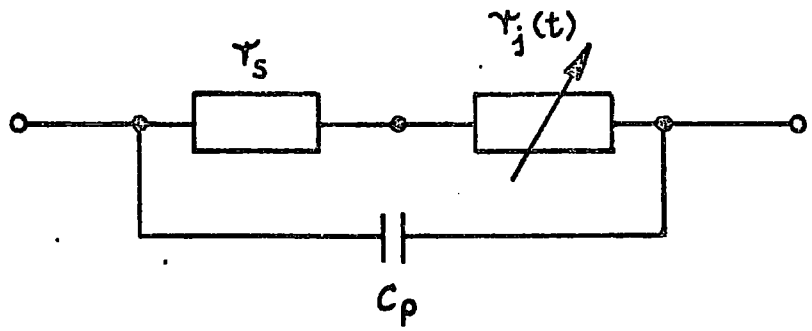

(a)

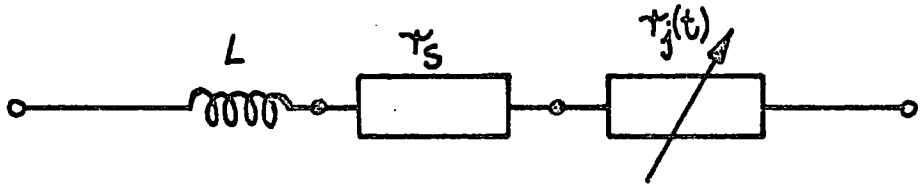

(b)

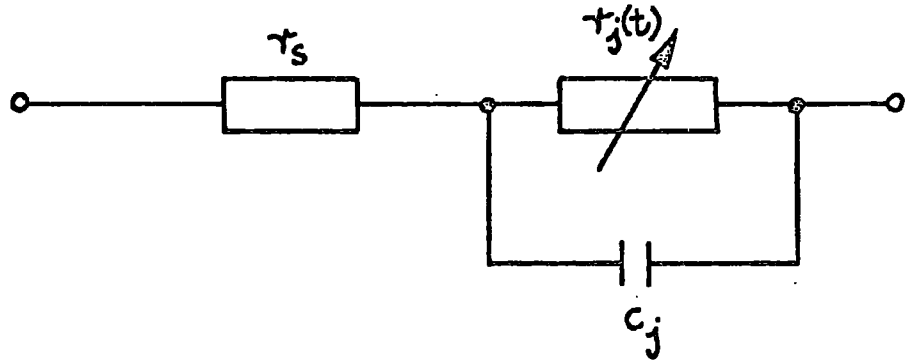

(C)

FIG. 4.12. THE DIODE EQUIVALENT CIRCUITS.

(b) The Time-Varying Incremental Impedance When the Diode Inductance is Being Considered

The non-varying parasitic inductance is considered to be in series with the series combination of spreading resistance and time- varying resistive element of diode, as shown in Fig. 4.12(b).

Then:

$$Z(t) = r(t) + j\omega_f L$$

where L = the diode inductance

By the application of the bisection theorem, the diode inductance can be placed symmetrically at the input and output outside the lattice of diodes. For a narrow-band open-circuit mixer, the inductance at the input may be included in the series resonant circuit at the signal frequency when the mixer is "hot tuned". The magnitude of the inductance present at the output of the lattice is, generally, less than the leakage inductance of the i.f. transformer. Thus because of this and the fact that the reactance is low (in many cases comparable to the spreading resistance of the diode), the presence of diode inductance is usually a second-order effect when considering this type of lattice mixer.

(c) The Time-Varying Incremental Impedance When the Junction Capacitance is Present

In this particular case the junction capacitance is shunting the time-varying resistive element of the diode; the spreading resistance being in series with this combination.

For the diode equivalent circuit considered in Fig. 4.12(c)

$$Z(t) = r_s + \frac{r_j(t)}{1 + j\omega_f c_j r_j(t)}$$

This case is possibly the most difficult to analyse as the incremental time-varying resistive element is varying from r_b down to small values of resistance (which tend to zero for high values of drive, X).

4.4 The Lattice Network Equations

It is assumed that the four diodes are identical and are current-drive at the radian frequency of the local oscillator, ω_p

The time-varying diode incremental resistances $r_+(t)$ and $r_-(t)$ are the same expressions as obtained in Chapter 2, namely:

$$r_+(t) = r_s + r_b \frac{1}{1 + X(t) + X(t)\,S(t)}$$

and

$$r_-(t) = r_s + r_b \frac{1}{1 - X(t) + X(t)\,S(t)}$$

Figs. 4.13 and 4.14 show the basic mixer circuit and the equivalent lattice of four time-varying incremental impedances.

Referring to Fig. 4.15, the equations for the lattice can be written as follows:

$$v_s\left[1 + j\omega_s C\left\{\frac{2r_+(t)\,.\,r_-(t)}{r_+(t) + r_-(t)}\right\}\right] = i_s\left[\frac{2r_+(t)\,.\,r_-(t)}{r_+(t) + r_-(t)}\right] + v_L\left[\frac{r_-(t) - r_+(t)}{r_+(t) + r_-(t)}\right] \quad \ldots 1$$

$$i_L\left[1 + j\omega_L C\left\{\frac{2r_+(t)\,.\,r_-(t)}{r_+(t) + r_-(t)}\right\}\right] = i_s\left[\frac{r_-(t) - r_+(t)}{r_+(t) + r_-(t)}\right] - 2v_L\left[\frac{(1 + j\omega_L C r_+(t))(1 + j\omega_L C r_-(t))}{r_+(t) + r_-(t)}\right] \quad \ldots 2$$

where i_s and v are assumed to be complex; i.e.

$$i_s = \mathcal{R}_e(i_s) + j\mathcal{I}_m(i_s)$$

$$v_L = \mathcal{R}_e(v_L) + j\mathcal{I}_m(v_L)$$

whilst v_s and i_L are restricted to be real

Equating the real and imaginary components in eqn. 1 (Appendix 1) results in two expressions from which we get

<u>at ω_q</u>

$$v_q = r_b A_0 \mathcal{R}_e(i_q) + \frac{A_1}{2}\mathcal{R}_e(v_{-1}) \quad \ldots 3$$

and

$$v_q \omega_q C = \mathcal{I}_m(i_q) + \frac{B_1}{2r_b}\mathcal{I}_m(v_{-1}) \quad \ldots 4$$

The solution of B_1 is given in Appendix 1.

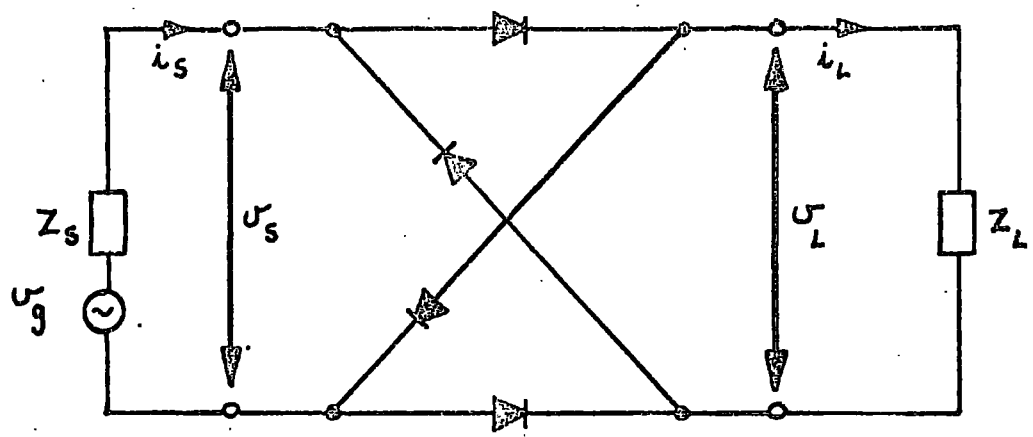

FIG. 4.13. THE BASE MIXER CIRCUIT.

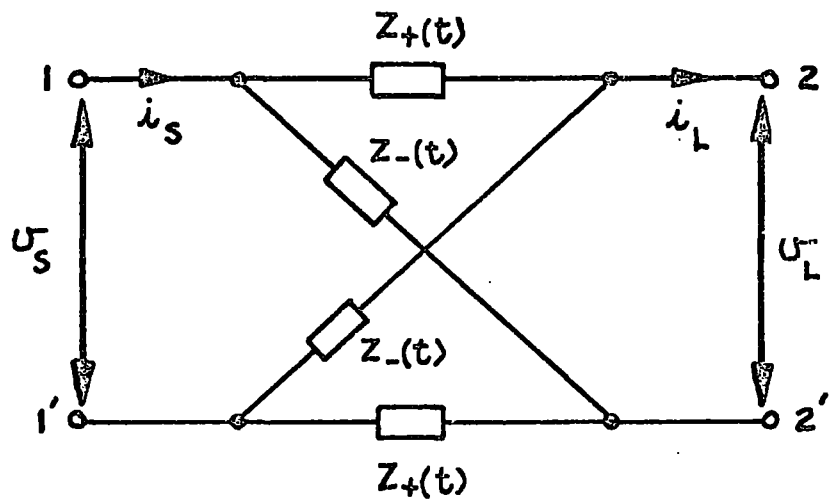

FIG. 4.14. THE NETWORK OF TIME - VARYING. INCREMENTAL IMPEDANCE.

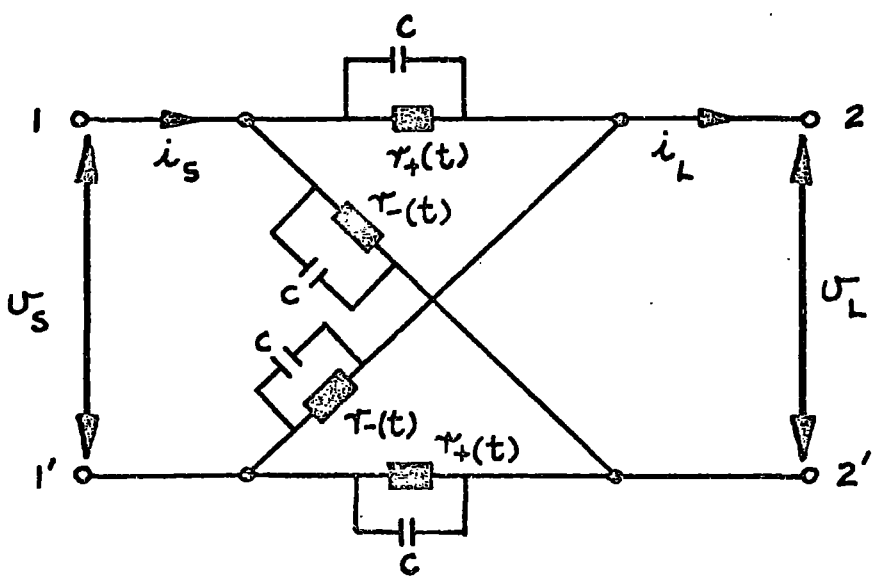

FIG. 4.15. THE MIXER AS A 4 TERMINAL NETWORK.

Similarly on equating the real and imaginary components in eqn. 2

<u>at ω_{-1}</u>

$$i_{-1} = \frac{A_1}{2}\mathcal{R}_e(i_q) - \left\{\frac{A_0'}{r_b} - \omega_{-1}^2 C^2 r_b A_0\right\}\mathcal{R}_e(v_{-1}) + 2\omega_{-1}C\,\mathcal{I}_m(v_{-1}) \qquad \ldots 5$$

and

$$i_{-1}\omega_{-1}C = \frac{B_1}{2r_b}\mathcal{I}_m(i_q) - \left\{\omega_{-1}C\frac{D_0}{r_b}\right\}\mathcal{R}_e(v_{-1}) - \left\{\frac{E_0}{r_b^2} - \omega_{-1}^2 C^2\right\}\mathcal{I}_m(v_{-1}) \qquad \ldots 6$$

The solutions of D_0 and E_0 are given in Appendix 1.

From eqns. 3 to 6, the following relations are obtained:

$$\mathcal{R}_e(v_{-1}) = v_q \frac{2}{A_1}\left[1 - G_i' A_0\right] = (v_q P_1)$$

$$\mathcal{R}_e(i_q) = i_{-1}\frac{2}{A_1}\left[1 + R'A_0' - 2X'\tau_{-1}\right] = (i_{-1} P_2)$$

$$\mathcal{I}_m(v_{-1}) = v_q \frac{2}{B_1}\left[\tau_q - B_i'\right] = (v_q P_3)$$

$$\mathcal{I}_m(i_q) = i_{-1}\frac{2}{B_1}\left[\tau_{-1} + R_L'D_{0\,-1} + X_L'(D_0 - \tau_{-1}^2)\right] = (i_{-1} P_4)$$

where

the input admittance is given as $Y_i = G_i + jB_i$ and

the output impedance as $Z_L = R_L + jX_L$

The other parameters (normalised with respect to r_b) which appear in the previous equations are as follows:

$$\tau_{-1} = \omega_{-1} C r_b \qquad \tau_q = \omega_q C r_b$$

$$B_i' = B_i r_b \qquad G_i' = G_i r_b$$

$$R_L' = \frac{R}{r_b} \qquad X_L' = \frac{X}{r_b}$$

It then follows that

$$G_i' = \frac{P_1 P_2}{R_L'} = \frac{P_2}{\frac{A_1 R_L'}{2} + 2A_0 P_2} \qquad \ldots 7$$

In this last equation the input conductance is expressed in terms of the diode constants (r_s'), the normalised current drive level (X), the normalised susceptance (at the i.f. frequency) of the diode package capacitance present at the output of the lattice (τ_{-1}) and the normalised output impedance.

Similarly,

$$B_i' = \frac{P_3 P_4}{X_L'} = \frac{\tau_q P_4}{\frac{B_i X_L'}{2} + P_4} \qquad \ldots 8$$

4.5 Conversion Power Loss Under Matched Conditions

4.5.1 Conversion Loss

The conversion loss of the mixer is defined as:

$$\frac{\text{Voltage x Current at } \omega_q}{\text{Voltage x Current at } (\omega_p - \omega_q)} = \frac{V_q * i_q}{V_{-1} i^*_{-1}} = \frac{V_q(i_{-1}P_2 + j i_{-1}P4)}{i_{-1}(V_q P_1 + j V_q P3)}$$

$$= \frac{P_2 + jP_4}{P_1 + jP_3}$$

Thus $$|C_L| = \left\{ \frac{P_2^2 + P_4^2}{P_1^2 + P_3^2} \right\}^{\frac{1}{2}}$$

4.5.2 Conversion Power Loss

The conversion power loss (or c.p.l.) of the mixer is defined as:

$$\frac{\text{available input power at } \omega_q}{\text{available output power at } (\omega_p - \omega_q)} = |C_L| \frac{\cos \theta_i}{\cos \theta_L}$$

where

$$\cos \theta_i = \frac{\mathcal{R}e(Y_i)}{|Y_i|} = \frac{P_2}{(P_2^2 + P_4^2)^{\frac{1}{2}}}$$

and

$$\cos \theta_L = \frac{\mathcal{R}e(Z_L)}{|Z_L|} = \frac{P_1}{(P_1^2 + P_3^2)^{\frac{1}{2}}}$$

Thus

$$\text{c.p.l.} = \frac{\mathcal{R}e(V_q * i_q)}{\mathcal{R}e(V_{-1} i^*_{-1})} = \frac{P_2}{P_1}$$

$$= (1 + y) + \frac{K}{R'_L} (1 + y)^2 \qquad \ldots 9$$

where,

$$y = A'_0 R'_L + 2 \tau_{-1} X'_L$$

and

$$K = \left(\frac{2}{A_1}\right)^2 A_0$$

4.6 Optimum Terminations

Differentiating eqn. 9 with respect to y gives:

$$\frac{d(c.p.l.)}{dy} = 1 + \frac{K}{(R'_L)^2}\left\{2R'_L(1+y) - (1+y)^2\frac{dR'_L}{dy}\right\} \qquad \ldots 10$$

The assumption is made that the bisector theorem is valid for the lattice of diodes. A substitution for X'_L is made in terms of R'_L and τ_{-1}; $\frac{dR'}{dy}$ thus being obtained in terms of only R'_L and τ_{-1}.

Equn. 10 is equated to zero and the optimum load resistance found by solving the cubic equation:

$$\left(\frac{1}{\left[R'_L(opt)\right]^3}\right) = \frac{A'_0}{K}\left(\frac{1}{R'_L opt}\right) + \frac{4\tau_{-1}^2}{K} \qquad \ldots 11$$

It can be readily seen from eqn. 11 that when no capacitance is present (i.e. $\tau_{-1} = 0$)

$$R'_L opt = \frac{2}{A_1}\left\{\frac{A_0}{A'_0}\right\}^{\frac{1}{2}}$$

This is the result obtained for the narrow-band open circuit mixer by Kulesza[8].

A solution to eqn. 11 is achieved by Cardan's Method [9], and for $\tau_{-1} > 10$ the solution is as follows:

$$R' opt = \left(\frac{K}{4\tau_{-1}^2}\right)^{\frac{1}{3}} = \left(\frac{A_0}{A_1^2\tau_{-1}^2}\right)^{1/3} \qquad \ldots 12$$

For most practical microwave diodes (i.e. $r_s < 15\Omega$, $r_b > 10^5\Omega$) used in a mixer to produce an i.f. of 30 MH_2, the condition that $\tau_{-1} > 10$ is usually met.

Then

$$X'_{L}(\text{opt}) = \tau_{-1}\left\{\frac{A_0}{A_1^2\,\tau_{-1}^2}\right\}^{\frac{2}{3}} \qquad \ldots 13$$

The other mixer parameters can now be found by the substitution of R'opt into the eqns. 7, 8:

$$G'_{i}(\text{opt}) = \frac{1}{R'_{L}\text{opt}}\left(\frac{2}{A_1}\right)^2\left\{1 + R'_{L}\,A'_0\right\} \qquad \ldots 14$$

For practical mixer diodes at high normalised current-drive levels (i.e. $X \geqslant 10^5$) this equation approximates to:

$$G'_{i}(\text{opt}) = \frac{1}{R'_{L}\text{opt}}\left(\frac{2}{A_1}\right)^2 = \frac{1}{R'\text{opt}}\,\frac{\pi^2}{4} \qquad \ldots 14a$$

This is the same result that is obtained for the narrow-band open circuit mixer when there is no parasitic diode package capacitance present.

Again, considering the parameters of practical mixer diodes eqn. 8 can be more simply expressed as:

$$B'_{i} = \tau_{q} \qquad \ldots 15$$

This physically implies that at the signal frequency (ω_q), the input susceptance is equal to the diode package capacitance shunting the input to the lattice of diodes.

4.7 The Effect of the Diode Package Capacitance on the c.p.l.

For practical mixer diodes at high drive levels the optimum value of c.p.l. is given as follows:

$$(\text{c.p.l.})_{\text{opt}} = (1 + A'_0\,R'_{L\text{opt}} + 2\tau_{-1}^2\,R'^2_{L\text{opt}}) + \left(\frac{2}{A_1}\right)^2\frac{A_0}{R'_{L\text{opt}}}\,(1 + A'_0\,R'_{L\text{opt}} + 2\tau_{-1}^2 R'^2_{L\text{opt}})^2 \qquad \ldots 16$$

This expression indicates that for a diode with $r_s' = 10^{-6}$, $X > 10^6$ and a diode package capacitance as high as 1 pF, a c.p.l. below 3 dB may be achieved.

4.8 The Graphical Representation of the Results Obtained in the Analysis

The input admittance (Y_i), the load impedance (Z_L) and the optimum conversion power loss $(c.p.l.)_{opt}$ are all functions of:

(i) the diode parameters (r_s' and r_b)

(ii) the normalised current drive level (X)

(iii) the diode package capacitance (C)

(iv) the signal frequency (ω_q)

and (v) the i.f. frequency $(\omega_p - \omega_q)$

To present a set of graphical results of these mixer parameters, even over a small range of each of these, would be a vast undertaking. In order to give an indication of the magnitudes of both the optimum terminations and conversion power loss, and how they vary with diode package capacitance and local oscillator drive, just one set of diode parameters have been assumed. The diode in question has $r_s = 10\Omega$ and $r_b = 10^7\Omega$ (these parameters are similar to those of a silicon Schottky-barrier diode).

Fig. 4.16 shows a graph of τ_{-1} for this diode plotted for a number of values of package capacitance over the i.f. frequency range of 10 to 200 MH_2.

τ_q, which is also the normalised input susceptance (B_i'), is shown in Fig. 4.17; plotted for the same values of package capacitance and for signal frequencies from 0.1 GHz to 60 GHz.

The optimum conversion power loss, Fig. 4.18, is plotted as functions of both the diode package capacitance and the normalised drive level (X). It has been assumed that the i.f. frequency is 30MHz in this

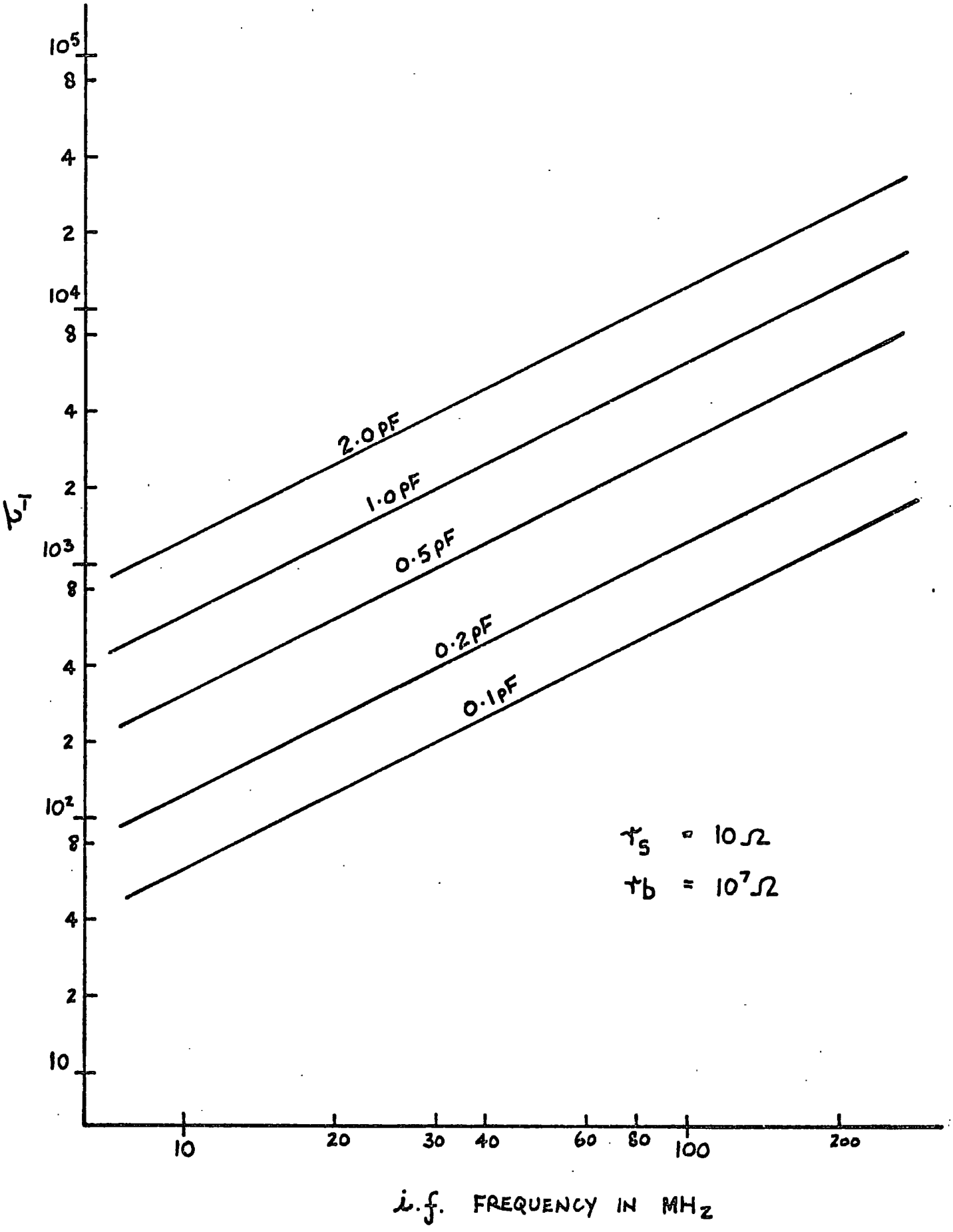

FIG. 4.16. τ^{-1} AGAINST i.f. FREQUENCY.

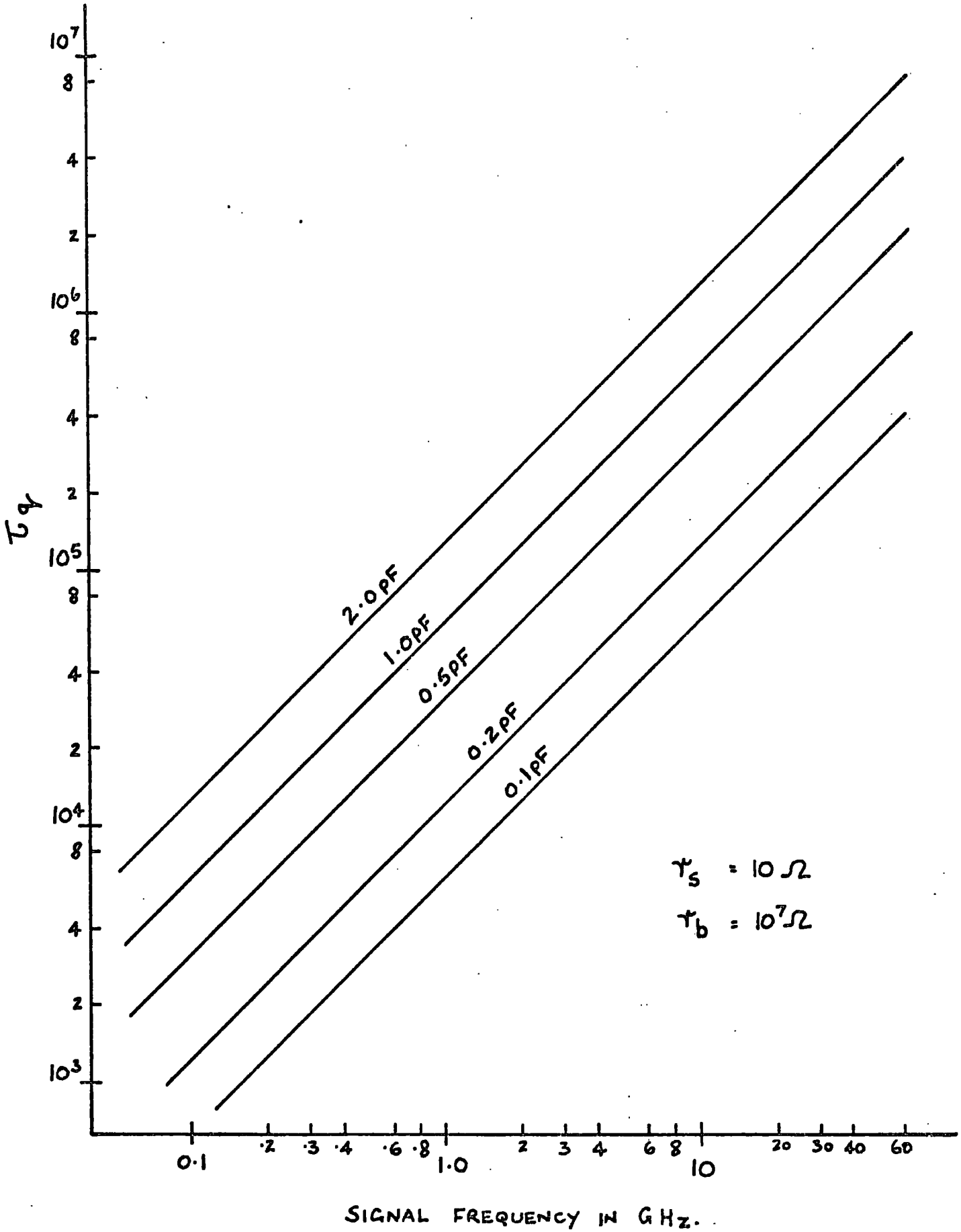

FIG. 4.17. τ_q AGAINST SIGNAL FREQUENCY.

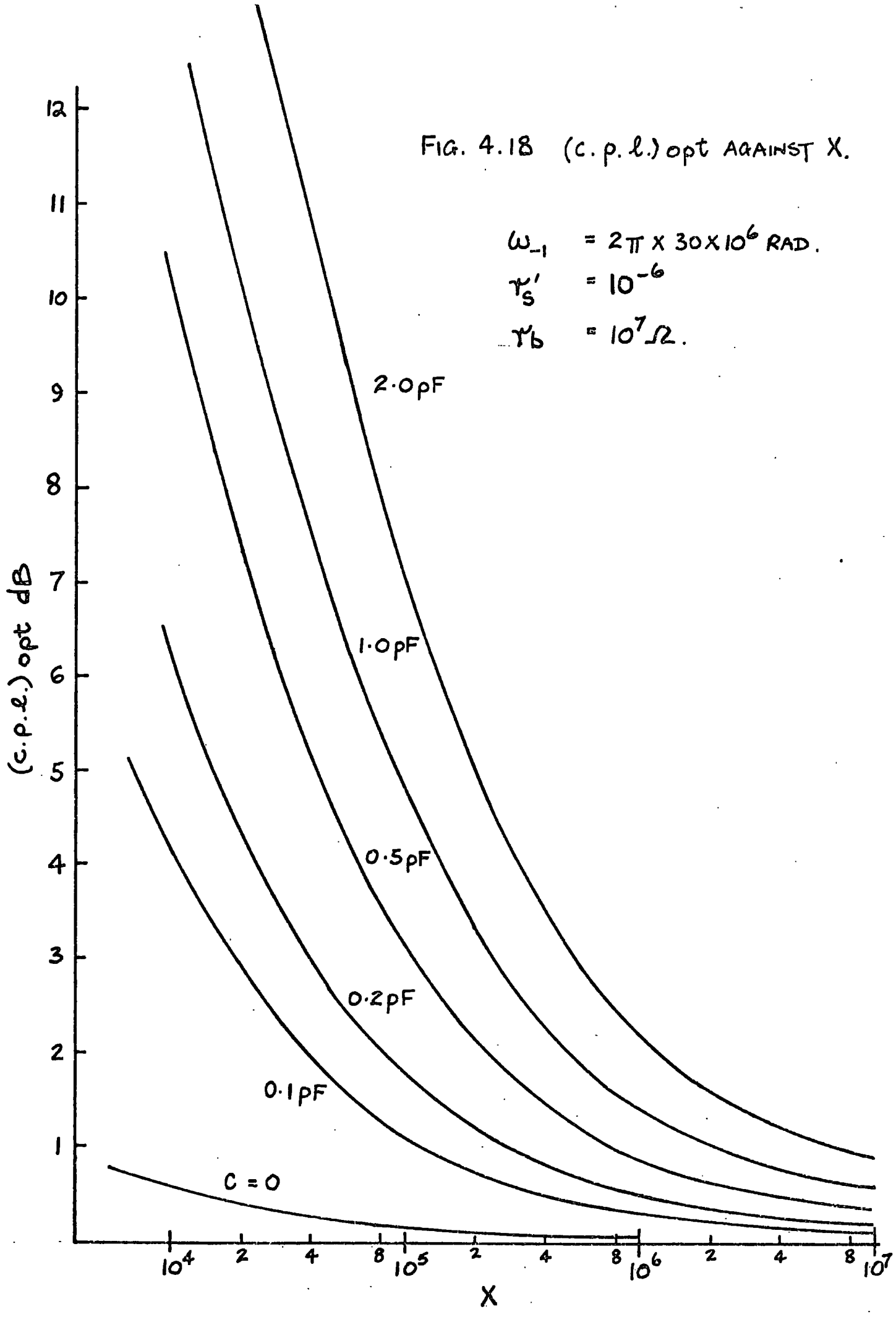
FIG. 4.18 (c.p.l.) opt AGAINST X.
ω_{-1} = 2π X 30X10^6 RAD.
r_s' = 10^-6
r_b = 10^7 Ω.
2·0pF
1·0pF
0·5pF
0·2pF
0·1pF
C = 0
(c.p.l.) opt dB
X
12
11
10
9
8
7
6
5
4
3
2
1
10^4
2
4
8
10^5
2
4
8
10^6
2
4
8
10^7

particular case. It can be seen that even a diode with a relatively large package capacitance of 2.0 pF may theoretically produce a c.p.l. below 2.5 dB for $X > 10^6$ (for the conditions previously stated). It can be considered that at high local oscillator drive levels the average incremental diode resistance is considerably reduced, and thus the effect of the diode capacitance, in parallel with this, will reduce as X increases.

$R'_L(opt)$, $X'_L(opt)$ and $G'_i(opt)$ are given in Figs. 4.19 to 4.21 respectively. As a comparison Fig. 4.22 shows $R'_{L(opt)}$ and $R'_{i(opt)}$ for this particular diode in a narrow-band open-circuit lattice mixer for the case when there is no diode package capacitance present. It can be seen from these results that R'_L is considerably reduced when even a small amount of parasitic diode package capacitance is present.

For example, at $X = 10^6$ with no capacitance, $R'_{L(opt)} = 3.75 \times 10^{-3}$ i.e. $R_L = 37.5K\,\Omega$ for this particular diode with $r_b = 10^7\Omega$. When the package capacitance is 0.1 pF, $R'_{L(opt)} = 0.58 \times 10^{-3}$ i.e. $R_L = 5.8K\Omega$.

The input resistance of the lattice for the same conditions is reduced from $15K\,\Omega$(no package capacitance) to $2.3K\,\Omega$; the c.p.l. being 0.30 dB.

Thus when matching the mixer input or output to the relatively low impedance of a coaxial line (eg. 50Ω) the presence of a small amount of diode package capacitance may be considered as being beneficial and the c.p.l. theoretically is still a low value.

4.9 Local Oscillator Power

Fig. 4.23 shows the lattice of diodes as 'seen' by the local oscillator. The current is restricted by the longitudinal resonance to be sinusoidal at the local oscillator frequency; its amplitude will be $2i_p$.

This then leads to the relationship:

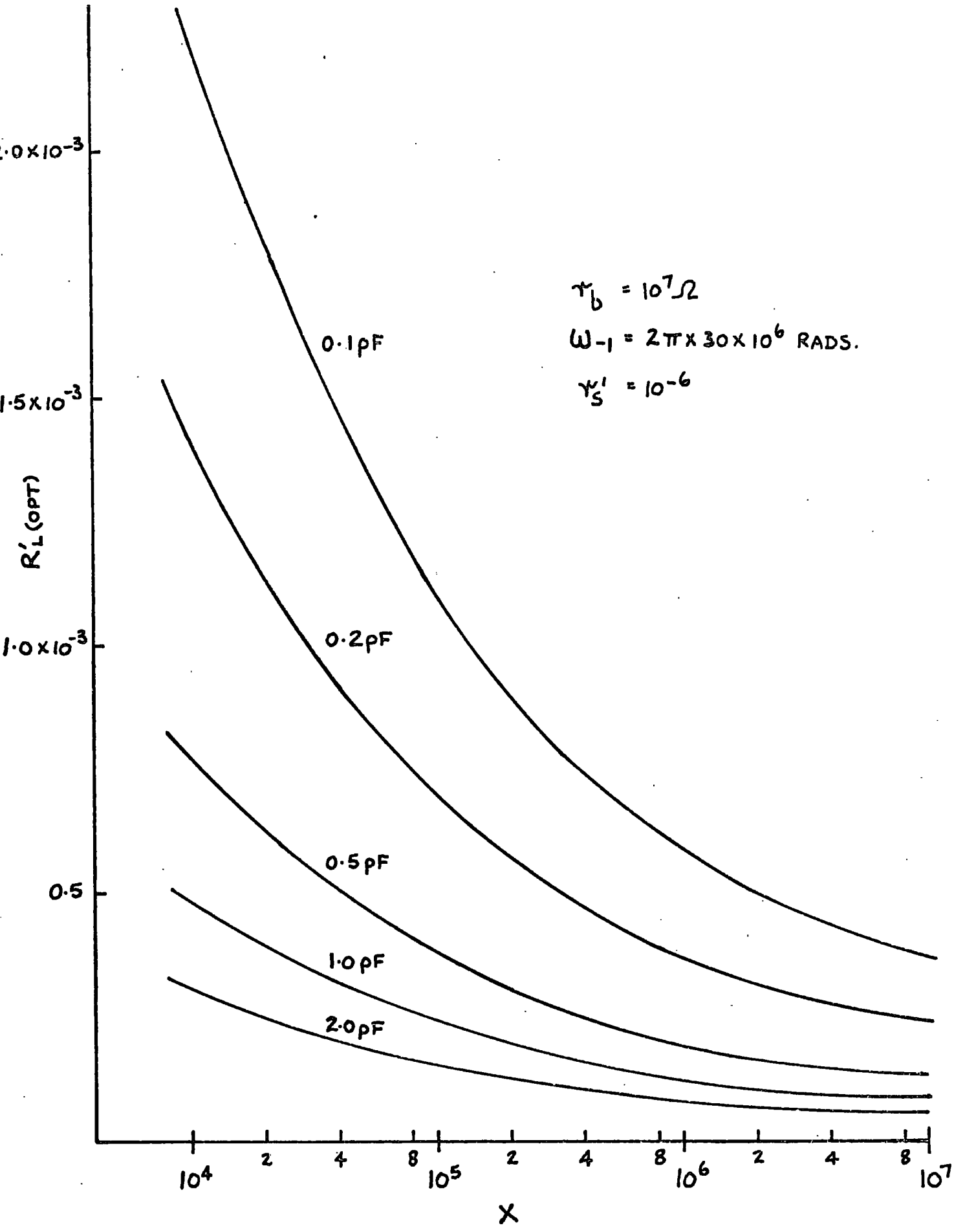

FIG. 4.19. R'_L (OPT) AGAINST X.

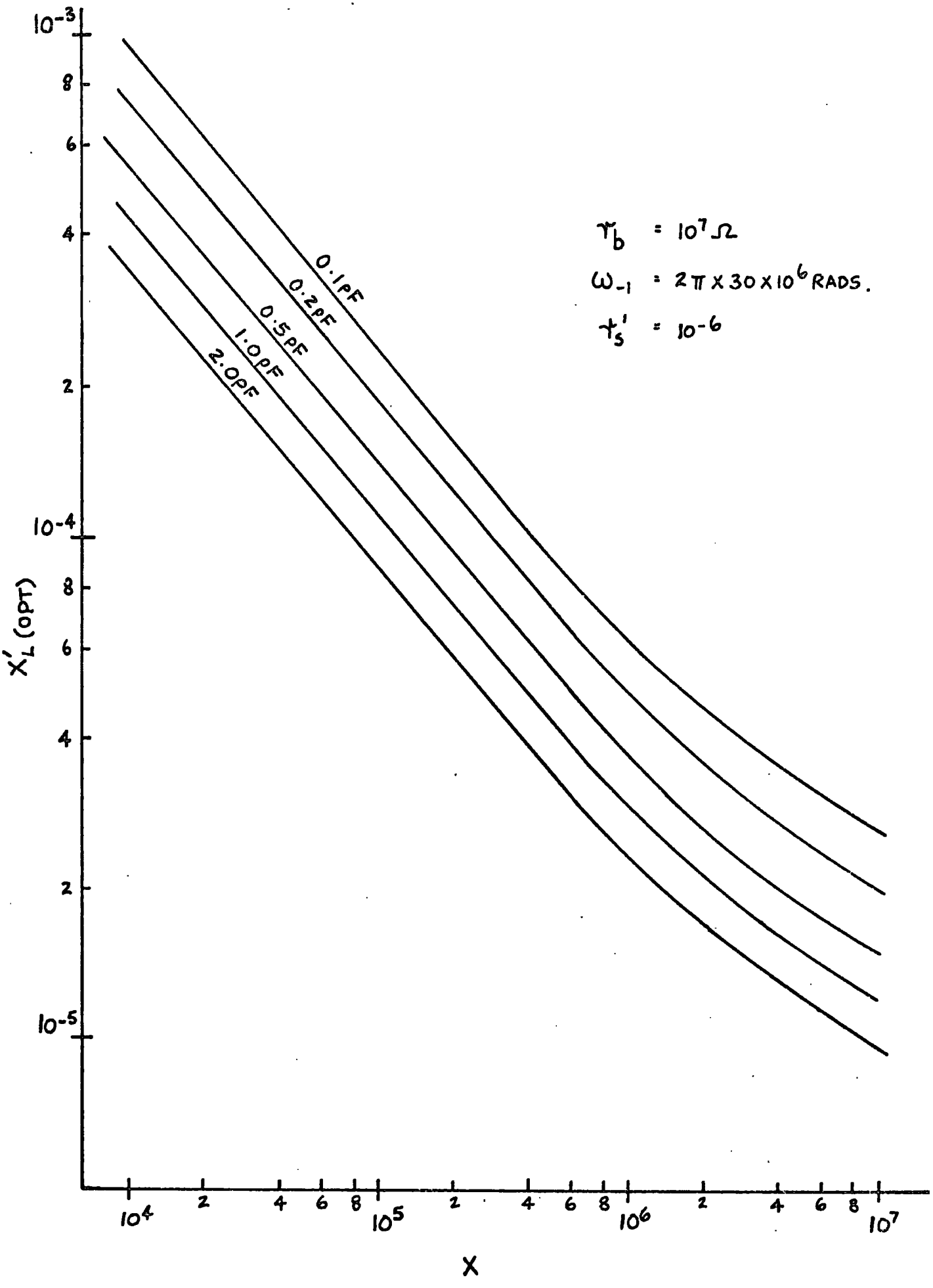

FIG. 4.20. X'_L(OPT) AGAINST X.

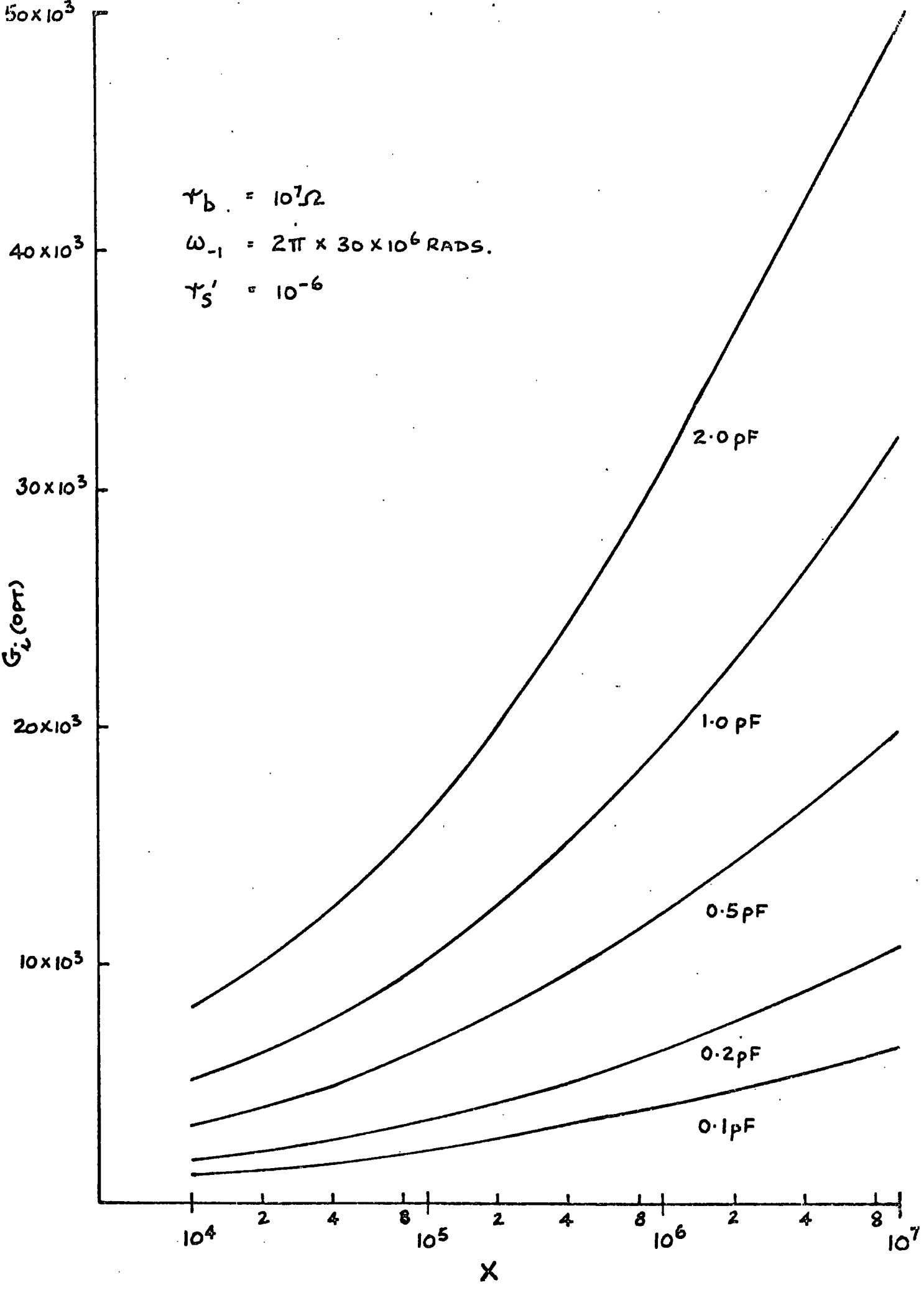

FIG. 4.21. G'_i (OPT) AGAINST X.

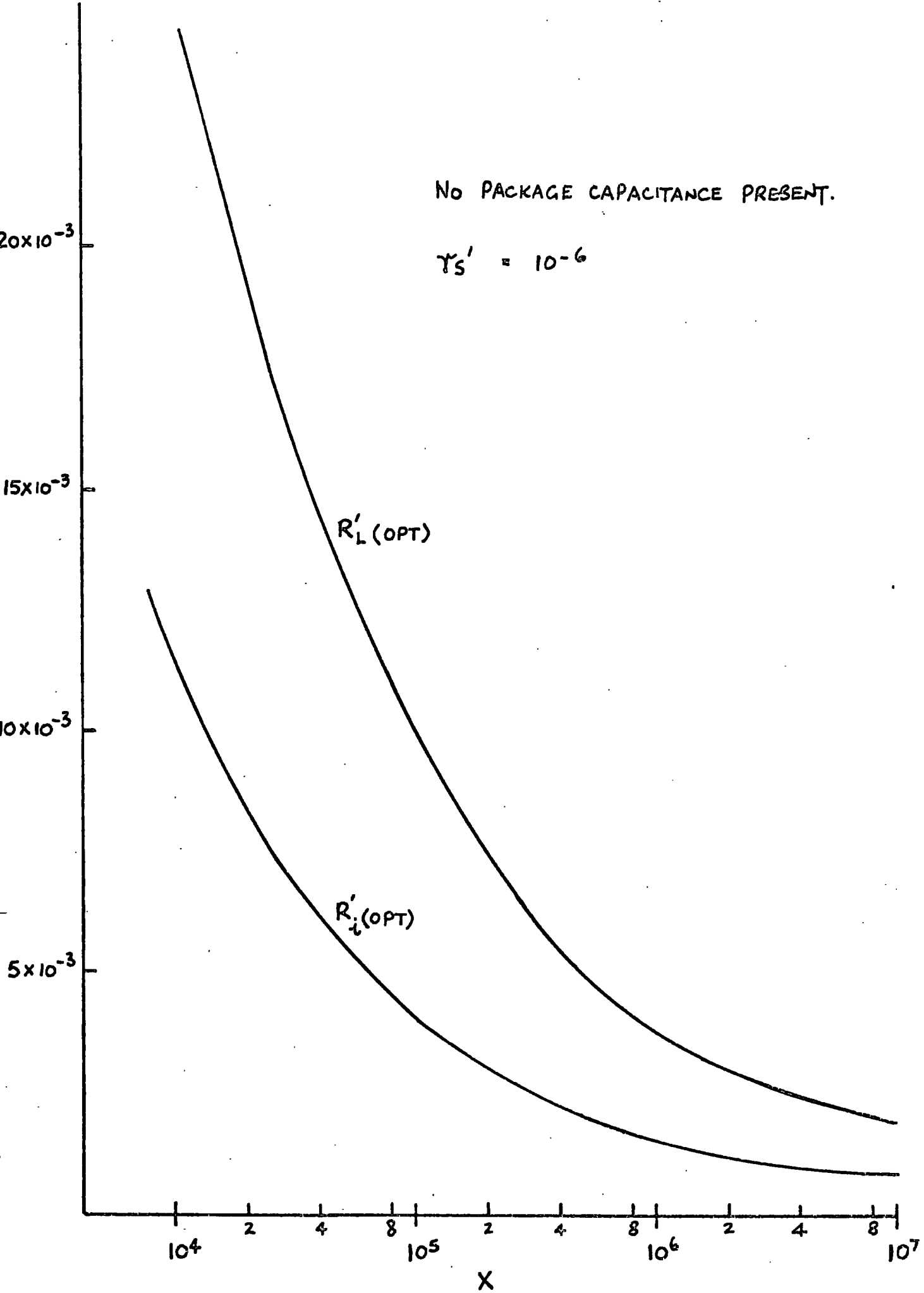

FIG. 4.22. R_L' (OPT) } AGAINST X.
R_i' (OPT) }

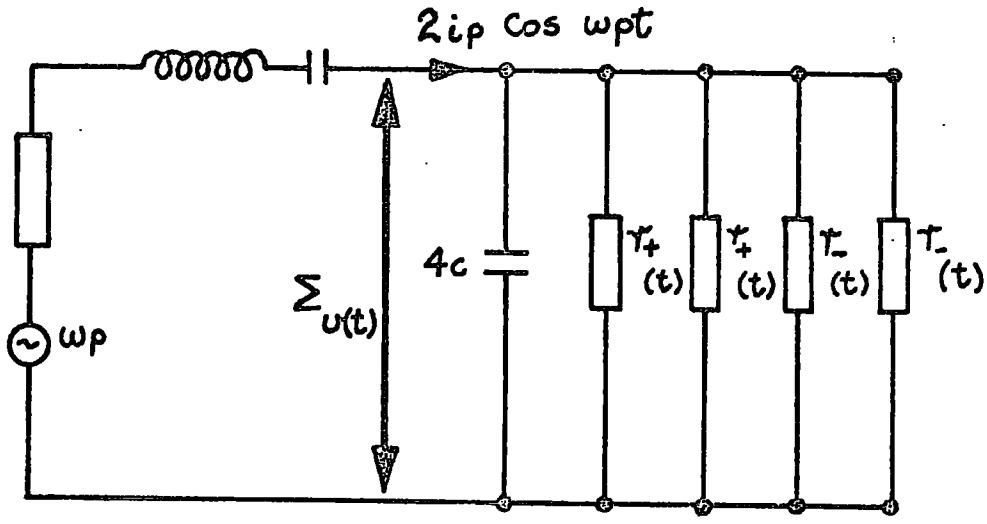

FIG. 4.23. THE LOCAL OSCILLATOR CIRCUIT.

$$\sum v(t) = 2i_p(\cos \omega_p t) \cdot Z(t)$$

where

$\sum v(t)$ is the summation of the voltages across the diodes

and $Z(t)$ is the time-varying impedance of the four diodes.

$$\sum v(t) = 2i_p(\cos\omega_p t) \cdot \frac{1}{\frac{2\left[r_+(t) + r_-(t)\right]}{r_+(t) \cdot r_-(t)} + j4\omega_p C}$$

at radian frequency, ω_p we obtain:

$$v_p = 2i_p \frac{r_b}{4}\left(Q_0 + \frac{Q_2}{2}\right)$$

Q_0 and Q_2 are given in the appendix (2)

$$v_p = 2i_p \frac{r_b}{4(1 + 2j\omega_p C r_s)}\left\{2r_s' + \frac{4}{\pi X}\right\}$$

The power delivered by the local oscillator is given by:

$$P_0 = \left| v^*_{p(rms)} \cdot i_{p(rms)} \right| \cdot \cos\theta$$

$$P_0 = \left| \left(\frac{2i_p}{\sqrt{2}}\right)^2 \frac{r_b}{4(1 - 2j\omega_p C r_s)}\left\{2r_s' + \frac{4}{\pi X}\right\} \right| \cdot \cos\theta$$

where $\theta = \tan^{-1}(2\omega_p C r_s)$

$$P_0 = \left(\frac{2i_p}{\sqrt{2}}\right)^2 \frac{r_b}{4}\left\{2r_s' + \frac{4}{\pi X}\right\} \frac{1}{(1 + 4\omega_p^2 C^2 r_s^2)}$$

For most practical cases $4\omega_p^2 C^2 r_s^2 \ll 1$

$$P_0 = \left[\left(\frac{2i_p}{\sqrt{2}} \right)^2 \frac{r_b}{4} \left\{ 2r_s' + \frac{4}{\pi X} \right\} \right] \text{ watts}$$

and

$$\frac{P_0}{I_s} = 10^{-7} \left(r_s' X^2 + \frac{2}{\pi} X \right) \text{ milliwatts per nanoampere}$$

This is the same relationship that is obtained for the purely resistive diode.

Fig. 4.24 shows the total local oscillator power plotted against X for the diode with $r_s = 10\Omega$ and $r_s' = 10^{-6}$. The reverse saturation current (I_s) is obtained from:

$$I_s r_b = \frac{kT}{q} \approx \frac{1}{40} \text{ eV} \quad \text{at } 300^\circ K$$

For practical mixers using these diodes X falls in the range of 2×10^6 to 2×10^7.

4.10 Conclusion

The analysis of the narrow-band open-circuit lattice mixer when there is diode package capacitance present was obtained by equating the four diodes (current driven at radian frequency ω_p) to four time-varying impedances.

The general network equations, were then solved by making two assumptions. Firstly, that v_s and i_L were restricted to be real and any phase shift was associated only with i_s and v_L, respectively. Secondly, that Bartlett's bisection theorem was valid for the lattice of diodes; the justification for this has been outlined in the first part of this chapter.

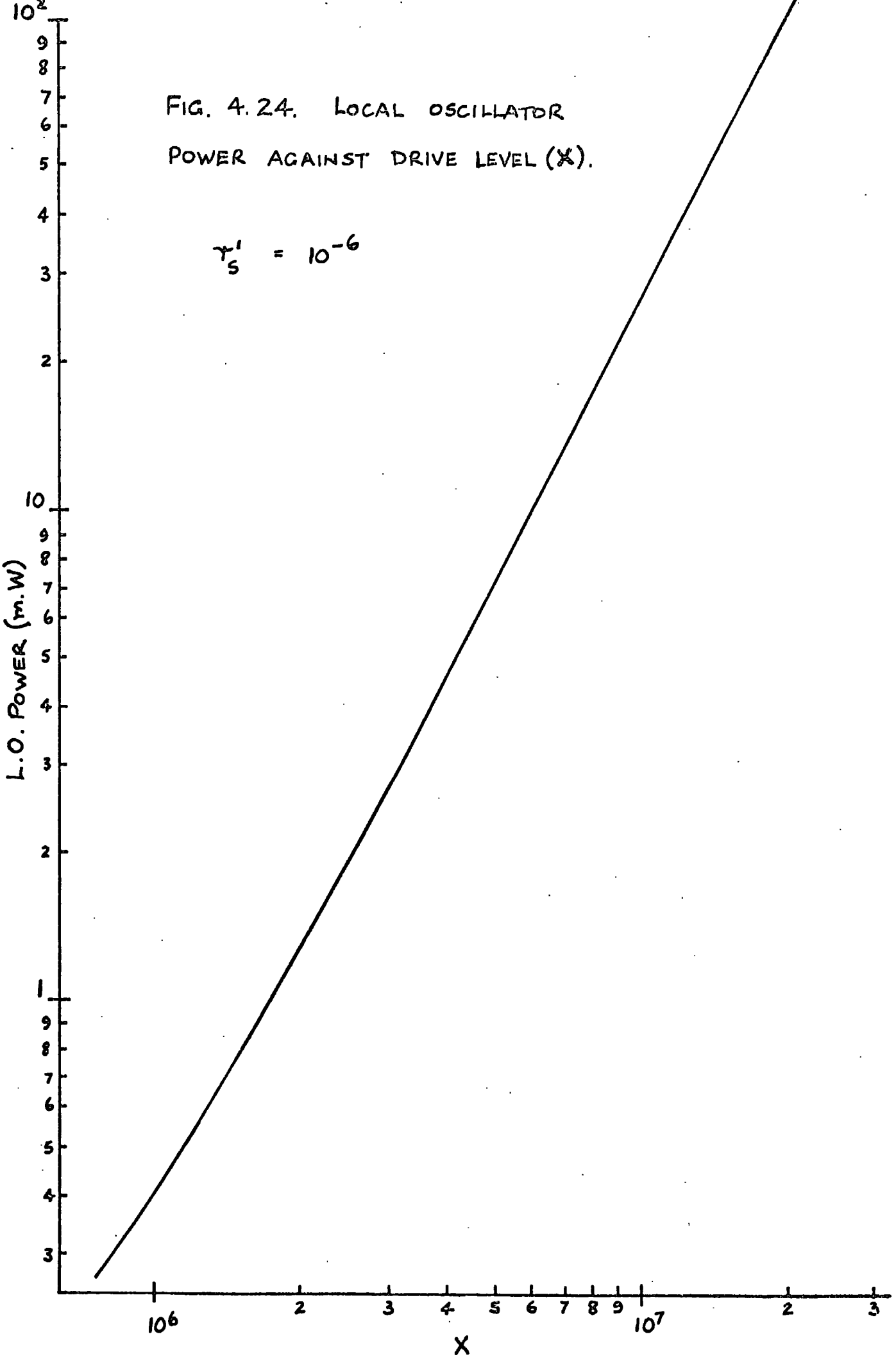

FIG. 4.24. LOCAL OSCILLATOR POWER AGAINST DRIVE LEVEL (X).

$\tau_s' = 10^{-6}$

The mixer parameters were then obtained as functions of the diode package capacitance and the normalised current-drive level by assuming a good quality diode ($r'_s = 10^{-6}$). At practical local oscillator drive levels (eg. $X = 5 \times 10^6$, which is just less than 10 mW of local oscillator power for these diodes), it is theoretically possible to achieve a low c.p.l. even when relatively high package capacitances are present.

The optimum input and output terminating impedances are reduced to more practically realisable values when each diode possesses even a small amount of parasitic package capacitance. It is interesting to note that the relationship:

$$\frac{R_{(opt)}}{R_{i(opt)}} = \frac{\pi^2}{4}$$

is still valid for the mixer terminating resistances.

As the l.o. drive is increased the incremental resistance of the diode generally becomes lower than the reactance of the parasitic capacitance. Thus the effect of this capacitance on the conversion efficiency of the mixer has a greater effect at low l.o. drive levels (eg. $X < 10^5$). This is one of the results obtained in the above analysis.

The parasitic junction capacitance has not been considered in the analysis as this is the subject of a separate project. If a junction capacitance is assumed to be a function of the bias voltage, then, under certain conditions it may be possible to obtain a parametric conversion gain from the lattice of diodes.

CHAPTER 5

AN EXPERIMENTAL L-BAND LATTICE MIXER

5.0 Introduction

This chapter is concerned with the construction and evaluation of a practical low-loss, L-band lattice mixer. The initial aim was to make the mixer as small and as cheap as possible so that it would have a greater number of applications in commercial communication and radar systems.

Lumped components were chosen because at the signal frequency of 1.5225 G Hz these can be made smaller and cheaper than either stripline or cavity components. They also have the added advantage that variable components may be easily introduced for tuning the mixer circuit resonances in situ.

The expressions given in the previous chapter were used in conjunction with the diode measurements to calculate the optimum terminating impedances and the c.p.l.

The experimental verification of the analysis by simulating additional diode package capacitance was the second objective in constructing the mixer.

5.1 Diode Measurements

5.1.1 Introduction

In Chapter 3 various techniques for diode measurements were discussed. In this section the results of these measurements are presented, from which the required parameters of the Schottky-barrier diodes used in the mixer are directly obtained.

5.1.2 The Voltage-Current Law

The diodes chosen for the mixer were a quad selected from matched pairs of wire-ended Si devices (Hewlett-Packard type 2578). Little information was supplied by the manufacturer except that they were suitable for mixer applications up to 2 GHz.

Fig. 5.1 shows the forward V-I characteristic for a typical 2578 diode used in the quad.

The diode obeys the law to within $\pm 2\%$:

$$V = Ir_s + \frac{kT}{q} \ln \left(1 + \frac{I}{I_s}\right)$$

where

$r_s = 2.63\,\Omega$

$I_s = 4.72$ nA which gives $r_b = 5.3 \times 10^6\,\Omega$

Four pairs of diodes were obtained and from these a quad of diodes was selected to give r_s and r_b within $\pm$ 10%. The price for four such diodes was under £15 at the time of purchase.

The average parameters of the diodes for the quad were:

$r_s = 2.7\,\Omega$

$r_b = 5.5 \times 10^6\,\Omega$ giving $r_s' = 4.9 \times 10^{-7}$

5.1.3 Diode Measurements at Microwave Frequencies

A slotted line which operated at the signal frequency of the mixer was not available so measurements were taken at the frequencies from 2.0 G Hz to 9.0 G Hz. The results on diodes type 2578 are shown in Fig. 5.2. The Smith's chart is drawn as a reactance chart, giving a series equivalent $\frac{R}{Z_0} + j\frac{X}{Z_0}$.

The incident power level on the diode was 0.5 mW; greater power than this would have produced errors due to the non-linearity of the resistive and capacitive components of the diode. Less power would have caused the detected signal at the voltage minimum to be lost in the noise.

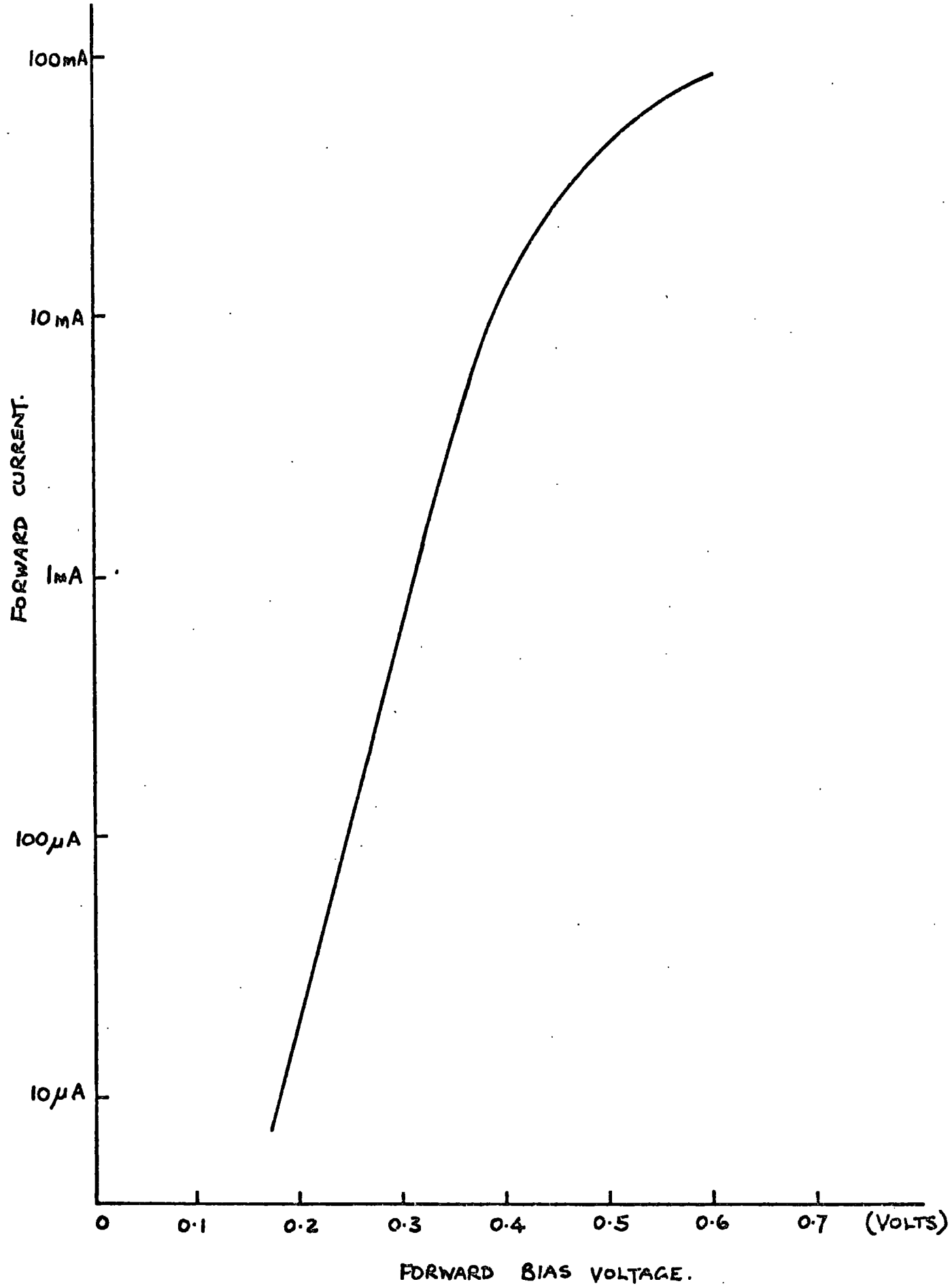

FIG. 5.1. THE DIODE V-I CHARACTERISTIC.

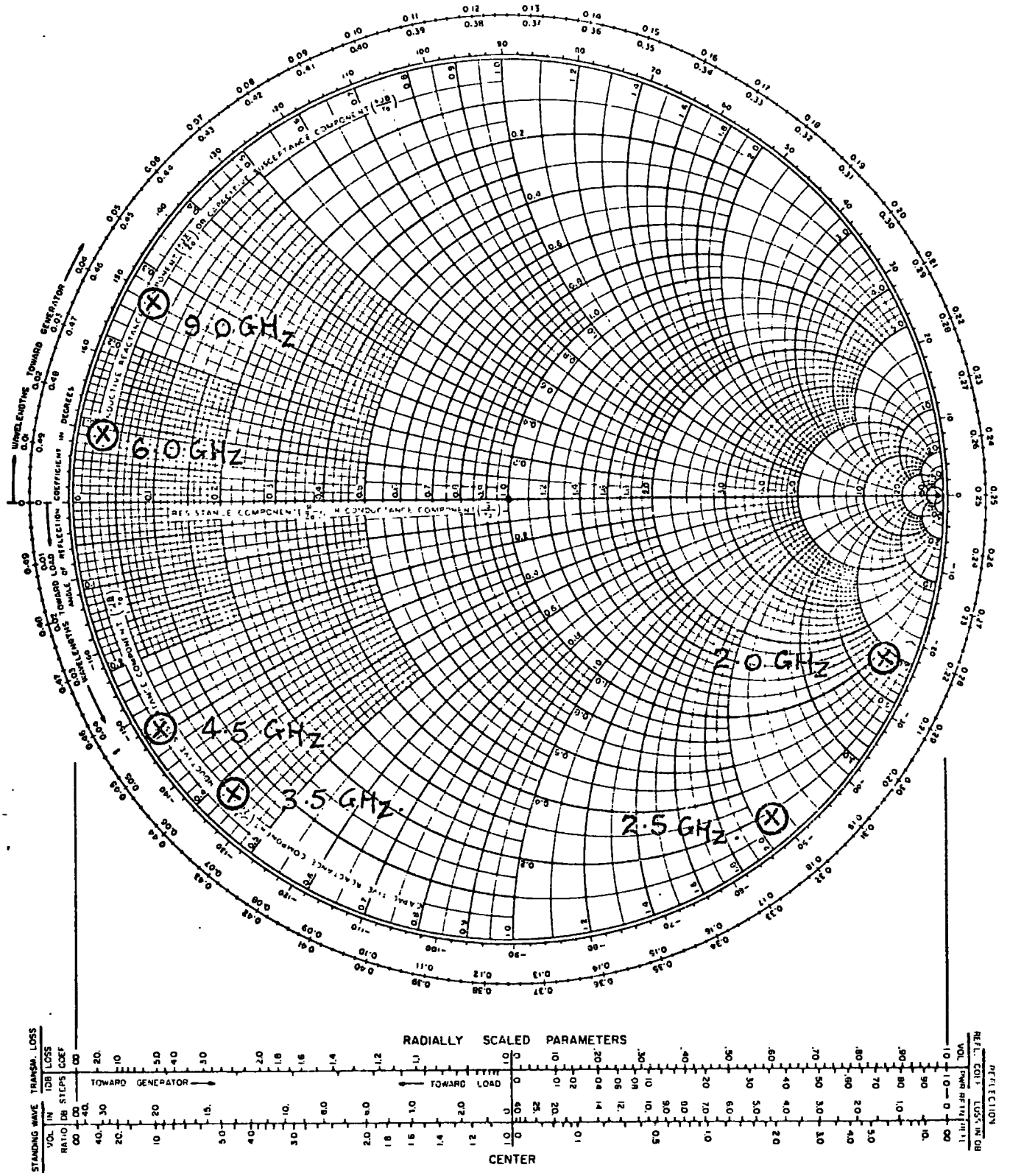

FIG. 5.2. THE SMITHS (IMPEDANCE) CHART FOR THE MEASUREMENT OF DIODE PARASITICS.

The reactance results for the diode are given in Table 5.1

Frequency (G H_z)	$j\frac{X}{Z_0}$
2.0	-4.8
2.5	-2.1
3.5	-0.43
4.5	-0.30
6.0	+0.08
9.0	+0.24

Table 5.1

Taking the readings at 2.5 G H_z and 3.5 G H_z, the diode inductance is calculated to be 3.87 nH and the diode capacitance as 0.35 pF. This capacitance was confirmed by an audio frequency bridge measurement.

5.1.4 The Variation of Junction Capacitance with Voltage

Fig. 5.3 (a) shows the variation of the diode capacitance with reverse bias voltage at a frequency of 100 K H_z. The diode measured was type 2900 (the same construction as 2578 but with a larger capacitance).

The equation of capacitance variation with voltage[2] is given by:

$$C = C_p + \frac{C_{jo}}{\left(1 - \frac{V}{\phi}\right)^n}$$

where C_p = package capacitance (0.19 pF)

C_{jo} = junction capacitance at zero bias (0.47 pF)

ϕ = contact potential (0.45 eV)

FIG. 5.3. (a) THE VARIATION OF DIODE CAPACITANCE WITH VOLTAGE.

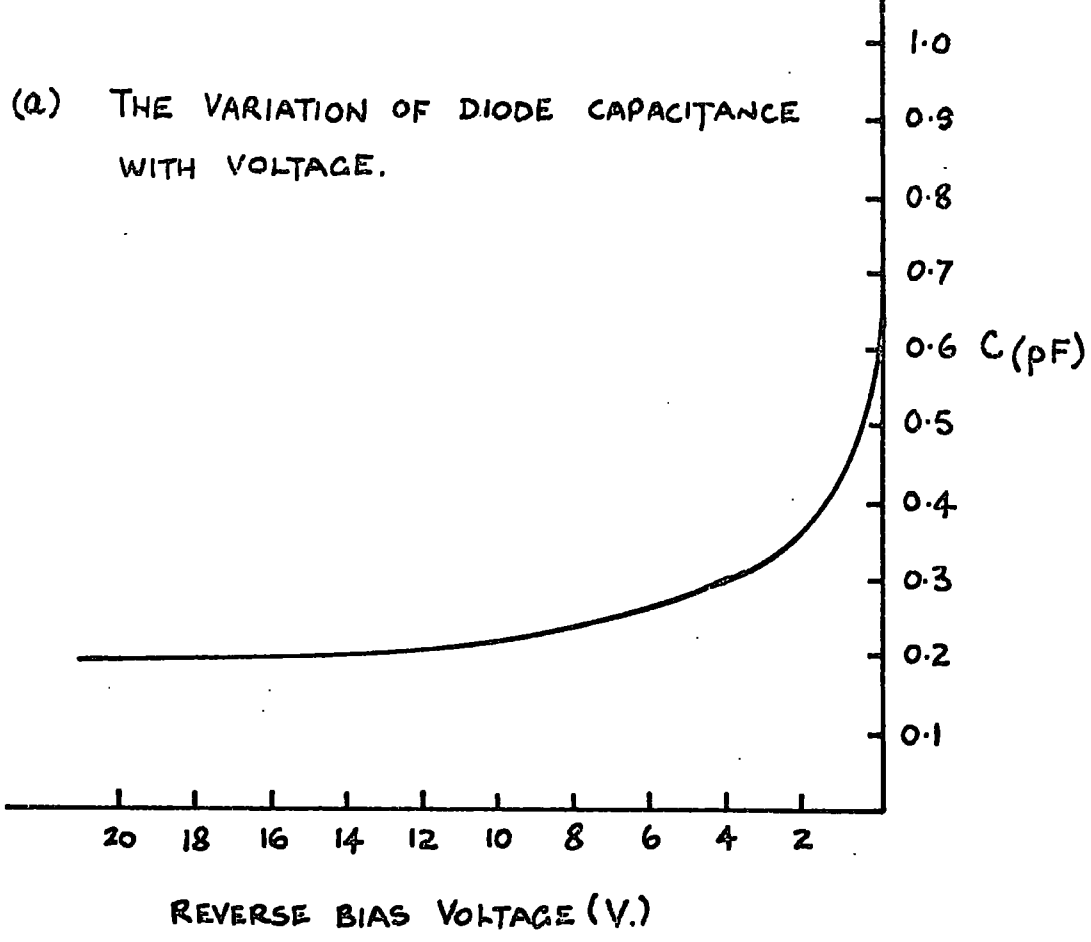

FIG. 5.3. (b) THE DETERMINATION OF 'n'.

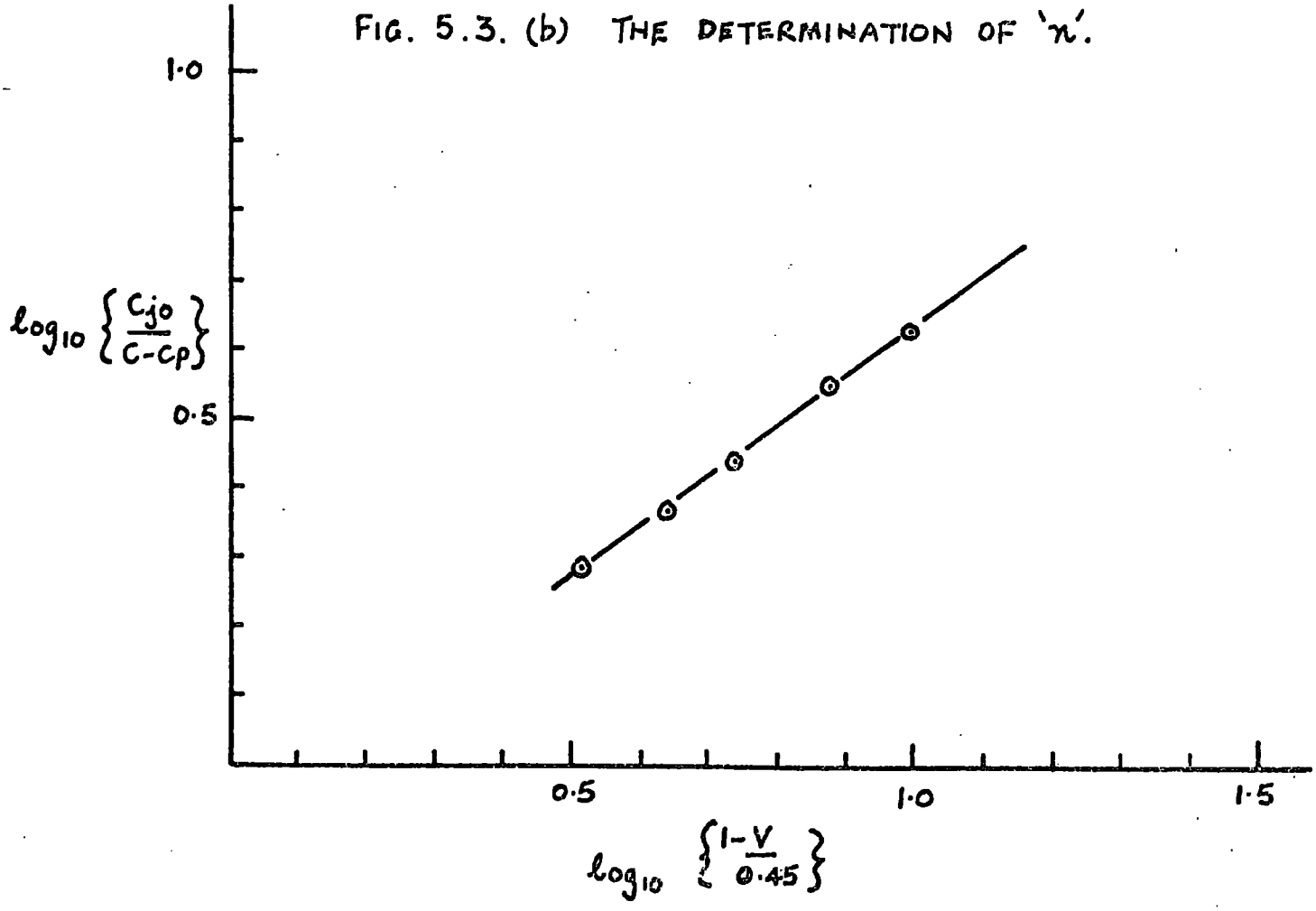

If $\log_{10}\left\{1 - \frac{V}{\phi}\right\}$ is plotted against $\log_{10}\left\{\frac{C_{jo}}{C - C_p}\right\}$

the slope gives the factor 'n' (0.72)

Errors arise in determining C_{jo} accurately as $\frac{dC}{dV}$ is large for $V = 0$.

5.2 The Construction of the L-Band Mixer

5.2.1 The Mixer Parameters

The optimum terminating impedances and the c.p.l. had to be calculated, using the results of the analytical work of Chapter 4 and the diode measurements, before the mixer could be constructed.

The local oscillator power as a function of X (the current drive level) for the quad of diodes is shown in Fig. 5.4. It was aimed to have a local oscillator power in the region of 10 mW to 20 mW; X was chosen to be 8×10^6 (equivalent to 17 mW).

The i.f. frequency of the mixer was chosen to be 30 MHz. The frequency of the local oscillator was fixed at 1.5525 GHz by a crystal-controlled varactor multiplier source, giving the signal frequency of 1.5225 GHz.

Using eqns. 12 and 13, in Chapter 4, the output equivalent circuit at the i.f. frequency is 1.21 KΩ in parallel with 0.35 pF, and similarly from eqns. 14a and 15, the input equivalent circuit at the signal frequency is 490 Ω in parallel with 0.35 pF. From eqn. 16 in Chapter 4 the optimum c.p.l. of this mixer will be approximately 0.1 dB for the narrow-band open-circuit case; assuming loss-less resonant circuits.

5.2.2 Practical considerations

The basic mixer circuit is reproduced in Fig. 5.5. There are a number of criteria which exist in the circuit that must be preserved when constructing the mixer.

FIG. 5.4. THE LOCAL OSCILLATOR POWER AGAINST DRIVE LEVEL (X).

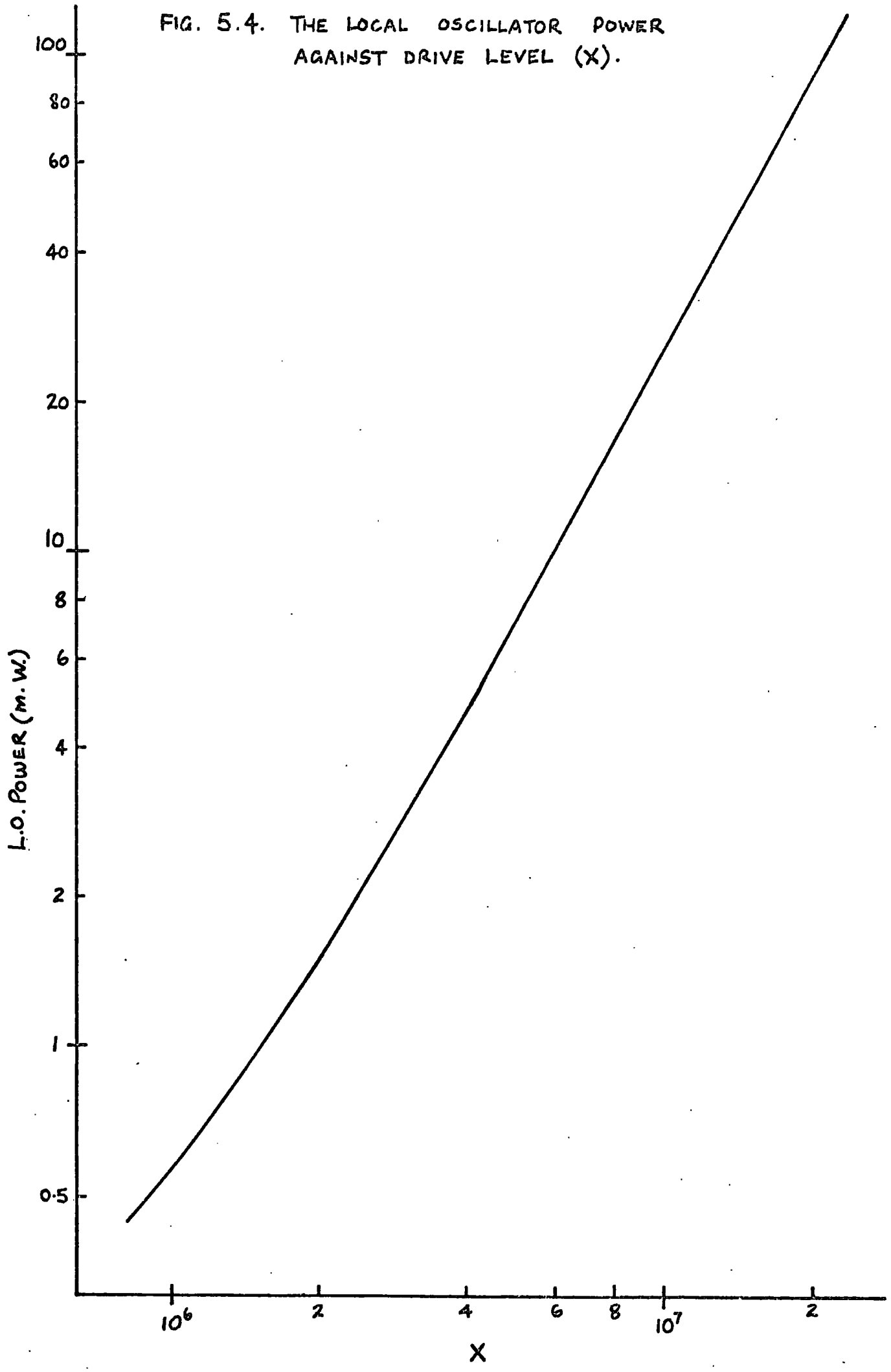

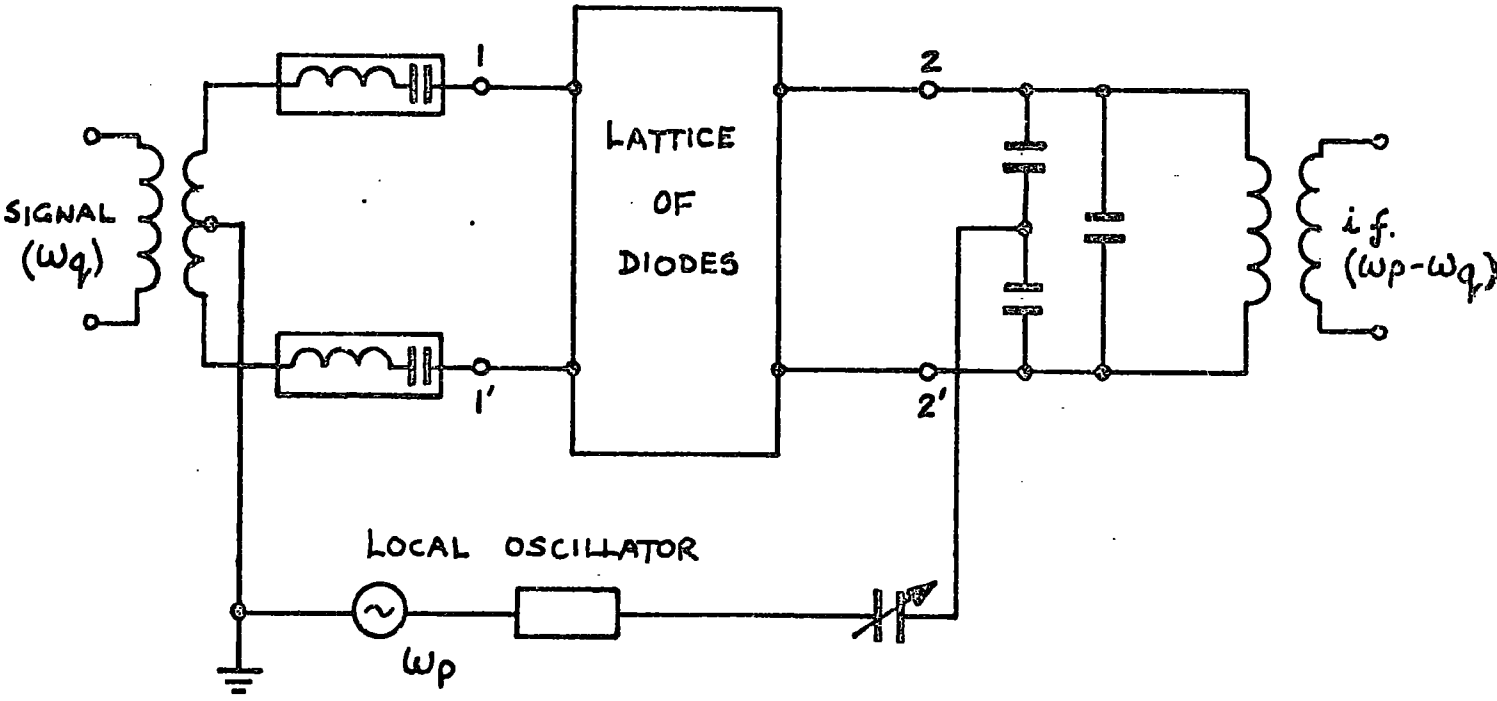

FIG. 5.5. THE BASIC MIXER CIRCUIT.

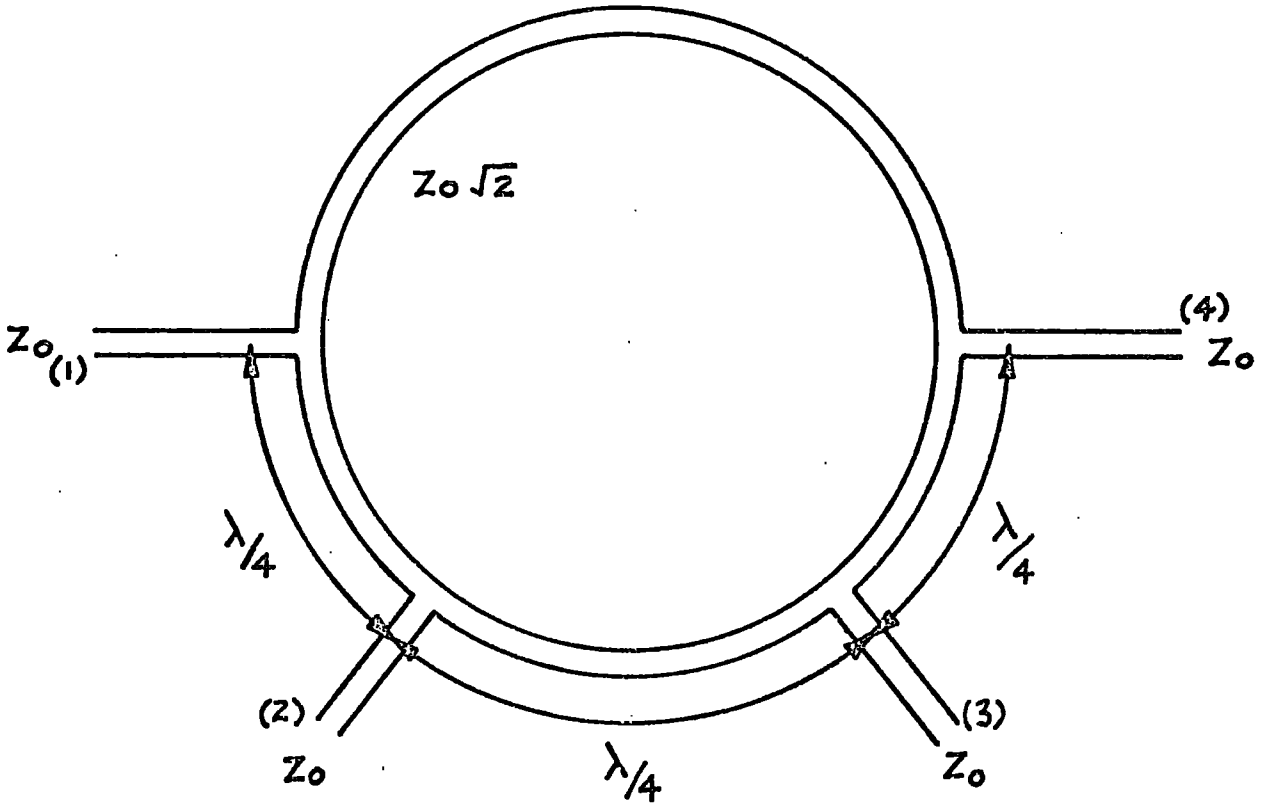

FIG. 5.7. THE RING HYBRID.

Firstly, the series resonance at the signal frequency must be highly selective and even-order currents must be prevented to flow. To obtain the narrow-band open-circuit condition, i.e. no current at the image frequency allowed to flow in the input circuit, the ratio of the reactance of this resonant circuit to the resistive components at the image frequency, present at the input, must tend to infinity. Fig. 5.6 shows the input terminating circuit.

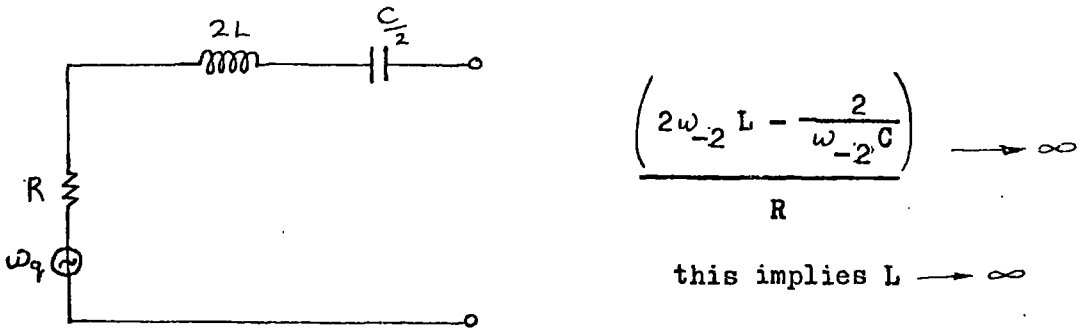

Fig. 5.6 The narrow-band open-circuit mixer input termination

It is thus impossible to achieve the ideal theoretical open-circuit image condition in practice. In most practical cases the image frequency termination will possess a resistive and an inductive reactive components. The effect on the mixer performance for this case is given by Kulesza[3].

If the reactance, of the series resonant circuit, at the image frequency is low in comparison with the input resistance then the mixer may be considered as tending towards the broad-band case.

If, on the other hand, the input transformer is arranged to be part of a parallel resonant circuit (resonant at the signal frequency), the mixer may, under certain conditions, be considered as approaching the narrow-band short-circuit case. These last two mixer circuits have also been analysed by Kulesza[4].

At the output of the mixer the transformer must be included in a parallel resonant circuit at the i.f. frequency which presents a low capacitive reactance (ideally zero impedance) to higher odd order frequency components.

The final requirement is that the sinusoidal local oscillator current drive through the diodes must be retained. Any imbalance in the circuit due to either stray impedances or mismatch between the diodes will produce a local oscillator break through in the signal and i.f. ports.

5.2.3 Review of Suitable Microwave Circuits

Firstly stripline techniques were considered for the construction of the mixer. A departmental memorandum[5] was written by the author on strip lines which reviewed their different configurations and applications. A translation of the mixer circuit into a stripline form was attempted.

The mixer was divided into parts which required a stripline equivalent, i.e.

(a) the input transformer

(b) the series resonance at the signal frequency

(c) the longitudinal resonance at the local oscillator frequency

Because of the balanced nature of the input transformer, theoretically, no l.o. voltage will be present at the signal terminals. An equivalent of this transformer in stripline is a hybrid junction. One such hybrid (a 'rat race') is shown diagrammatically in Fig. 5.7.

The signal input at port 1 will have outputs at ports 2 and 4 (the power being equally divided between the two), but, will have no output at port 3 as there is destructive interference due to a 180° phase difference in the two paths.

Similarly the local oscillator input at port 3 will have equal outputs at ports 2 and 4, but no output at the signal port 1.

The series resonance circuits were to be replaced by two four section Chebyshev band pass filters at ports 2 and 4, allowing both the signal and local oscillator currents to flow but presenting a high rejection (>15 dB) at the image frequency.

There are two major advantages that stripline techniques could have offered, over the lumped components, in the construction of the mixer.

Firstly, higher unloaded Q's may be obtained in stripline eg. up to 400 as compared to approximately a maximum of 120 which may be obtained for the lumped components at L-band frequencies.

Secondly, fringing field capacitances and parasitic inductances, because of the method of construction of the stripline, are readily calculated and reduced.

Unfortunately, there were two factors which led to the abandonment of stripline approach as the method of constructing the mixer, these were:

(a) The equipment needed for the photoresist and etching techniques to produce the filters with the precise frequency response was not readily available, and

(b) Only "polyguide" substrate (a polythene dielectric sandwiched between two thin copper sheets) was available. This, because of its relatively low dielectric constant ($\varepsilon_r = 2.2$) would have required in size approximately 6" by 2" for the filters and 3" by 3" for the rat-race hybrid. This would have been prohibitively too large and expensive.

Stripline may be a practical proposition at a higher frequency, or if a dielectric such as alumina ($\varepsilon_r = 10$) had been obtainable.

Construction of the microwave circuits using end-loaded cavity techniques was considered but the size of the cavities at L-band would have been too large. One way of reducing the size would have been to use a dielectric in conjunction with the cavity. A lattice mixer has been constructed at 4.5 G Hz using end loaded cavities[6].

Lumped circuit components were chosen because at L-band they can be made smaller and cheaper than either stripline or cavity components. The values of the lumped circuit components were obtained using the formulae in Appendix 5.

The major limitations of lumped components at microwave frequencies are:

(i) They must be less than approximately $\frac{\lambda}{8}$ in length otherwise they may not be considered as purely lumped elements but, rather transmission lines.

(ii) There are maximum values of the components which may be practically obtained due to either the presence of self-capacitance in the inductors or parasitic inductance in the capacitors. If care is not taken in the design, these reactances may become dominant.

It was found at L-band that approximately 50 nH was the maximum inductance which could be reliably obtained.

Tubular ceramic capacitors could produce a maximum of 5 pF and silver mica capacitors with short leads up to 10 pF.

(iii) The spacing of the components inside the metal case (with respect to each other and the metal walls) was found to be critical. This is especially true for the series resonant circuits at the signal frequency.

Early attempts at constructing the mixer in a box 1.25" x 1.25" x 2.5" were abandoned because of the stray capacitances between adjacent components and also with the walls of the box. A box 1.1" x 2.75" x 2.75" was found to give a considerable improvement to the mixer performance.

5.2.4 The Practical Mixer

Fig. 5.8 shows the circuit of the L-band mixer; the component values are given in Table 5.2.

The capacitors C_3 and C_3' were low-loss "polyguide" discs. This enabled low capacitance values with minimum parasitic lead inductances to be fabricated.

As has already been outlined in 5.3.2, to approach the narrow-band open-circuit condition the inductance L_3 (which is equal to L_3') has to be as large as practically possible. For a lumped circuit component there is a maximum limitation to its value. Two such limitations have been discussed (i.e. length $\frac{\lambda}{8}$ and reduction of self-capacitance). A third concerns the condition that there must be a sinusoidal current drive at the local oscillator frequency.

The capacitance required in the local oscillator circuit for the longitudinal resonance $= \left(\frac{\omega_g}{\omega_p}\right)^2 \cdot C_3$. Now, if C_3 is small (i.e. L_3 large), the additional capacitance which has to be placed in series with C_3 (to retain the sinusoidal current drive) could be impractically large. For example, in the L-band mixer $C_3 = 0.40$ pF the additional capacitance which has to be added in series with this, in the l.o. circuit is 10.3 pF. Too small a value of C_3 may produce a situation where it would be practically difficult to obtain a large lumped capacitance at these frequencies.

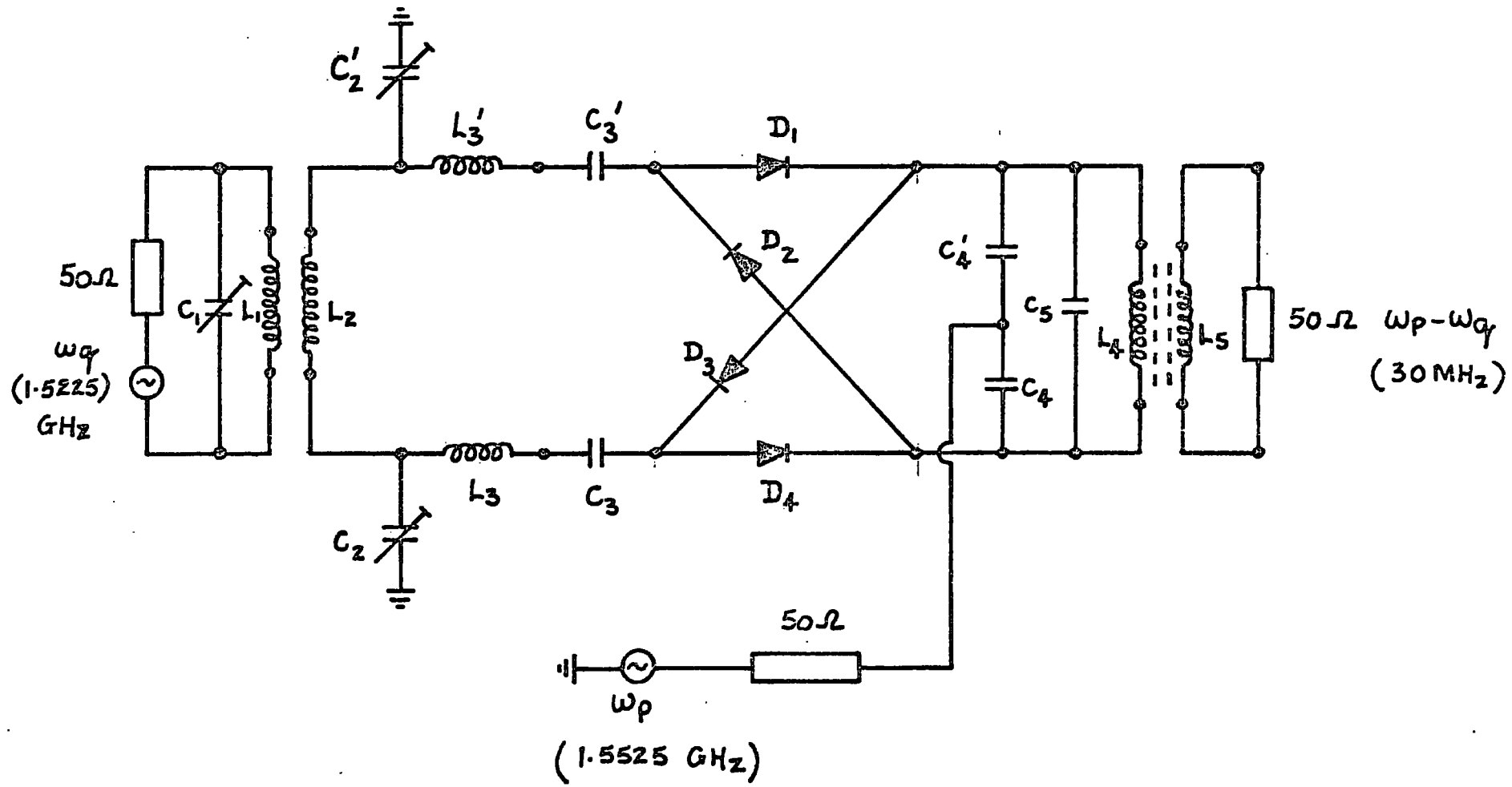

FIG. 5.8. THE EXPERIMENTAL MIXER.

TABLE 5.2

COMPONENT	VALUE	DESCRIPTION OF COMPONENT
C_1	1.7 pF	4.0 pF high frequency tubular ceramic pre-set
C_2	1.2 pF	" " " " " "
C_2'	1.4 pF	" " " " " "
C_3	0.40 pF	0.150" diameter "polyguide" $\frac{1}{32}$" thick
C_3'		
C_4	10.0 pF	silver-mica
C_4'		
C_5	23 pF	1pF "polyguide" capacitor in parallel with 22 pF silver-mica
L_1	6.5 nH	loop 0.35" long; 0.067" diameter wire
L_2	11.7 nH	0.80" long; " " "
L_3	27.3 nH	see details below
L_3'		
L_4*	0.91 μH	5t 0.0105" diameter wire (unloaded Q = 115 @ 30MHz)
L_5*	0.37 μH	1t 0.0105" " " (unloaded Q = 80 @ 30MHz)
$D_1 - D_4$	HP2578	

* both coils coupled with U.H.F. ferrite slugs

Details of L_3 and L_3'

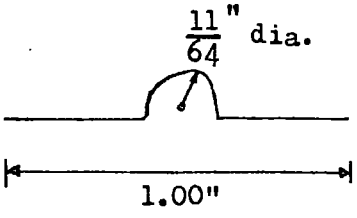

Total Wire Length = 1.25"

Wire Diameter = 0.0245"

Capacitors C_2 and C_2' play a number of roles in the circuit. Firstly, there are parasitic diode inductances in the l.o. path; they provide a small variable capacitance which produces a series resonance with these. Secondly, they provide a balanced earth input for the local oscillator. By adjustment of the two capacitors, the local oscillator breakthrough in the signal input was minimised (similarly, in the output circuit, the l.o. breakthrough was minimised by adjusting two ferrite slugs in the i.f. transformer). Finally, they produce a parallel resonance with the secondary of the input transformer; this combination when "hot tuned" provides a conjugate match with the input of the lattice of diodes.

The input transformer was approximately 3:1 turns ratio, obtained by the coupling between two parallel wires (see photograph).

The apparatus for the c.p.l. measurement is shown in Fig. 5.9. Because of the frequency drift in the L-band transistor oscillator, the i.f. output was displayed on an oscilloscope rather than using a wave analyser. The oscilloscope was then calibrated against a power meter (see Appendix 4.b)

The performance of the mixer is given in Fig. 5.10, this shows a minimum c.p.l. of 2.8 dB at the local oscillator input power of 20 mW.

As the slotted line, which operated at the signal frequency, was not available a method was devised to determine the input V.S.W.R. of the mixer at low power levels of the signal (Appendix 4.a). The disadvantage of this method is that there is no means of finding the phase angle or reactive component of this input impedance. Fig. 5.11 shows the input V.S.W.R. of the mixer against the l.o. power. If a 3:1 turns ratio is assumed for the input transformer, the input impedance to the lattice of diodes (Z_i) can be found and is shown in Fig. 5.12.

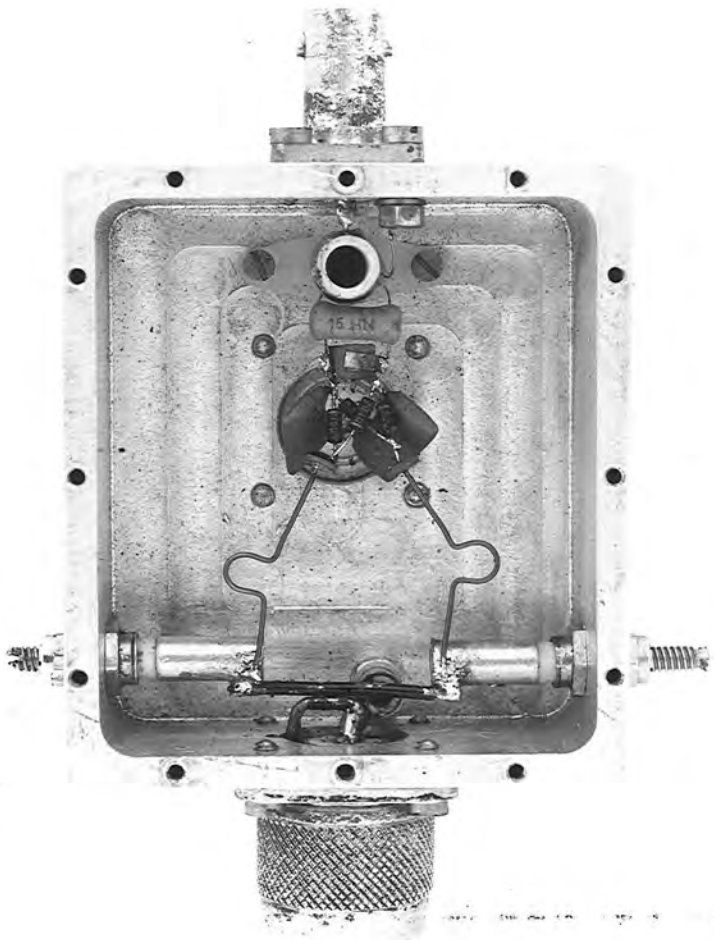

The Experimental Mixer

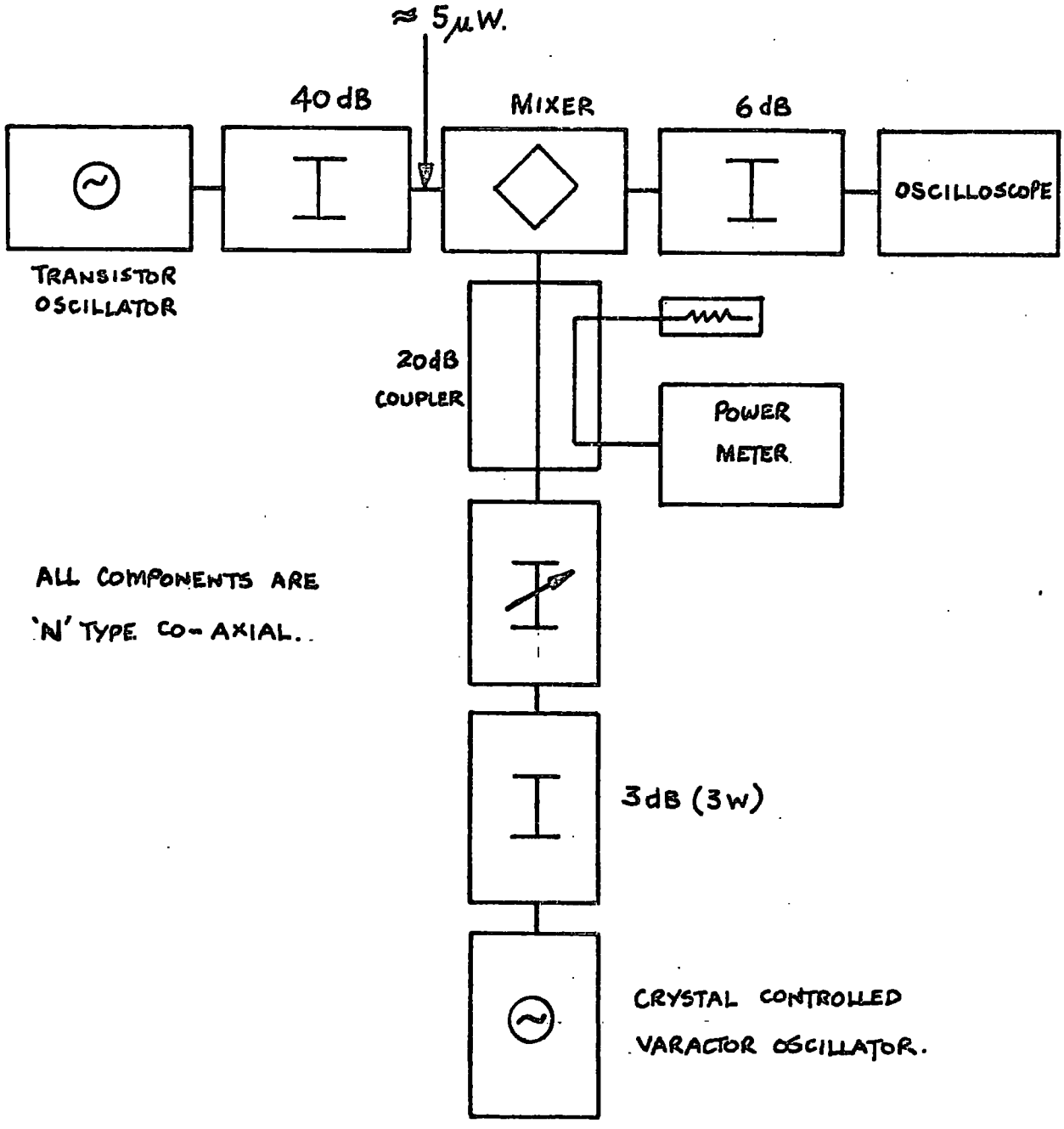

FIG. 5.9. APPARATUS USED FOR MEASURING C. P. L.

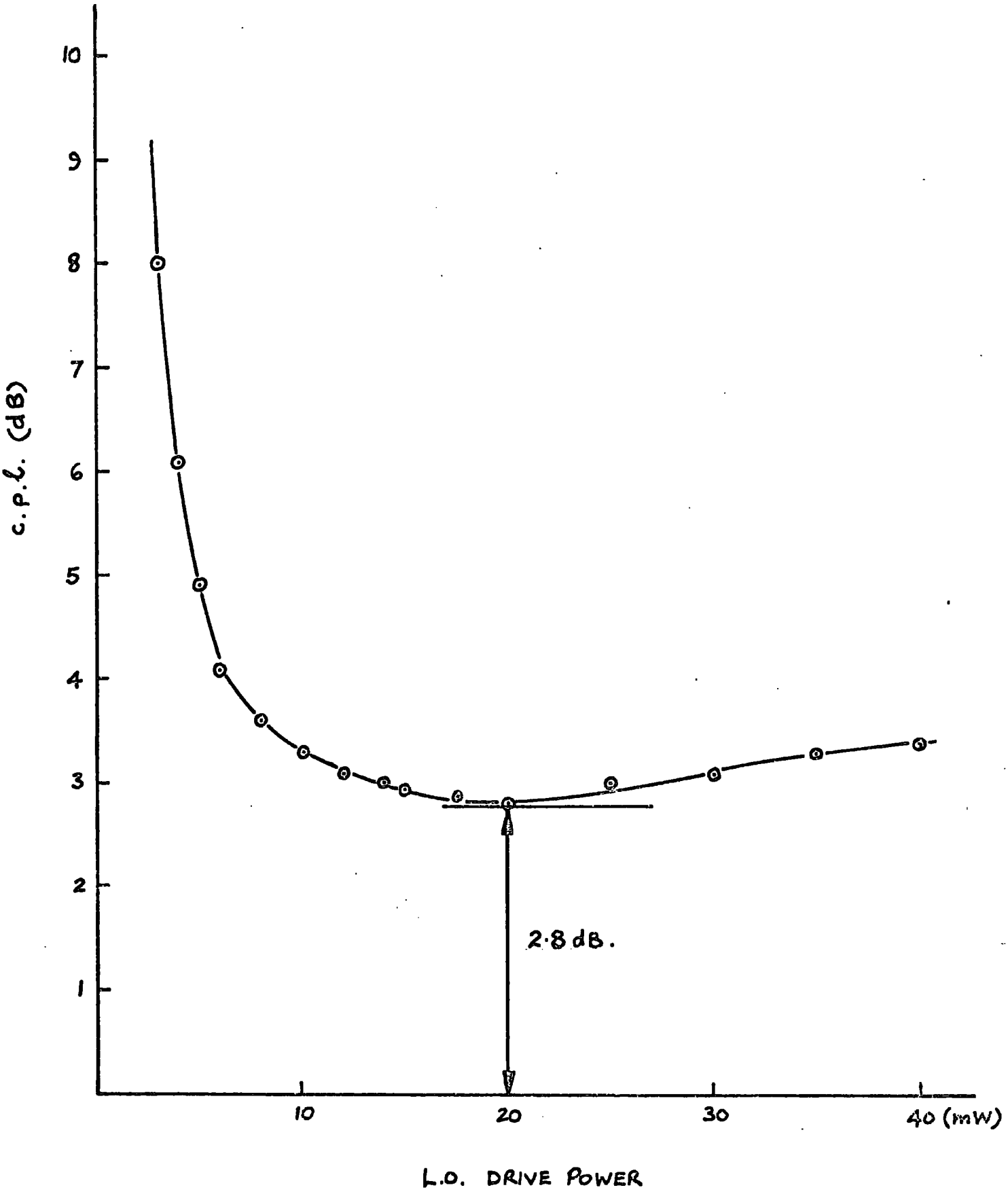

FIG. 5.10. THE C.P.l. AGAINST L.O. POWER.

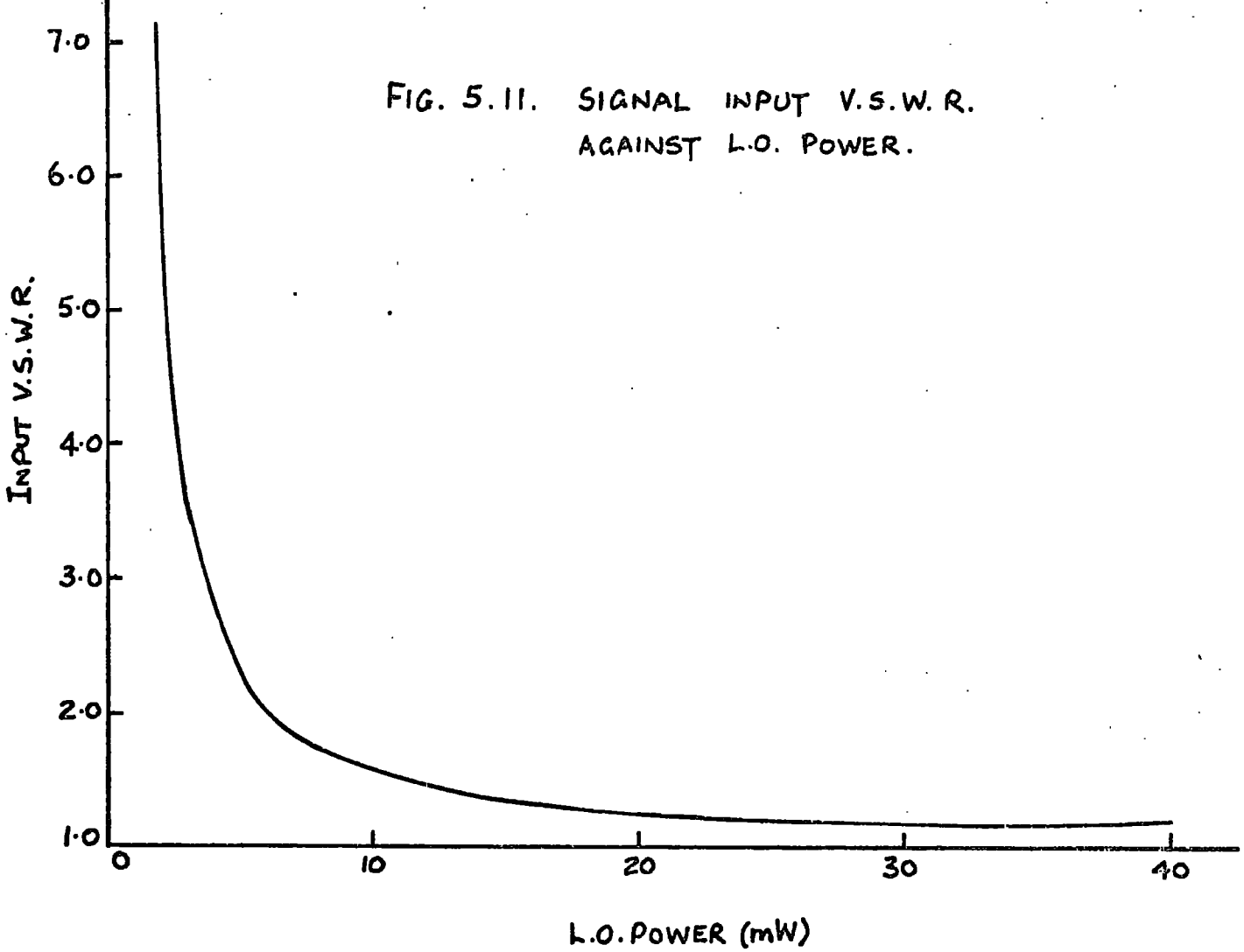

FIG. 5.11. SIGNAL INPUT V.S.W.R. AGAINST L.O. POWER.

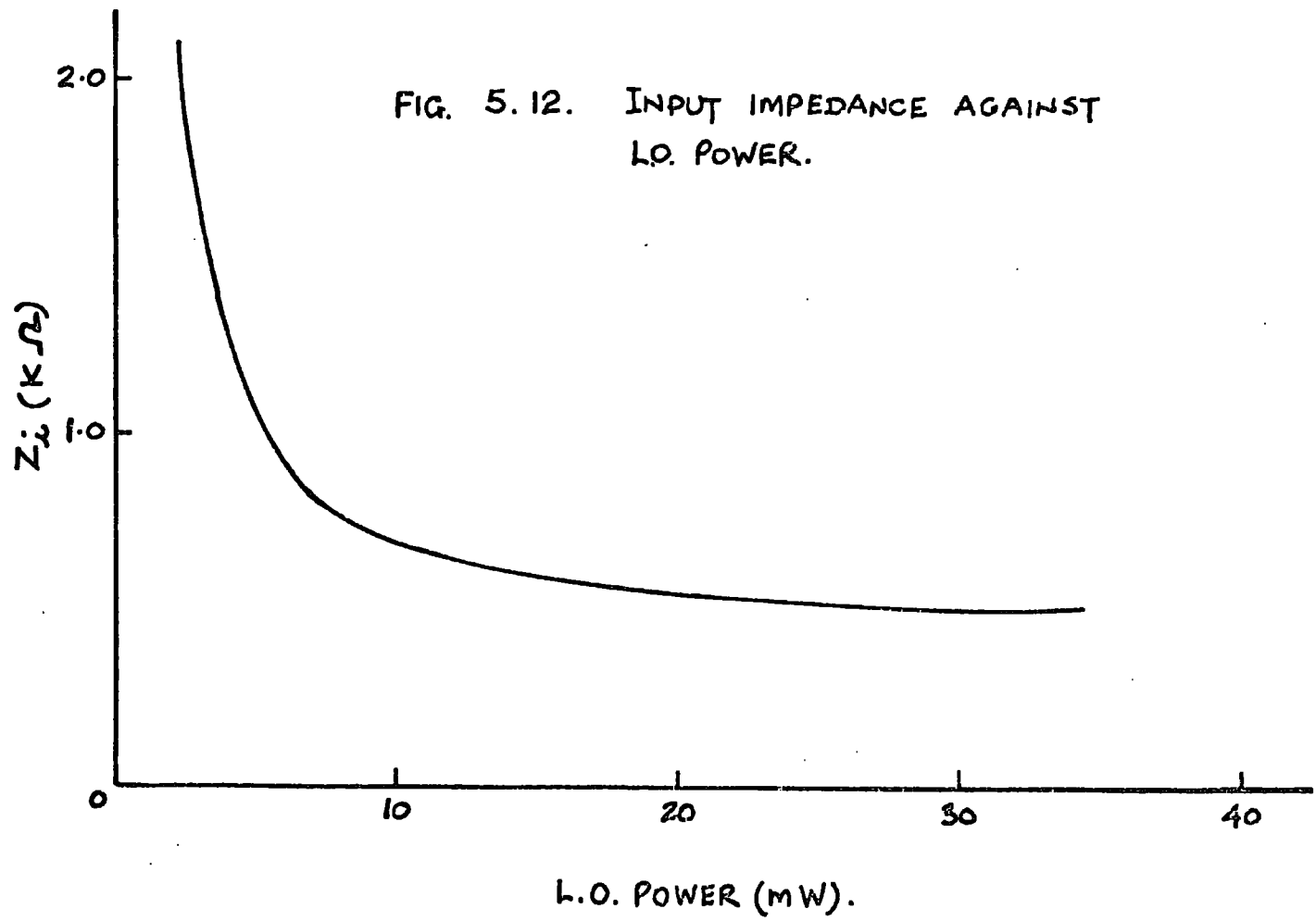

FIG. 5.12. INPUT IMPEDANCE AGAINST L.O. POWER.

By changing the signal frequency, the 3 dB bandwidth points at the i.f. were given at 17.5 MHz and 42.5 MHz; this corresponds to the signal frequencies of 1.535 GHz and 1.510 G Hz respectively (i.e. a 3 dB bandwidth of 25 MHz).

5.2.5 The Simulation of Diode Package Capacitance

The aim of this section was to find experimentally the effect that additional diode capacitance would have on the c.p.l. of the L-band mixer. Small "polyguide" capacitors were fabricated and a matched set of 4 selected to give values 0.24, 0.38, 0.42, 0.60 and 1.15pf(each value $\pm$ 2%), respectively.

These capacitors were placed across each diode of the lattice. The theoretical (c.p.l.) opt and R_L opt as functions of X are given in Figs. 5.13 and 5.14.

Because of the range of R_L and R_i over which the mixer was now required to function, the input and output were matched at every point when the c.p.l. was being measured. This was achieved at the input by the use of a three stub co-axial tuner, and at the output by a π reactive matching network. A conjugate match to the input of the quad of diodes was also obtained by adjusting capacitors C_2 and C_2' ; and at the output by adjusting the ferrite slug in the i.f. coil.

The introduction of additional diode capacitance also produced an increase in the capacitive susceptance as seen by the local oscillator. Thus a three stub tuner was found necessary to match the local oscillator circuit.

The experimental results obtained by the simulation of additional diode package capacitance is shown in Fig. 5.15.

FIG. 5.13. THE THEORETICAL (c p ℓ) opt AGAINST X.

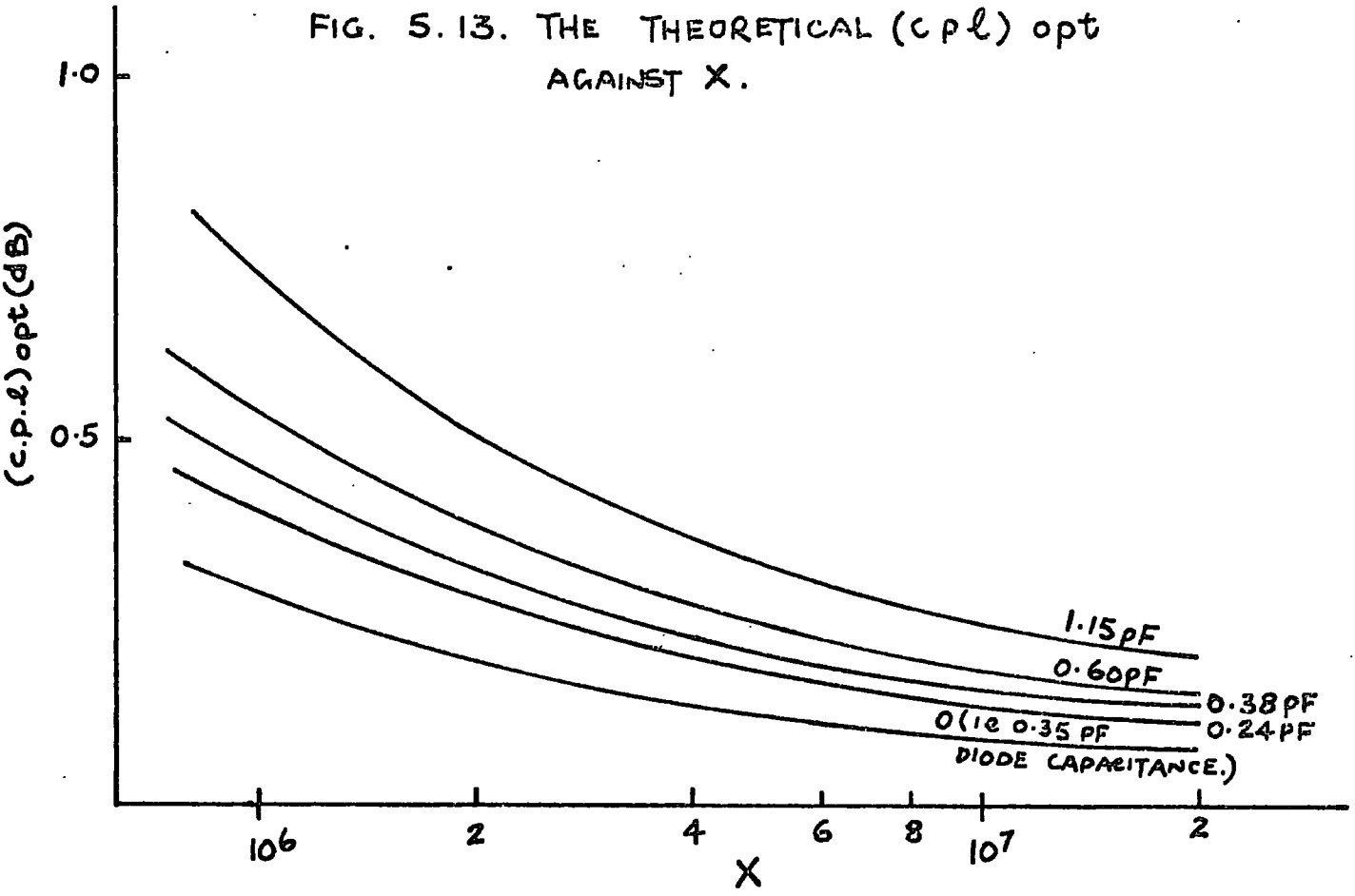

FIG. 5.14. THE THEORETICAL R_L (opt) AGAINST X.

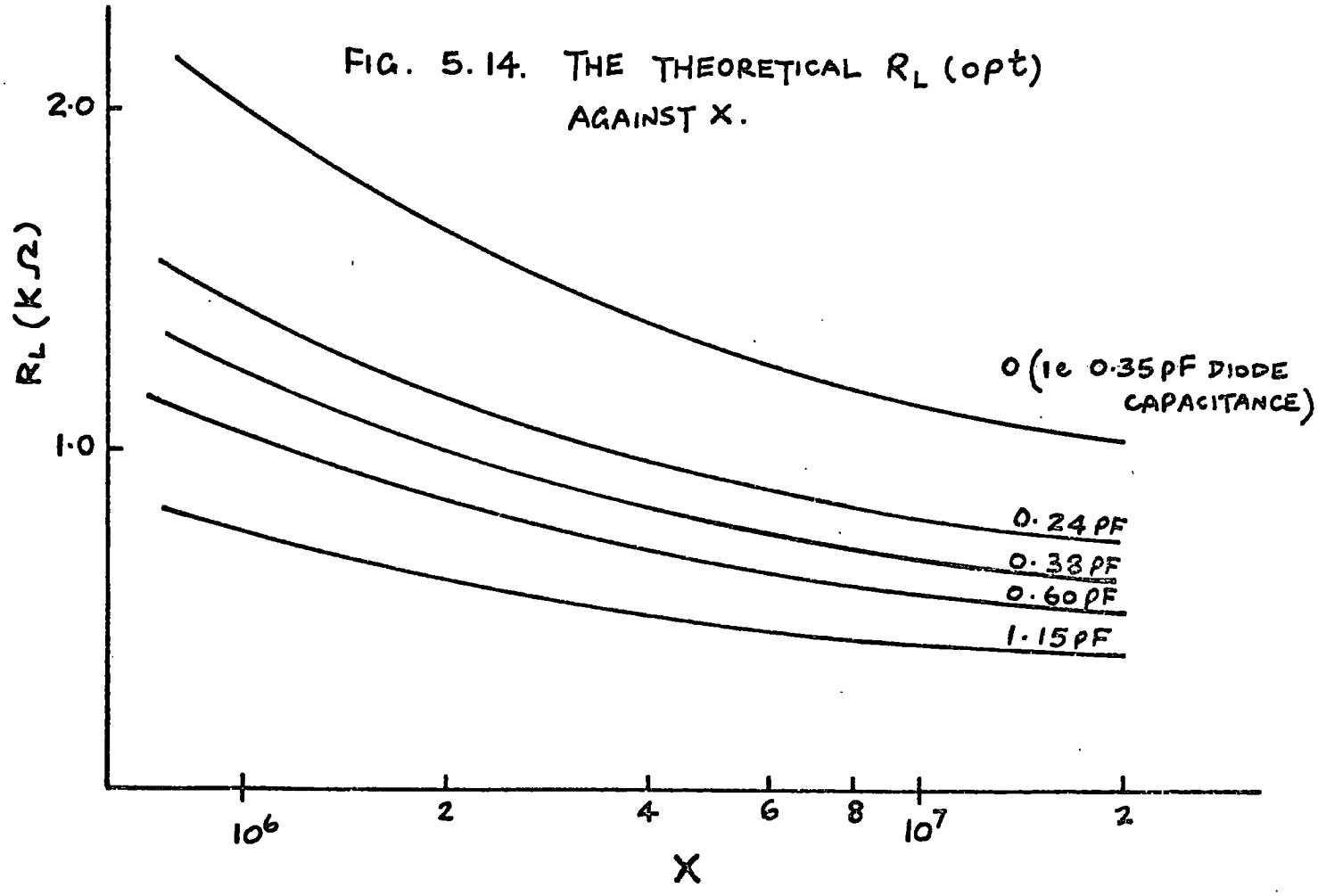

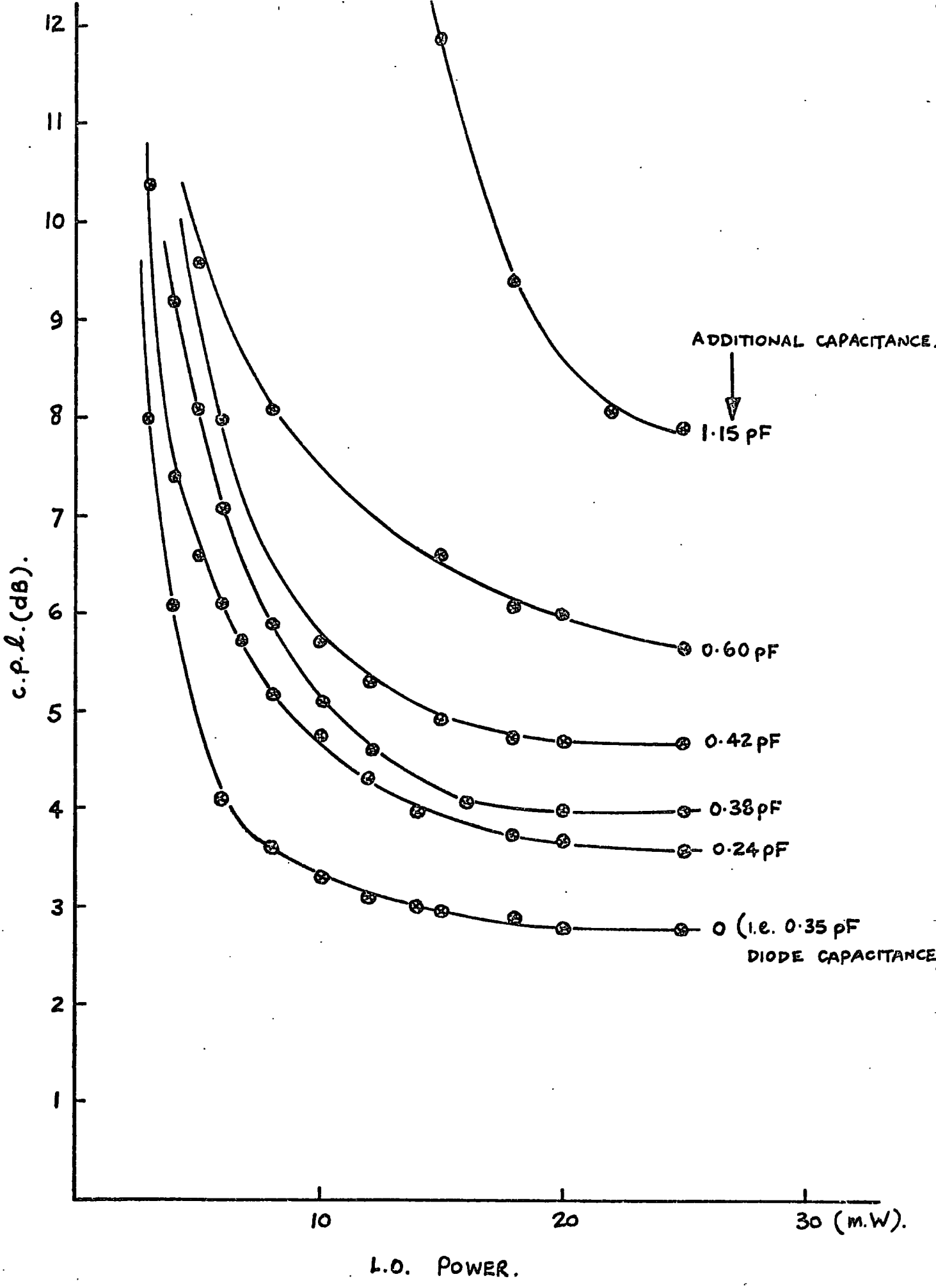

FIG. 5.15. THE SIMULATION OF ADDITIONAL DIODE CAPACITANCE.

5.3 Discussion of the L-band Mixer Results

5.3.1 The L-band Mixer Losses

The input equivalent circuit is given in Fig. 5.16. The resistive loss in the series resonant circuit (R) is calculated from the formula 2 in Appendix 5.

At the image frequency (1.5825 G Hz) the series resonant circuit will have an impedance of $(0.33 + j\,40)\Omega$. The input parallel resonant circuit will have a series equivalent impedance of $(93 - j\,169)\Omega$, the series losses in $2L_3$ can thus be neglected.

At the current drive of $X = 8 \cdot 10^6$, x is given as:

$$x = \frac{A_2}{2A_0} = -\frac{\ln 2x - 2}{\ln 2x + \pi r_s' X} \simeq -0.55$$

This then gives:

$R''_{-2} = 8.0$

$X''_{-2} = 11.1$, from which $|K| = 0.0628$ and $|K|^{\frac{1}{2}} = 0.25$.

The (c.p.l.) opt for this reactively terminated case is then given as 2.44 dB.

Had the mixer been a broad-band lattice mixer a c.p.l. of 3.6 dB would have been obtained. On the other hand a narrow-band short-circuit mixer would have given 3.75 dB. These latter two cases are given by Kulesza[4] and are shown as functions of X for two values of r_s' (i.e. the practical L-band mixer diodes $r_s' = 0.5 \times 10^{-6}$ and $r_s' = 0$) in Figs. 5.17 and 5.18.

Considering a broad-band mixer and non-ideal diodes, as the drive is increased the minimum loss levels off at 4.77 dB. For a narrow-band short-circuit mixer, as the drive is increased, the c.p.l. under matched conditions becomes independent of r_s' and in the limit is a constant loss of 7.65 dB.

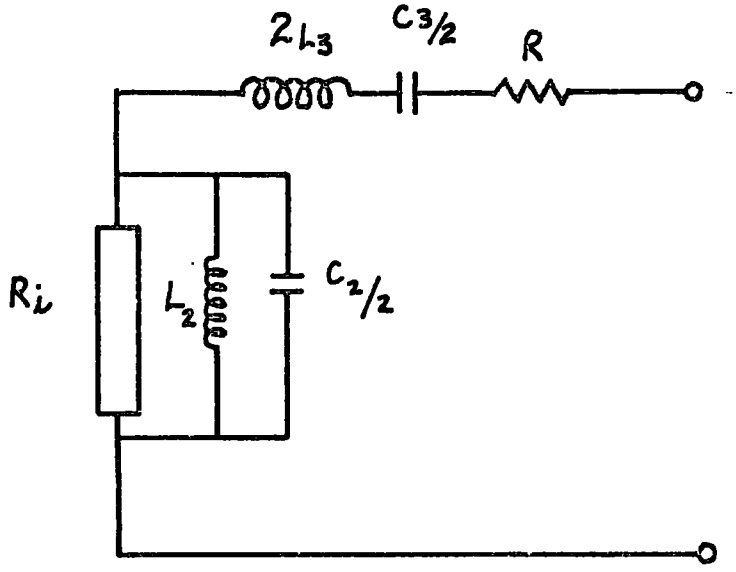

$R_i = 490\ \Omega$

$L_2 = 11{\cdot}7\ nH$

$\left(\frac{C_2}{2}\right) = 0{\cdot}65\ pF$

$2L_3 = 54{\cdot}6\ nH$

$\left(\frac{C_3}{2}\right) = 0{\cdot}20\ pF$

$R = 0{\cdot}33\ \Omega$

FIG. 5.16. THE INPUT EQUIVALENT CIRCUIT.

FIG. 5.17. BROAD BAND MIXER.
(THE THEORETICAL c.p.l. (opt) AGAINST X.)

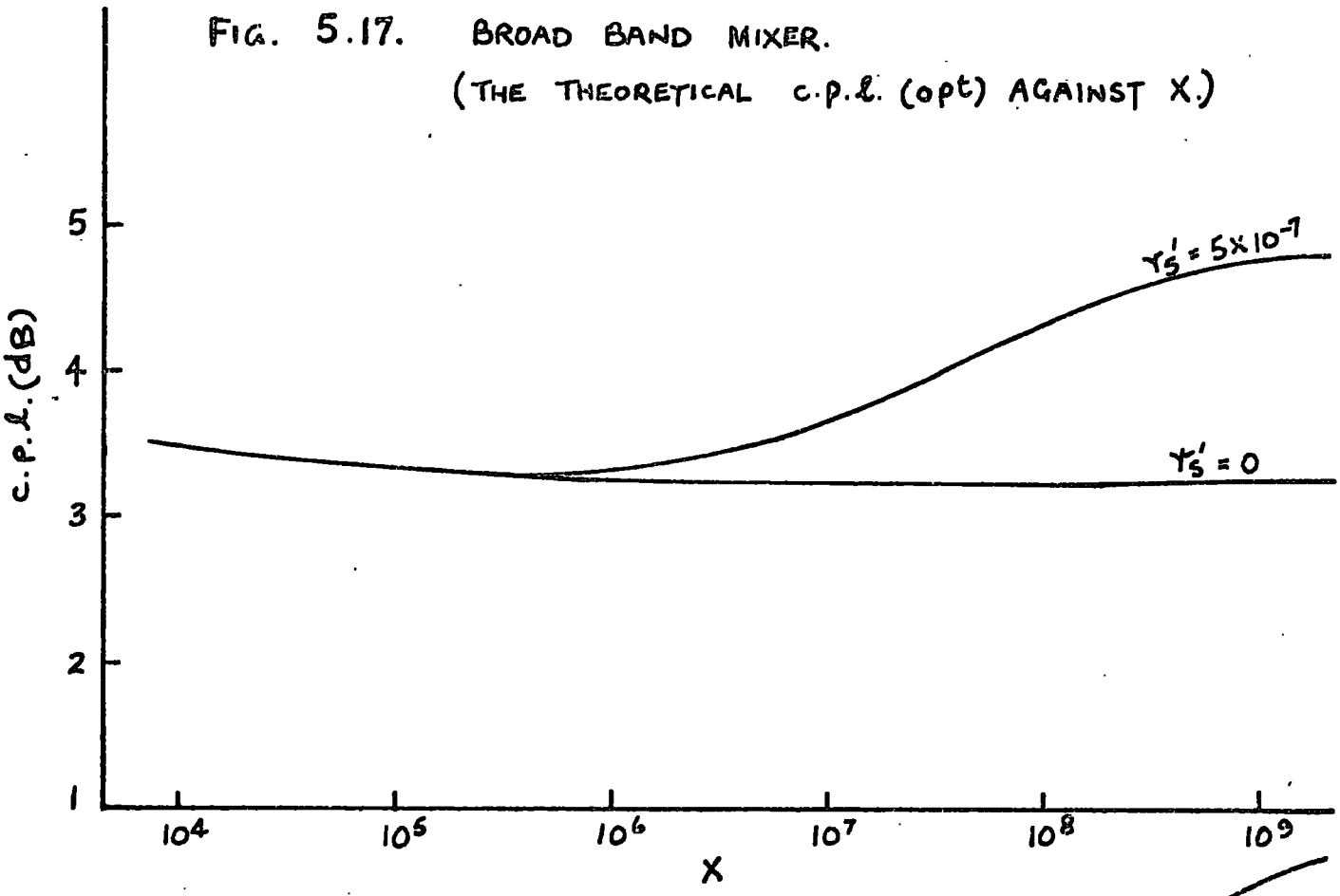

FIG. 5.18 NARROW-BAND SHORT-CIRCUIT MIXER.
(THE THEORETICAL c.p.l. (opt) AGAINST X.)

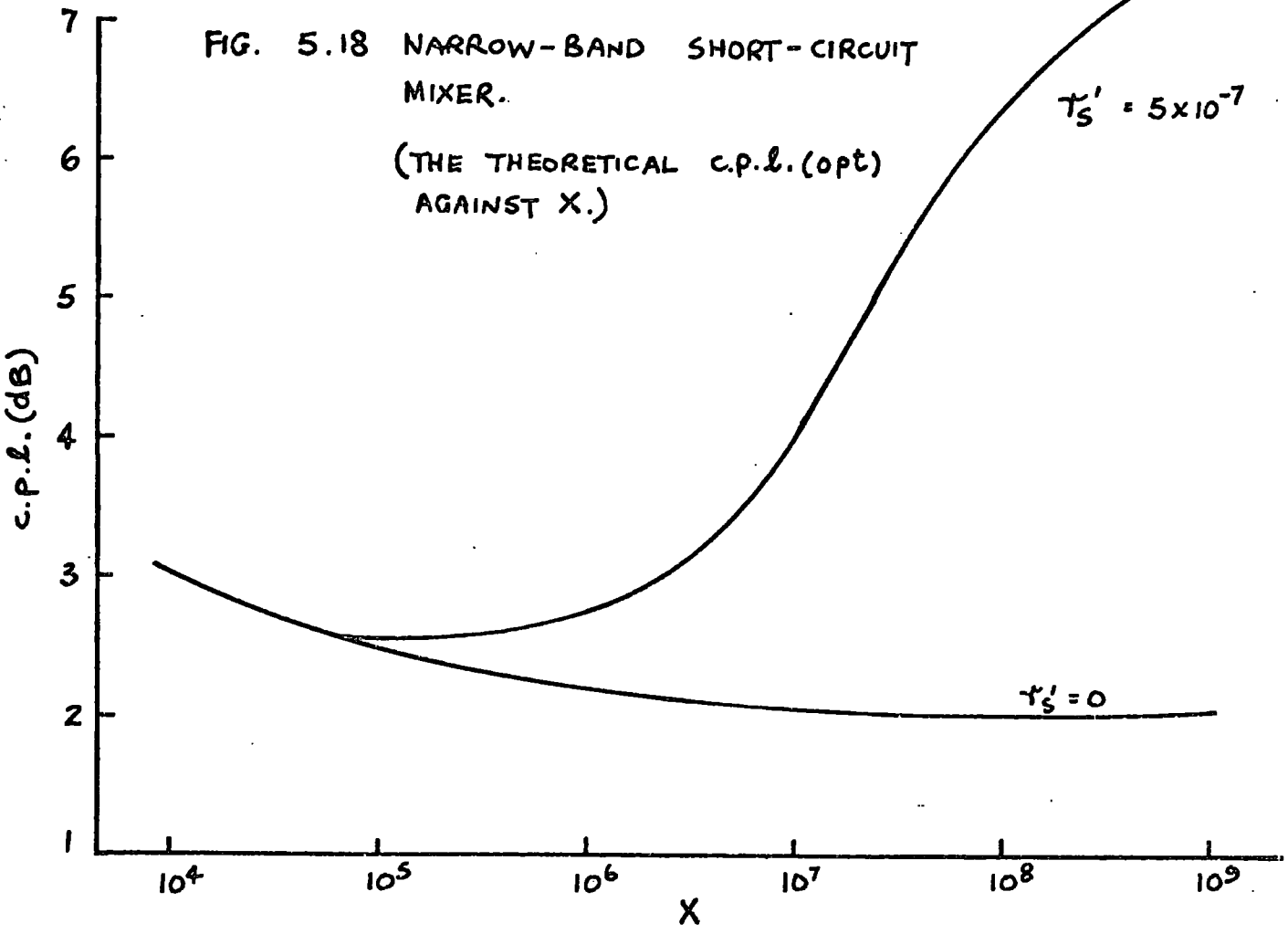

It is interesting to note how the experimental mixer could tend to either the narrow-band short-circuit or the broad-band case by a simple change of the input circuit. Had $\frac{C_2}{2}$ been much larger (i.e. a low reactance at the image frequency from the parallel resonant circuit), the mixer could have been considered as approximating to the narrow-band short-circuit case. Alternatively, if there had been no $\frac{C_2}{2}$ capacitance present the circuit could have been considered as approximating to the broad-band case.

If the losses in the i.f. coils are calculated from the Q figure results obtained at 30 MHz a loss of approximately 0.1 dB is obtained for the output transformer. A loss of 0.3 dB was obtained by connecting two transformers back-to-back. The discrepancy may be accounted for by the lead and transformer leakage inductances in the secondary. If a lead inductance of 25 nH is assumed this gives a value of approximately 0.6 for 'k' (the coefficient of coupling).

A further 0.10 dB loss is due to the presence of 0.35 pF diode package capacitance. Another 0.05 dB may be associated with the input V.S.W.R. of 1.2.

Thus the theoretical minimum c.p.l. is 2.9 dB, which compares favourably with the measured value of 2.8 dB.

5.3.2 The Simulation of Additional Diode Capacitance

The theoretical results for the (c.p.l.) opt. when different capacitors are placed across the diodes (as presented in Fig. 5.13) differ from those obtained in practice (as given in Fig. 5.15). The major differences between the theory and experiment have been accounted for in section 5.3.1.

For the case when large package capacitances are introduced into the practical L-band mixer, there are two considerations which have to be taken into account.

Firstly, the theory requires a sinusoidal local oscillator current drive. With increasing diode capacitance this becomes harder to achieve in practice when conducting experiments on a mixer constructed for only one value of diode capacitance.

Secondly, the required input and output matching terminations, over a large range of the additional package capacitance, proved difficult to obtain.

Ideally, a separate mixer should have been designed and constructed for each value of the package capacitance.

The experimental results did show the expected change in the c.p.l. when a replacement quad of diodes, with a higher package capacitance, was introduced into the L-band mixer.

5.4 Conclusion

The diode constants r_s, r_b, I_s and C were obtained from simple diode measurements. These constants were able to give directly, from the expressions obtained in the previous analysis, the local oscillator power, the optimum terminating impedances and the optimum conversion power loss.

The construction of the mixer using lumped circuit components (as compared with either stripline or cavity circuits) was found to have a number of advantages in its small size and low cost at L-band. A considerable amount of care in assembly had to be exercised when using lumped circuit techniques at these frequencies to minimise the stray reactances.

The mixer resulted in a minimum c.p.l. of 2.8 dB which compared favourably with a theoretical value of 2.9 dB. The major part of the loss being accounted for by the termination at the image frequency rather than due to the presence of parasitic diode capacitance (which was moderately high for these medium-priced diodes). The image in this

particular mixer, because of the secondary of the input transformer was a parallel resonance circuit, was terminated in a series combination of resistance and capacitance. This was confirmed by replacing the series resonant circuits at the signal frequency by the ones with twice the inductance and half the capacitance. This gave a c.p.l. of 2.95 dB at the same l.o. power level (X''_{-2} in this case was reduced from 11.1 to 8.6; R''_{-2} in both cases was 8.0)

A typical commercially available "low-loss" mixer at L-band is quoted with a c.p.l. of 6.5 dB[7]. Thus the mixer has shown a considerable improvement in performance over the commercial models.

The mixer has a great number of potential applications in the commercial, military and scientific fields, where low-loss frequency changer circuits are required. The capital out-lay for the equipment for diode measurements, mixer measurements and mixer construction could be low; in fact most of the test equipment should normally be available in electronics laboratories.

CHAPTER 6

Conclusions and Comments

6.0 Introduction

Each important aspect of the project will now be briefly reviewed and comparisons made, wherever possible, with other published work.

The non-linear diodes are essential to the mixing process and any improvements that may be made in the reduction of:

(a) the spreading resistance (r_s)

(b) the reverse saturation current (I_s)

and (c) the parasitic reactances

will, generally, also yield lower conversion power losses.

There are, naturally, alternative methods of analysing mixer circuits. Some of these approaches will be outlined.

Other workers have obtained microwave mixers with comparable or even lower c.p.l.s than the experimental L-band mixer described. The salient features of their mixers will be given.

6.1 The Mixer Diodes

Research into the methods of diode fabrication and materials technology have brought with it progressive improvements in the quality of mixer diodes.

One of the greatest achievements was the Schottky-barrier diode. The Si devices were found to have a lower spreading resistance and a better noise performance than the Si point contacts. The GaAs diodes, available commercially only within the last decade, have been found to have a lower reverse saturation current than the Si diodes; as low as 2×10^{-13} amp. has been estimated[9] as compared to approximately 5×10^{-9} amp. for the Si diodes used in the L-band mixer.

Some workers[1,2] prefer to specify the cut off frequency of the diode given by:

$$f_{co} = \frac{1}{2\pi C_j R_s} \quad \ldots 1$$

where C_j = the diode capacitance at zero bias

and R_s = the diode spreading resistance

For high frequency applications Si diodes are available with cut off frequencies up to 150 G Hz, and GaAs devices may theoretically attain up to 1000 G Hz due to an even lower R_s and C_j [2].

The introduction of special diode encapsulations, including beam lead, and leadless integrated constructions have reduced the package capacitance to values less than 0.05 pF.

The use of the cut off frequency (as defined in eqn. 1) as the sole parameter used to assess the mixer diodes' quality must be criticized. In frequency converting networks it is the non-linearity of the element which has to be considered (whether it be resistance, capacitance or even inductance), when a comparison is made. It is for this reason that the ratio of the diode spreading resistance to the slope resistance at the origin (i.e. r_s') used in the analysis by Kulesza [3] is the parameter which is chosen to represent the quality of the diode.

At higher frequencies the diode's parasitic reactances have to be accounted for. The best way to achieve this is to obtain the time varying incremental impedance from the diode's equivalent circuit and then to solve the equations of the network, rather than using f_{co} in the analysis. It is interesting to note that had GaAs diodes (which are usually more expensive than Si) been used in the L-band mixer, its performance would not have shown an improvement as most of the losses occurred in the image termination. With higher signal frequencies the effect of the parasitic

diode capacitance becomes more significant. Using the Si diodes, the input impedance of the lattice would be reduced and it may prove difficult to obtain the optimum input termination. For frequencies above approximately 4 G Hz (C-band) the use of GaAs diodes, with their inherently lower C and r_s', may show an improvement in the mixer performance.

6.2 The Analysis of a Lattice Mixer

6.2.1 The General Theory

The theoretical semiconductor diode equation has been shown by experience not to accurately apply to the forward V/I characteristics of practical diodes.

Some references are made in the literature[6,7] to the diode equation being expressed as:

$$I = I_s \left(\exp \frac{qV}{nkT} - 1 \right) \qquad \ldots 2$$

where 'n' is the ideality factor found by empirical methods. This equation gives a relatively poor agreement in practice especially for high forward currents, as no account is made for the spreading resistance.

The practical diode law as proposed by Kulesza[3] was an expression for the voltage which is an explicit function of the diode current. The mixer was thus chosen to be analysed driven by the l.o. current rather than voltage. Solutions were obtained for the network equations in terms of the Fourier coefficients. Approximations for practical diode constants and l.o. drive levels yielded expressions which could be calculated easily using a slide rule or hand calculator.

Some workers[4] have based their mixer analysis on the diode equation given by Crowell and Sze[5] i.e.:

$$I = I_s \left\{ \exp\left[\frac{q}{n' k T} (V - IR_s) \right] - 1 \right\} \qquad \ldots 3$$

Here the diode current is expressed as a function of the voltage. Schneider and Snell then assumed a sinusoidal local oscillator voltage which gave an expression for the diode current as an infinite series of modified Bessel functions. If this approach was applied to the analysis of the lattice mixer the expressions for the mixer parameters would not be so readily obtained.

6.2.2 The Analysis when Diode Capacitance is Present

The effect of parasitic diode reactances on the performance of microwave mixers has, generally, received little attention.

Torrey and Whitmer[8] in their analysis of a single diode mixer have considered a non-linear junction resistance (this case would correspond to Fig. 4.12(c)). Their analysis also assumed the theoretical semiconductor diode I/V characteristic and a sinusoidal local-oscillator drive. They found, theoretically, that at low local-oscillator drive levels that the diode capacitance was the principal factor limiting the performance of the mixer; as the drive inoreased, the effect of the capacitance on the c.p.l. was reduced. This was one of the conclusions obtained from the analysis of a lattice mixer in Chapter 4.

Other published work on the effects of diode capacitance on low-loss frequency changers (mainly modulators) has been referred to in section 4.2. They also have used approximations for the practical diode I/V forward characteristic in their analyses.

It is considered that the approach given in the analysis of a lattice mixer in Chapter 4, which used the practical diode V/I law and a sinusoidal current drive produced accurate results for the optimum terminations and c.p.l.'s of practical microwave mixers.

Perhaps a more elegant method of analysing the mixer when diode capacitance is present, would have been to have used 'K' parameters (as given by Kulesza[3]). Appendix 6 gives these 'K' parameters for the narrow-band open-circuit lattice mixer when diode package capacitance is considered.

The approach to the analysis as given in Chapter 4 does give the "physical picture" of the mixer circuit from the equations and does yield (when practical diodes and local oscillator drive levels are assumed) simple expressions which may be solved without having to resort to the use of a digital computer.

Any future work on the analysis of parasitic diode reactances in lattice mixers must include the image frequency component. The method followed in Chapter 4 may prove cumbersome when the image termination is considered and thus the 'K' parameters would be of great benefit in the solution of this particular case.

6.3 The Experimental Results and Other Mixers

In Chapter 5 a lumped circuit L-band mixer with a minimum c.p.l. of 2.8 dB at 20 mW local oscillator drive was described. Although this shows a considerable improvement over commercially available models, mixers have been constructed with c.p.l.'s as low or even lower than this; these will be considered in the following.

Johnson[7] has obtained a 4.1 dB c.p.l. for a short-circuit image, two diode, balanced mixer at 8.6 G Hz. This mixer was constructed using microstrip technique on an alumina substrate, and was approximately 0.7" by 0.45" in size.

A c.p.l. of 3.1 dB at 4.5 G Hz has been obtained by Wright, Emmett and Kulesza[9] for an open-circuit narrow-band lattice mixer constructed using end-loaded cavities and GaAs diodes. They found that using GaAs diodes gave an improvement of approximately 0.9 dB over Si.

More recently a mixer designed by Dickens and Maki[2] gave a c.p.l. of 2.6 dB at 9.6 G Hz. They described their mixer as being an "image and sum enhanced" two diode, balanced mixer; it would more correctly be described, however, as a narrow-band open-circuit mixer. (The 'sum' component they referred to is the frequency component $\omega_p + \omega_q$.) It used a combination of strip and slot lines on an alumina substrate with GaAs diodes.

A novel mixer described by Schneider and Snell[5] uses a local oscillator half the frequency that would normally be used in a conventional superhetrodyne. The two diodes in the balanced mixer were used as a 2 x multiplier of this frequency which then mixes with the signal frequency in the conventional way. A c.p.l. of 3.2 dB at 3.45 G Hz was reported for the mixer.

6.4 Future Work

Any future research programme should include noise investigations on the mixer.

One such method of approach would be to measure close-to-carrier amplitude modulated and frequency modulated noise components in a narrow-band width eg. 10 Hz on the signal and i.f. output, up to frequencies approximately 100 K Hz from the carrier. It is possible to measure such noise spectra on the signal with the system described by Ondria[10]. For measurements of the noise at the i.f. frequency a lumped-circuit version of this equipment could be built.

Any increase in the amplitude of the noise spectra of the i.f., compared with the signal, may be associated with either the flicker $\frac{1}{f}$, shot or thermal noise contribution from the mixer. If there was a deterioration in the close-to carrier noise this would probably be due to flicker noise in the mixer diodes. For frequencies greater than 10 K Hz from the carrier this $\frac{1}{f}$ noise component does not play such a dominant

part in the noise spectrum; so noise measurements above 10 K Hz could yield an indication of the shot and thermal noise components.

The development of low-loss mixers at X (6.2 G Hz - 10.9 G Hz) and even up to Q (33 G Hz - 46 G Hz) frequency bands would be a worthwhile project. In long distance communication systems, higher frequencies in X and J (up to 17.25 G Hz) are being demanded as it is possible to transmit more channels at this increased frequency. A more sensitive receiver at these and any other communication frequencies brings with it an improved performance of the system and the possibility of an increased range of reception. The shorter wavelengths enable higher definition radar systems to be built. A mixer with a lower loss would improve the range and performance of these.

6.5 Conclusion

The importance of a low-loss mixer in radar and long distance communication systems cannot be overemphasised. It was shown in section 1.0 that for a receiver that consisted basically of a mixer followed by an i.f. amplifier, the noise figure (and hence the sensitivity) of such a system is directly proportional to the conversion-power-loss of the mixer.

For a purely resistive mixer a c.p.l. below 3 dB cannot be obtained with a broad-band mixer circuit. The narrow-band open-circuit lattice mixer theoretically gives the maximum conversion efficiency. Although an infinite impedance at the image frequency cannot be achieved in practice, a low c.p.l. may be obtained even at low image rejection ratios.

The effect of diode parasitics on the performance of microwave mixers using practical diodes has not been previously investigated in any great detail. The importance of an analytical approach to the problem must be stressed. The results obtained in section 4.6 show that even a small amount of package capacitance (eg. 0.1 pF) can reduce R_L (opt) considerably (by a factor of 6.5 for this case). Any attempt to find the optimum

terminations by an empirical method could be time consuming and may not give the unique (c.p.l.) opt. Parasitic diode inductance was shown in section 4.3 to be of a secondary importance as compared to the capacitance as it may be included in the resonant circuits. The effect of the diode capacitance on the c.p.l. was more pronounced at low l.o. drives (i.e. $X < 10^6$). At higher l.o. power levels, used in practical mixers, the termination of the image frequency may have a greater contribution to the loss (this was the case in the L-band mixer).

Lumped circuits offered an advantage in the construction of the experimental mixer as they were inexpensive and small in size. At higher frequencies stray reactances become more important and cavity circuits or thick or thin film techniques would have to be employed. To obtain an experimental verification of the effects of diode capacitance a separate mixer would have to be built for each value of capacitance.

In the mixers described in paragraph 6.3 (excluding the lattice) a major part of the research and development effort has been directed towards the technology of fabricating the microwave circuits. The results obtained with the mixer described in Chapter 5 (i.e. 2.8 dB c.p.l. at 1.5 G Hz) and 3.1 dB at 4.5 G Hz [9] have shown that low-loss mixers may be obtained using a lattice of diodes in conjunction with readily constructed lumped or cavity circuits.

It is the inherent balanced configuration of the lattice mixer, together with the separation of the even order frequency components to the input of the lattice and odd order components to the output, that aids construction and filtering.

7. REFERENCES

7.1 References for Chapter 1

1. Friis, H.T.: 'Noise figures of radio receivers', Proc. Inst. Radio Engrs., 1944, 32, pp. 419— 422
2. Danglish, H.N. et al: 'Low-noise microwave amplifiers', Cambridge University Press (1968)
3. Faraday, M.: 'Experimental researches in electricity', Bernard Quaritch, London Vol. 1, pp. 122 - 124 (1833)
4. Becquerel, A.E.: 'On electric effects under the influences of solar radiation', Comptes Rendues de l'Academie des Sciences (Nov. 1839), Vol. 9, pp. 711 - 714
5. Braun, F.: 'Veber die stomleitung durch schwefelmstalle', Annalen der Physik und Chemie (1874), Vol. 153, No. 4, pp. 556 - 563
6. Schuster, A.: 'On unilateral conductivity', Phil. Mag., 1874, Vol. 48, pp. 251 - 257
7. Grondahl, L.O., and Geiger, P.H.: 'A new electronic rectifier', Trans. Am. I.E.E., Feb. 1927, Vol. 42, pp. 357 - 366
8. Hall, E.H.: 'On a new action of the magnet on electric current', Am. J. of Maths., Nov. 1879, Vol. 2, pp. 287 - 291
9. Bose, J.C.: U.S. patent 755840 (1904)
10. Dunwoody, H.H.C.: U.S. patent 837616 (1906)
11. Pickard, G.W.: U.S. patent 836531 (1906)
12. Pierce, G.W.: 'Crystal rectifiers for electric currents and electrical oscillators', Phys. Rev., July 1907, Vol. 25, pp. 31 - 60
13. Schottky, W., and Deutschmann, W.: Physic A., 1929, 30, p. 839
14. Torrey, H.C., and Whitmer, C.A.: 'Crystal rectifiers', (M.I.T. Press, 1948)
15. North, H.Q. et al: 'Wealded germanium crystals', G.E. Final Report Contract O.E. Msr. 262, Sept. 20, 1945

16. Bordeen, J., and Brattain, W.H.: 'The transistor, a semiconductor triode', Phys. Rev., July 1948, Vol. 74, pp. 230 - 231

17. Schockley, W.: 'The theory of p-n. junctions in semiconductors and p.n. junction transistors', Bell Syst. Tech. J., 1949, Vol. 28, pp. 435 - 489

18. Hall, R.N., and Dunlap, W.C.: 'p-n. junctions prepared by impurity diffusion', Phys. Rev., 1950, 80, pp. 867 - 868

19. Scaff, J.H., and Theurer, H.C.: US. patent 2, 567, 970, Sept. 1951

20. Pfann, W.G.: 'Principles of zone refining', Trans A.M. I. of Mining and Met. Engrs., 1952, 194, pp. 747 - 753

21. Meacham, L.A., and Micheals, S.E.: 'Observations of the rapid withdrawal of stored holes from germanium transistors and varistors', Phys. Rev, 78, p. 175

22. Pell, E.M.: 'Recombination rate in germanium by observation of pulsed reverse characteristics', Phys. Rev. 90, p. 278, 1953

23. Rhoderick, E.H.: 'The physics of schottky barriers', J. Phys. D., 1970, Vol. 3, pp. 1153 - 1167

24. Esaki, L.: 'New phenomenon in narrow germanium p-n. junctions', Phys. Rev., 1958, 109, pp. 603 - 604

25. Hall, R.N.: 'Tunnel diodes', I.R.F. Trans. E.D., 1960, E.D. 7, pp. 1 - 9

26. Van der Graff, J.: Unpublished report on modulators, Dr. Neter Laboratory, Netherlands Post and Telecommunication Service

27. Pound, R.V.: 'Microwave mixers', (M.I.T. Press, 1948)

7.2 References for Chapter 2

1. Kulesza, B.L.J.: 'General theory of a lattice mixer', Proc. I.E.E., 1971, 118 No. 7, pp. 864 - 870

2. Kulesza, B.L.J.: 'Broad-band and narrow-band lattice mixers', European Microwave Conference, 1971, Stockholm.

3. Belevitch, V.: 'Linear theory of bridge and ring modulator circuits', Elect. Commun., 1948, 25, p. 62

4. Tucker, D.G.: 'Modulators and frequency changes', (Macdonald 1953)

5. Howson, D.P., and Tucker, D.G.: 'Rectifier modulators with frequency-selective terminations', Proc. I.E.E., 1960, 107B, pp. 261 - 272

6. Van der Graff, J.: Unpublished report on modulators, Dr. Neter Laboratory, Netherlands Post and Telecommunication Service

7. Kulesza, B.L.J.: 'Characteristics of point contact Ge diodes', Memorandum 186, and Ph. D. thesis, Part I, Department of Electronic & Electrical Engineering, University of Birmingham, 1967

8. Armstrong, H.L.; Metz, E.D. and Weiman, I.: 'Design theory and experiments for abrupt hemispherical p-n junction diodes', I.R.E. Trans., 1956, Ed. 3, pp. 86 - 92

7.3 References for Chapter 3

1. Kulesza, B.L.J.: 'General theory of a lattice mixer', Proc. I.E.E., Vol. 118, No. 7, July 1971

2. H.P.A. Application Note No. 907: 'The hot carrier diode, theory, design and applications'

3. Rhoderick, E.H.: 'The physics of schottky barriers', J. Phys. D: Appl. Phys., 1970, Vol. 3

4. Blackwell, L.A., and Kotzebue, K.L.: 'Semiconductor-diode parametric amplifiers', Prentice-Hall, 1961

5. 'Handbook of microwave measurements', Vols. I and III edited by Sucher and Fox, Brooklyn Polytechnique Press

7.4 References for Chapter 4

1. Bartlett, A.C.: 'An extension of a property of artificial lines', Phil. Mag., Ser. 7, 4, p. 902 (1927)

2. Montgomery, C.G.: 'Principles of microwave circuits', Chapter 4, p. 110, M.I.T. Radiation Lab Series (1947)

3. Brune, O.: 'Notes on Bartlett's bisection theorum for four terminal networks', Phil. Mag., Ser. 7, 14, p. 806 (1932)

4. Tucker, D.G.: 'Losses in a lattice switch', University of Birmingham, Dept. of Electronic & Electrical Engineering, memorandum 309, June 1967

5. Kruse, S.: 'Theory of rectifier modulators', Ericsson Technics, No. 2, p. 17 (1939)

6. Belevitch, V.: 'Théorie des circuits non linéaires en régime alternatif', Librairie Universitaire Uystpruyst, Louvain, 1959, Chapter 4, p. 85

7. Belevitch, V.: 'Linear theory of bridge and ring modulator circuits', Elect. Comm. 25, p. 62 (1948)

8. Kulesza, B.L.J.: 'General theory of a lattice mixer', Proc. I.E.E., Vol. 118, No. 7, p. 864, July 1971

9. Korn, G.A., and Korn, T.M.: 'Manual of mathematics', p. 18, McGraw-Hill (1967)

10. Kulesza, B.L.J.: 'Broad-band and narrow-band lattice mixers', Proc. 1971, European Microwave Conference, Vol I, A11/2:1

7.5 References for Chapter 5

1. Hewlett-Packard; 'Components - diodes and microwave products', January, 1971

2. Hewlett-Packard Applications Note 907: 'The hot carrier diode, theory design and applications'

3. Kulesza, B.L.J.: 'General theory of a lattice mixer', Proc. I.E.E., 1971, Vol. 118, No. 7, pp. 864 - 870

4. Kulesza, B.L.J.: 'Broad-band and narrow-band lattice mixers', European Microwave Conference, Stockholm, 1971

5. Gregory, J.F.: 'Strip transmission lines', Solid State Microwave Electronics research group, Durham University, memorandum No. 1

6. Wright, J.P., Emmett, J.R., and Kulesza, B.L.J.: '4.5 G H_z narrow-band open-circuit lattice mixers', European Microwave Conference, Stockholm, 1971

7. Anoren Microwave Inc.: Product Catalog, March 1971

7.6 References for Chapter 6

1. Watson, H.A.: 'Microwave semiconductor devices and their circuit applications', (McGraw-Hill, 1969)

2. Dickens, L.E., and Maki, D.W.: 'An integrated-circuit balanced mixer, image and sum enhanced', I.E.E.E. Trans. M.T.T., 23, No. 3, March 1975, pp. 276 - 281

3. Kulesza, B.L.J.; 'General theory of a lattice mixer', Proc. I.E.E., Vol. 118, No. 7, July 1971

4. Schneider, M.W., and Snell, W.W.: 'Harmonically pumped stripline down converter', I.E.E.E. Trans. M.T.T., 23, No. 3, March 1975, pp. 271 - 275

5. Crowell, C.R., and Sze, S.M.: 'Current transport in metal-semiconductor barriers', Solid-State Electronics, Vol. 9, pp. 1035 - 1048, Nov/Dec 1966

6. Hewlett-Packard Application Note 907; 'The hot carrier diode, theory, design and application', May 1967

7. Johnson, K.M.: 'X-band integrated-circuit mixer with reactively terminated image', I.E.E.E. Trans. M.T.T., 16, No. 7, July 1968

8. Torrey, H.C., and Whitmer, C.A.: 'Crystal rectifiers', (M.I.T. Press, 1948), p. 157

9. Wright, J.P., Emmett, J.R., and Kulesza, B.L.J.: '4.5 GH_z narrow-band open-circuit lattice mixer', European Microwave Conference, Stockholm, 1971

10. Ondria, J.G.: 'A microwave system for measurements of AM and FM noise spectra', I.E.E.E. Trans. 1968 M.T.T., 16, No. 9, pp. 767 - 781

7.7 References for Appendices

1. Bois, G.P.: 'Tables of indefinite integrals', Dover (1961)

2. Froberg, C.-E.: 'Introduction to numerical analysis', Addison-Wesley (1965), p. 217

3. Terman, F.E.: 'Radio engineer's handbook', McGraw-Hill (1943)

4. Kulesza, B.L.J., Private communication

8. THE APPENDICES

8.1 Appendix 1 The General Fourier Coefficients

Equating the real and imaginary components in eqn. 1 of chapter 4 results in the two expressions:

$$v_s = r_b\left\{\sum_{n\ \text{even}} A_n \cos n\omega_p t\right\}\mathcal{R}e(i_s) + \left\{\sum_{n\ \text{odd}} A_n \cos n\omega_p t\right\}\mathcal{R}e(v_L)$$

and

$$v_s\omega_s C = \mathcal{I}_m(i_s) + \left\{\frac{1}{r_b}\sum_{n\ \text{odd}} B_n \cos n\omega_p t\right\}\mathcal{I}_m(v_L)$$

Similarly equating the real and imaginary components in eqn. 2 gives:

$$i_L = \left\{\sum_{n\ \text{odd}} A_n \cos n\omega_p t\right\}\mathcal{R}e(i_s) - \left\{\sum_{n\ \text{even}} A'_n \cos n\omega_p t - \omega_s^2 C^2 r_b \sum_{n\ \text{even}} A_n \cos n\omega_p t\right\}\mathcal{R}e(v_L)$$

$$+ 2\omega_L C\,\mathcal{I}_m(v_L)$$

and

$$i_L\omega_L C = \left\{\frac{1}{r_b}\sum_{n\ \text{odd}} B_n \cos n\omega_p t\right\}\mathcal{I}_m(i_s) - \left\{\frac{\omega_L C}{r_b}\sum_{n\ \text{even}} D_n \cos n\omega_p t\right\}\mathcal{R}e(v_L)$$

$$- \frac{1}{r_b^2}\left\{\sum_{n\ \text{even}} E_n \cos n\omega_p t - \omega_L^2 C^2 r_b^2\right\}\mathcal{I}_m(v_L)$$

Solutions of the integrals for the required Fourier coefficients

$$B_n = \frac{1}{\pi}\int_{-\frac{\pi}{2}}^{\frac{3\pi}{2}} \frac{X(t)\cos n\omega_p t\,.\,d\omega_p t}{1 + 2r'_s\left[1 + X(t)\,S(t)\right]} \qquad \text{where n is odd}$$

Thus

$$B_1 = \frac{1}{\pi}\int_{-\frac{\pi}{2}}^{\frac{3\pi}{2}} \frac{X \cos^2 \omega_p t \, d\omega_p t}{1 + 2r_s' \left[1 + X(t)\, S(t)\right]}$$

Generally for the integral:

$$\int \frac{\cos^2 x \, dx}{a + b \cos x}$$

The solution is given by Bois[1] as:

$$\frac{a^2}{b^2}\int \frac{dx}{a + b \cos x} - \frac{a}{b^2}\int dx + \frac{1}{b}\int \cos x \, dx$$

The solution to the integral:

$$\int \frac{dx}{a + b \cos x} = \frac{2}{(a^2 - b^2)^{\frac{1}{2}}} \tan^{-1}\left\{\left(\frac{a - b}{a + b}\right)^{\frac{1}{2}} \tan \frac{x}{2}\right\} \quad \text{for} \quad a > b$$

and

$$= \frac{1}{(b^2 - a^2)^{\frac{1}{2}}} \ln\left\{\frac{(b + a)^{\frac{1}{2}} + (b - a)^{\frac{1}{2}} \tan \frac{x}{2}}{(b + a)^{\frac{1}{2}} - (b - a)^{\frac{1}{2}} \tan \frac{x}{2}}\right\} \quad \text{for} \quad a < b$$

The solution for B_1 is thus given by:

$$\frac{1}{r_s'}\left\{\frac{2}{\pi r_s' X (1 - 4r_s'^2 X^2)^{\frac{1}{2}}} \tan^{-1}\left[\frac{1 - 2r_s' X}{1 + 2r_s' X}\right]^{\frac{1}{2}} - \frac{1}{2r_s' X} + \frac{2}{\pi}\right\} \quad 1 > 2r_s' X$$

and,

$$\frac{1}{r_s'}\left\{\frac{1}{r_s' X (4r_s'^2X^2 - 1)^{\frac{1}{2}}} \ln\left[2r_s' X + (4r_s'^2 X^2 - 1)^{\frac{1}{2}}\right] - \frac{1}{2r_s' X} + \frac{2}{\pi}\right\} \quad 2r_s'X > 1$$

$$D_0 = \frac{1}{2\pi}\int_{-\frac{\pi}{2}}^{\frac{3\pi}{2}} \frac{2(1 + X\cos\omega_p t\, S(t))\, d\omega_p t}{1 + 2r_s' X \cos\omega_p t.\, S(t)}$$

$$E_0 = \frac{1}{2\pi}\int_{-\frac{\pi}{2}}^{\frac{3\pi}{2}} \frac{1 + 2X\cos\omega_p t\, S(t)\, d\omega_p t}{1 + 2r_s' X\cos\omega_p t.\, S(t)}$$

The solutions to the above integrals are found by the same approach as for B_1. For $r_s' < 10^{-3}$ and $X > 10^3$

$$D_0 = E_0 = \frac{1}{r_s'}\left\{1 - \frac{4}{\pi(1 - 4r_s'^2 X^2)^{\frac{1}{2}}} \tan^{-1}\left[\frac{1 - 2r_s' X}{1 + 2r_s' X}\right]^{\frac{1}{2}}\right\} \qquad 1 > 2r_s' X$$

$$= \frac{1}{r_s'}\left\{1 - \frac{2}{\pi(4r_s'^2 X^2 - 1)^{\frac{1}{2}}} \ln\left[2r_s' X + (4r_s'^2 X^2 - 1)^{\frac{1}{2}}\right]\right\} \qquad 2r_s' X > 1$$

8.2 Appendix 2 The Fourier Coefficients for the Local Oscillator Circuit

$$Q_0 = \frac{1}{2\pi(1 + 2j\omega_p Cr_s)} \int_{-\frac{3}{2}}^{\frac{3}{2}} \left\{ (1 - 2r_s' a) \left(\frac{1}{a + X(t).S(t)} \right) + 2r_s' \right\} d\omega_p t$$

where $a = \dfrac{1 + j\omega_p Cr_b}{1 + 2j\omega_p Cr_s}$

For most practical cases $2r_s' / a / \ll 1$

Thus $$Q_0 = \frac{1}{(1 + 2j\omega_p Cr_s)} \left[2r_s' + \frac{1}{2\pi} \int_{-\frac{\pi}{2}}^{\frac{3\pi}{2}} \frac{d\omega_p t}{a + X(t).S(t)} \right]$$

$$\therefore \quad Q_0 = \frac{1}{(1 + 2j\omega_p Cr_s)} \left[2r_s' + \frac{1}{\pi(X^2 - a^2)^{\frac{1}{2}}} \ln\left(\frac{4X^2 - a}{a} \right) \right]$$

Similarly

$$Q_2 = \frac{1}{(1 + 2j\omega_p Cr_s)} \left[\frac{1}{\pi} \int_{-\frac{\pi}{2}}^{\frac{3\pi}{2}} \frac{\cos 2\omega_p t}{a + X(t).S(t)} \right]$$

$$= \frac{8}{\pi X} - \frac{2}{\pi(X^2 - a^2)^{\frac{1}{2}}} \ln\left(\frac{4X^2 - a}{a} \right) - \frac{4a}{X^2} + \frac{4}{\pi X^2 (X^2 - a^2)^{\frac{1}{2}}} \ln\left(\frac{4X^2 - a}{a} \right)$$

For practical values:

$$Q_2 \approx \frac{8}{\pi X} - \frac{2}{\pi(X^2 - a^2)^{\frac{1}{2}}} \ln\left(\frac{4X^2 - a}{a} \right)$$

8.3 Appendix 3 Summation of the Fourier Coefficients

Introduction

One approach to an analytical solution of the effect of the diode capacitance on the performance of an open-circuit lattice mixer required the solution of:

$$\sum_{n=0}^{\infty} A_n \qquad \text{for } n = 0, 2, 4 \ldots (\text{even})$$

Although, there was found to be an error in one of the assumptions and the analysis abandoned; the solution to the problem yields an elegant answer which may be of use to future work.

Solution

For n = 0

we have

$$A_0 = 2r_s' + \frac{1}{2\pi} \int_{-\frac{\pi}{2}}^{\frac{3\pi}{2}} \frac{d\omega_p t}{1 + X(t).S(t)}$$

The solution is:

$$A_0 = 2r_s' + \frac{2}{\pi X} \ln 2X$$

For n = 2, 4, 6 ... even

$$A_n = \frac{1}{\pi} \int_{-\frac{\pi}{2}}^{\frac{3\pi}{2}} \frac{\cos n\omega_p t}{1 + X(t).S(t)} d\omega_p t$$

The integrand is expressed as a power series of the form:

$$\frac{\cos^m \omega_p t}{1 + X(t)}$$

These terms can be expressed as:

$$\frac{1}{X^m}\left\{ X^{m-1} \cos^{m-1} \omega_p t - X^{m-2} \cos^{m-2} \omega_p t + X^{m-3} \cos^{m-3} \omega_p t - \ldots + \frac{(-1)^m 1}{1 + X \cos \omega_p t} \right\}$$

As $X \gg 10^3$ only integrals multiplied by the highest term in X, which is $\frac{1}{X}$, are considered for the evaluation.

The coefficients calculated by this method, up to and including A_{10}, are shown below:

$$A_2 = \frac{8}{\pi X} - \frac{4}{\pi X} \ln 2X$$

$$A_4 = \frac{4}{\pi X} \ln 2X - \frac{32}{3\pi X}$$

$$A_6 = \frac{184}{15\pi X} - \frac{4}{\pi X} \ln 2X$$

$$A_8 = \frac{4}{\pi X} \ln 2X - \frac{1408}{105\pi X}$$

$$A_{10} = \frac{4504}{315\pi X} - \frac{4}{\pi X} \ln 2X$$

Together with A_0, the coefficients form a slowly converging series which can be summed to infinity using Euler[2]'s transformation

As a result:

$$\sum_{n=0,2,4 \text{ even}} A_n = 2r_s' + \frac{1}{X}$$

8.4 Appendix 4 Measurement Techniques

(a) Measurement of V.S.W.R. at low power levels (by the return loss method)

A slotted line, which operated at the signal frequency was not available; so another method had to be devised for the measurement of the input V.S.W.R. of the mixer. The Apparatus is shown in Fig. A.1. The 10 dB attenuator was found necessary to prevent any reflections between the spectrum analyser and the dual directional coupler.

A comparison of the power levels at the two ports of the directional coupler was obtained using the switched i.f. attenuators of the spectrum analyser. Interpolation was possible between the 1 dB steps of the attenuator. The magnitude of the reflection coefficient is given by:

$$|\Gamma| = \left(\frac{Pr}{Pi}\right)^{\frac{1}{2}}$$

where Pr = reflected power

Pi = incident power

If the ratio between Pr and Pi is 'a' dB, measured on the spectrum analyser, then,

$$|\Gamma| = 10^{-\frac{a}{20}}$$

The V.S.W.R. is then given by:

$$\text{V.S.W.R.} = \frac{1 + |\Gamma|}{1 - |\Gamma|}$$

A graph of V.S.W.R. plotted against 'a' is shown in Fig. A.2

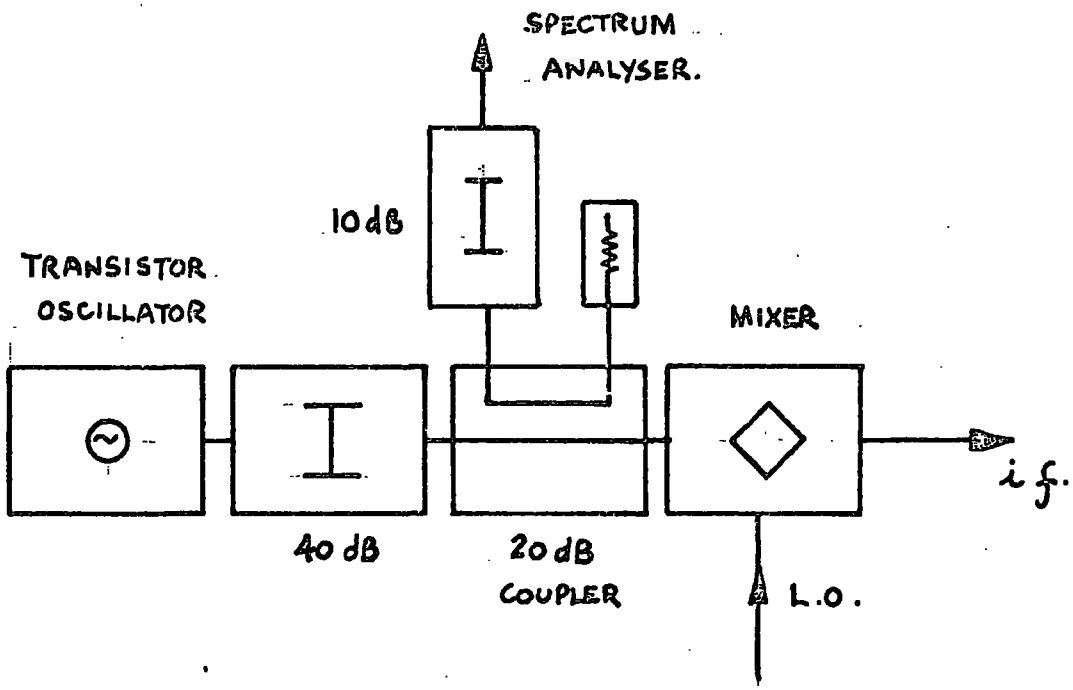

FIG. A1. THE MEASUREMENT OF THE INPUT V.S.W.R.

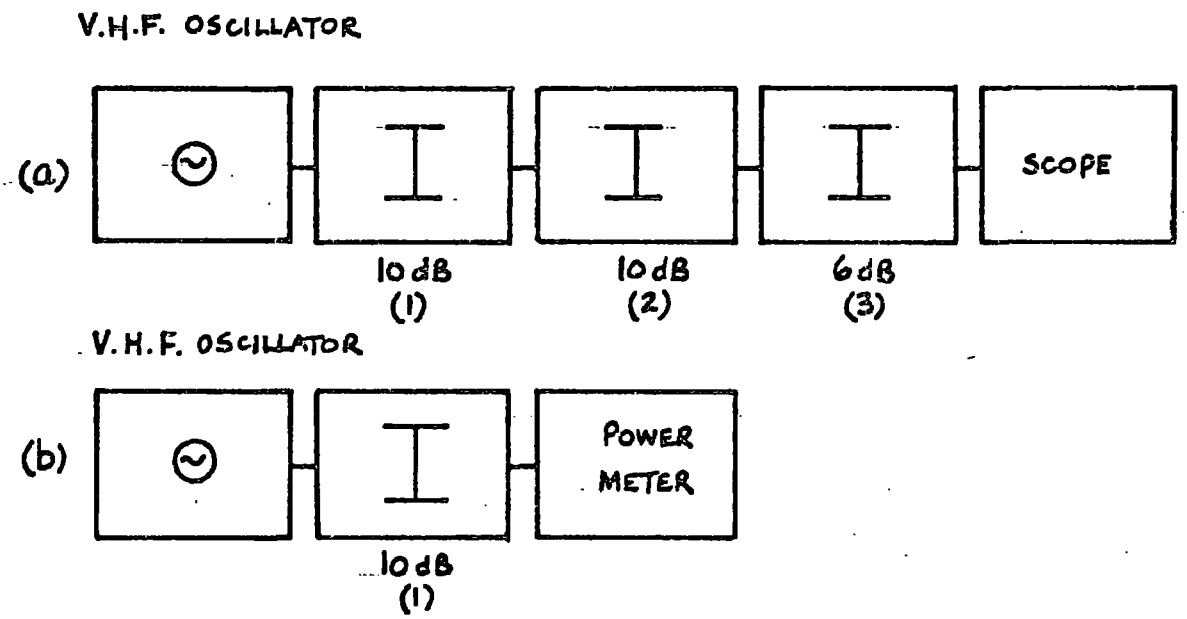

FIG. A3. THE CALIBRATION OF THE i.f. POWER MEASURING SYSTEM.

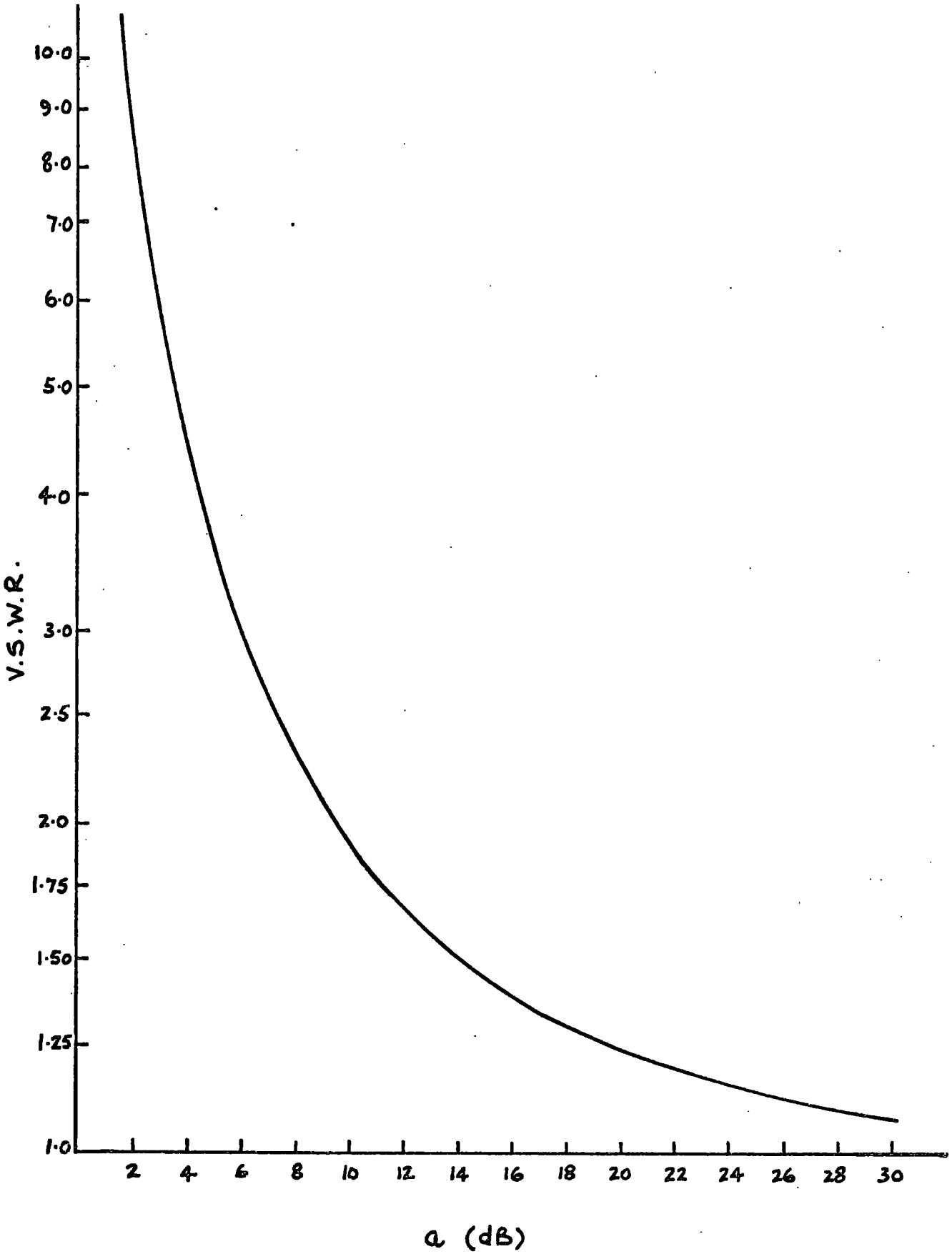

FIG. A2 THE V.S.W.R. AGAINST THE RETURN LOSS (a).

(b) Calibration of the i.f. power measuring system

Errors in the c.p.l. measurements, at the start of the experimental work, were found to be due to errors in the calibration of the i.f. power measuring system. It is thus thought important enough to warrant a short section on this measurement.

The measuring apparatus is shown diagrammatically in Fig. A.3(i). The U.H.F. oscillator had a piston attenuator output which was not a 50Ω impedance. The piston attenuator was adjusted to give the required peak to peak display on the oscilloscope. The power level at the input of attenuator 3 was $\leqslant 10\,\mu W$ and could not be reliably measured on the most sensitive range of the power meter. The power, instead, was measured at the output of attenuator 1, and from an accurate calibration of attenuator 2, the power at the input of attenuator 3 of the i.f. power measuring equipment could then be calculated.

A.5 Appendix 5 Lumped Circuit Formulae

The inductance of a straight wire is given to a good approximation by:[1]

$$L = 5.08 \cdot 10^{-3} \ell \left\{ \ln \frac{4\ell}{d} - 1 \right\} \mu H \qquad \ldots 1$$

where

ℓ is its length in inches

d is its diameter in inches

The resistance of a round copper wire as a frequency of f H_z

$$= \frac{83.2 \cdot f^{\frac{1}{2}} \cdot 10^{-9}}{d} \text{ ohms/cm} \qquad \ldots 2$$

where

d is the diameter in cms

The capacitance of two parallel plates is given as

$$C = 0.0885 \varepsilon_r \frac{A}{d} \text{ pF} \qquad \ldots 3$$

where

A = area of plates in cm^2

d = separation of the plates in cms.

ε_r = dielectric constant of the dielectric

A.6 Appendix 6 The 'K' Parameter Solution

In the following, the analysis, of the narrow-band open-circuit lattice mixer (when diode package capacitance is present), is considered using 'K' parameters.

Eqns. 1 and 2 of Chapter 4 have to be solved to obtain the K parameters as follows:

$$v_q = i_q r_b K_1 + v_{-1} (K_q)^{\frac{1}{2}} \quad \ldots 1$$

$$i_{-1} = i_q (K_{-1})^{\frac{1}{2}} - v_{-1} \frac{1}{r_b} K_2 \quad \ldots 2$$

where

$$K_3 = (K_q)^{\frac{1}{2}} (K_{-1})^{\frac{1}{2}} \quad \ldots 3$$

Thus:

$$K_1 = \frac{1}{2\pi} \int_{-\frac{\pi}{2}}^{\frac{3\pi}{2}} \frac{1 + 2r_s' X \cos \omega_p t . S(t) \, d\omega_p t}{(1 + j\omega_q C r_b) + X(1 + j 2\omega_q C r_s) \cos \omega_p t \, S(t)}$$

$$= \frac{1}{2\pi(1 + j 2\omega_q C r_s)} \left[2 r_s' + \frac{(1 - 2 r_s' b)}{\pi (X^2 - b^2)^{\frac{1}{2}}} \ln \left\{ \frac{4X^2 - b}{b} \right\} \right]$$

where

$$b = \frac{1 + j\omega_q C r_b}{1 + j 2\omega_q C r_s}$$

$$(K_q)^{\frac{1}{2}} = \frac{1}{\pi} \int_{-\frac{\pi}{2}}^{\frac{3\pi}{2}} \frac{X \cos^2 \omega_p t \, d\omega_p t}{(1 + j\omega_q C r_b) + X(1 + j 2\omega_q C r_s) \cos \omega_p t . S(t)}$$

$$= \frac{2}{\pi(1 + j\,2\omega_q C r_s)} \left\{ 2 - \frac{\pi b}{4X} + \frac{b^2}{X} \left[\frac{1 - 2r_s' b}{\pi (X^2 - b^2)^{\frac{1}{2}}} \ln \left(\frac{4X^2 - b}{b} \right) \right] \right\}$$

For practical drive levels (i.e. between 10^4 and 10^7) this becomes:

$$(K_q)^{\frac{1}{2}} = \frac{4}{\pi(1 + j\,2\omega_q C r_s)}$$

$$(K_{-1})^{\frac{1}{2}} = \frac{1}{\pi} \int_{-\frac{\pi}{2}}^{\frac{3\pi}{2}} \frac{X \cos^2 \omega_p t \; d\omega_p t}{(1 + j\,\omega_{-1} C r_b) + X(1 + j\,2\omega_{-1} C r_s) \cos \omega_p t . S(t)}$$

$$= \frac{2}{(1 + j\,2\omega_{-1} C r_s)} \left\{ 2 - \frac{\pi d}{4X} + \frac{d^2}{X} \left[\frac{1 - 2r_s' d}{\pi (X^2 - d^2)^{\frac{1}{2}}} \ln \left(\frac{4X^2 - d}{d} \right) \right] \right\}$$

where

$$d = \frac{1 + j\,\omega_{-1} C r_b}{1 + j\,2\omega_{-1} C r_s}$$

Again, for practical drive levels:

$$(K_{-1})^{\frac{1}{2}} = \frac{4}{(1 + j\,2\omega_{-1} C r_s)}$$

$$K_2 = 2 - \frac{1}{2\pi} \int_{-\frac{\pi}{2}}^{\frac{3\pi}{2}} \frac{d\omega_p t}{1 + X \cos \omega_p t . S(t)} + j\,\omega_{-1} C r_b$$

$$- \omega_{-1}^2 C^2 r_b \left(1 - \int_{-\frac{\pi}{2}}^{\frac{3\pi}{2}} \frac{X \cos \omega_p t}{1 + X \cos \omega_p t . S(t)} \right)$$

For practical drive levels and practical mixer diodes (i.e. $r'_s < 10^{-4}$)

$$K_{2} = 2 + j\omega_{-1} C r_b$$

8.7 Appendix 7 The General Theory of a Lattice Mixer

The mixer-network equations in terms of the time varying resistances are:

$$v_s = i_s \frac{2 r_+(t)\, r_-(t)}{r_+(t)+r_-(t)} + v_L \frac{r_-(t) - r_+(t)}{r_+(t) + r_-(t)} \qquad \ldots 1$$

$$i_L = i_s \frac{r_-(t) - r_+(t)}{r_+(t) + r_-(t)} - v_L \frac{2}{r_+(t) + r_-(t)} \qquad \ldots 2$$

On substitution for the time-varying resistances, and for $r'_s < 10^{-3}$, eqns. 1 and 2 approximate to:

$$v_s = i_s r_b \left\{ 2r'_s + \frac{1}{1 + X(t)\, S(t)} \right\} + v_L \left\{ \frac{X(t)}{1 + X(t)\, S(t)} \right\}$$

$$i_L = i_s \left\{ \frac{X(t)}{1 + X(t)\, S(t)} \right\} - v_L \frac{1}{r_b} \left\{ 2 - \frac{1}{1 + X(t)\, S(t)} \right\}$$

The general 'K' parameters are:

$$K_1 = \frac{A_0 \left\{ Z''_{-2} + (1 - x^2) \right\}}{(Z''_{-2} + 1)}$$

$$K_2 = \frac{A'_0 \left\{ Z''_{-2} + 1 + \left(\frac{A_1}{2}\right)^2 \frac{1}{A_0 A'_0} \right\}}{(Z''_{-2} + 1)}$$

$$K_3 = \left(\frac{A_1}{2}\right)^2 \frac{\left\{Z''_{-2} + (1 - x)\right\}^2}{(Z''_{-2} + 1)^2}$$

where

$$Z''_{-2} = \frac{Z_{-2}}{r_b A_0} \qquad \text{and} \qquad x = \frac{A_2}{2A_0}$$

The following expressions aid the calculation of the $(c.p.l.)_{opt}$, for the general case[4]

$$\theta_i = \tfrac{1}{2}\beta + \tfrac{1}{2}\gamma - \tfrac{1}{2}\alpha$$

$$-\theta_L = \tfrac{1}{2}\alpha + \tfrac{1}{2}\gamma - \tfrac{1}{2}\beta$$

$$\phi = \tfrac{1}{2}\gamma - \tfrac{1}{2}\alpha - \tfrac{1}{2}\beta$$

where

$$\beta = \tan^{-1} \frac{X''_{-2}}{R''_{-2} + 2(1 - x)}$$

$$\alpha = \tan^{-1} \frac{X''_{-2}}{R''_{-2} + 1}$$

and

$$\gamma = \tan^{-1} \frac{X''_{-2}}{R''_{-2} + (1 - x^2)}$$